Title: Multi-sensor remote sensing for drought characterization: current status, opportunities and a roadmap for the future

Authors: Wenzhe Jiao[1], Lixin Wang[1]*, Matthew F. McCabe[2]

[1]Department of Earth Sciences, Indiana University - Purdue University Indianapolis (IUPUI), Indianapolis, 46202, USA

[2]Hydrology, Agriculture and Land Observation Group, Water Desalination and Reuse Center, King Abdullah University of Science and Technology, Thuwal 23955-6900, Saudi Arabia

Abstract:

Satellite based remote sensing offers one of the few approaches able to monitor the spatial and temporal development of regional to continental scale droughts. One of the unique elements of remote sensing platforms is their multi-sensor capabilities, which enhances the capacity for characterizing drought from a variety of aspects. Such capabilities include monitoring drought influences on vegetation and hydrological responses as well as assessing sectoral impacts (e.g., agriculture). With advances in remote sensing capacity and the increasing range of platforms available for analysis, this contribution presents a systematic review of multi-sensor remote sensing drought studies, with a particular focus on drought related datasets, drought related phenomena and mechanisms, and drought modeling. To explore this topic, we first present a comprehensive summary of large-scale drought-related remote sensing datasets that can be used for multi-sensor drought studies. Then we review the role of multi-sensor remote sensing for important drought related phenomena and mechanisms, including vegetation responses to drought, land-atmospheric feedbacks during drought, drought-induced tree mortality, drought-related ecosystem fires, post-drought recovery and legacy effects, flash drought, as well as

This is the author's manuscript of the article published in final edited form as:

Jiao, W., Wang, L., & McCabe, M. F. (2021). Multi-sensor remote sensing for drought characterization: Current status, opportunities and a roadmap for the future. Remote Sensing of Environment, 256, 112313. https://doi.org/10.1016/j.rse.2021.112313

drought trends under climate change. We then provide a summary of recent modeling advances towards developing integrated multi-sensor remote sensing drought indices. We conclude that leveraging multi-sensor remote sensing provides unique benefits for regional to global drought studies, particularly in: 1) revealing the complex drought impact mechanisms on various ecosystem components; 2) providing continuous long-term drought related information at large scales; 3) presenting real-time drought information with high spatiotemporal resolution; 4) providing multiple lines of evidence of drought monitoring to improve modeling and prediction robustness; and 5) improving the accuracy of drought monitoring and assessment efforts. We specifically highlight that more mechanism-oriented drought studies that leverage a combination of sensors and techniques (e.g., optical, microwave, hyperspectral, LiDAR, and constellations) across a range of spatiotemporal scales are needed in order to progress and advance our understanding, characterization and description of drought in the future.

Keywords: data fusion; drought; drought impact; drought monitoring; ecohydrology; multi-sensor satellite; regional scale drought.

Contents:

80
81
82

1. Introduction

Drought is routinely described as a naturally occurring phenomena induced by precipitation deficiency and consequent hydrological imbalance (Pachauri et al., 2014; Trenberth et al., 2014). Drought can occur over all climatic conditions and has a wide range of damaging impacts (Dai, 2011; Vicente-Serrano et al., 2019). For instance, it can cause crop failures, which may lead to substantial food security concerns and financial loses (Daryanto et al., 2015; Daryanto et al., 2016; Godfray et al., 2010; Pandey et al., 2007); it can decrease the volumes of source waters from rivers, lakes, and groundwater, directly impacting water availability, distribution and energy supply (Van Loon, 2015); it can also amplify tree mortality, trigger ecosystem fires, and decrease carbon uptake in vegetation (Allen et al., 2010; Ciais et al., 2005; Zhao and Running, 2010), thereby influencing terrestrial carbon storage and sequestration potential. Given the wide-ranging scope of influences and impacts that droughts can have, it is no surprise that it is often classified quite broadly, based on the different systems affected. These classifications generally fall into: i) agricultural; ii) hydrological; iii) meteorological, and iv) socioeconomic drought (Wilhite and Glantz, 1985). Recent research has suggested additional drought types, such as ecological drought (Crausbay et al., 2017), environmental drought (Vicente-Serrano et al., 2019), and flash drought (Otkin et al., 2018; Svoboda et al., 2002). With the severity and frequency of droughts projected to increase under climate change, understanding the interrelated impacts and influence across and within sectors is an issue of considerable importance (Dai, 2013; Trenberth et al., 2014; Xu et al., 2019; Zhou et al., 2019). **Figure 1** illustrates a number of these drought impacts on different ecosystem components, together with the feedbacks between drought and climate.

105 Given the spatial and temporal advantage that remote sensing can offer, data from a range
106 of satellite-based platforms have played an increasingly important role in drought studies over
107 the last decade (AghaKouchak et al., 2015; West et al., 2019). In addition, advances in algorithm
108 development and the rise of cloud-based computing and storage capacity have greatly enhanced
109 the application potential of remote sensing for drought studies (Abdelwahab et al., 2014;
110 Faghmous and Kumar, 2014; Huntington et al., 2017; Sellars et al., 2013; Zhou et al., 2016).
111 Apart from offering an independent observational capacity, remote sensing data provides an
112 opportunity to reduce uncertainty and constrain modelling efforts directed towards drought
113 prediction (Smith et al., 2016). With all of these advances, there have been an increasing number
114 of studies on the subject of drought monitoring and impacts (Agutu et al., 2017; Asner et al.,
115 2016; Gonçalves et al., 2020; Hu et al., 2020a; Jiao et al., 2019a; Jiao et al., 2019b; Jiao et al.,
116 2019c; Liu et al., 2017a; Nicolai-Shaw et al., 2017; Park et al., 2017; Schwantes et al., 2016;
117 Thomas et al., 2017; Zhang et al., 2017b). However, while there has been considerable and
118 important research reviewing drought monitoring and its various impacts, with a number of these
119 studies highlighting the importance of integrated drought monitoring (AghaKouchak et al., 2015;
120 Liu et al., 2016b; Trnka et al., 2018; Van Loon et al., 2016; West et al., 2019; Zhang et al.,
121 2017a), there has been no systematic review focusing on some of the recent advances in multi-
122 sensor remote sensing for drought studies, and how these might further advance the modeling,
123 assessment and prediction fields.

124 **[Insert Figure 1 here]**

125 In this contribution, we undertake a timely and systematic review of multi-sensor remote
126 sensing based drought studies, motivated in part by recent and rapid developments in sensing
127 capability, as well as the significant advantages that can be gained by coupling multi-

platform/multi-sensor approaches to better understand drought phenomena and impacts. For example, many government agencies have space-based Earth observation programs, including the United States National Aeronautics and Space Administration (NASA), European Space Agency (ESA) and Japan Aerospace Exploration Agency (JAXA), all of which present opportunities for coupling multi-platform/multi-sensor approaches for enhanced monitoring (McCabe et al., 2008). A recent example is the effort to develop a Harmonized Landsat and Sentinel-2 (HLS) surface reflectance dataset, which combines United States Geological Survey (USGS)/NASA Landsat with ESA Sentinel-2 to provide near-daily reflectance observations at 30-meter resolution (Claverie et al., 2018). Such multi-sensor/multi-platform integration presents a number of advantages for the remote sensing of drought compared to single sensor approaches, including:

1. It is well recognized that drought has complex environmental impacts and can affect numerous ecosystems components in parallel (Vicente-Serrano et al., 2019). Used in isolation, a single drought index is unlikely to capture the complexity of process interactions and diverse impacts of drought, whereas multi-sensor platforms, facilitated by multivariate retrievals, may better reflect the extent and severity of drought conditions (Hao and AghaKouchak, 2013; Hao and Singh, 2015).

2. Current remote sensing products already make it possible to observe drought from various perspectives, including through monitoring precipitation, air and land surface temperature, soil moisture, evaporation, total water storage and vegetation health (AghaKouchak et al., 2015; Alizadeh and Nikoo, 2018; Pan et al., 2008). A number of remote sensing platforms provide continuous long-term drought related information for use at large scales, with an

obvious example being the series of National Oceanic and Atmospheric Administration (NOAA) satellites, which have provided global coverage from the Advanced Very High Resolution Radiometer (AVHRR) from 1979 to present (Van Leeuwen et al., 2006). Such long-term coverage is only possible through multi-sensor/multi-platform data fusion.

3. Up until the recent addition of CubeSat constellations to our Earth observation arsenal (McCabe et al., 2017a; Rahmat-Samii et al., 2017; Woellert et al., 2011), single satellite sensors were unable to provide real-time drought information with high spatiotemporal resolution, as traditional remote sensing approaches generally require a compromise between spatial resolution and temporal frequency (Price, 1994; Zhu et al., 2010). New systems, together with the fusion of data from different sensors and platforms, or multi-sensors from satellite constellations, can provide drought information with both high spatial and temporal resolution (Feng et al., 2006; McCabe et al., 2017b; Pohl and Van Genderen, 1998; Zhu et al., 2010), overcoming this spatiotemporal divide.

4. Drought studies using multiple sources of data can provide multiple lines of evidence and improve the robustness of analysis. Sensors from different instruments observe the Earth independently, thus allowing analysis from a variety of data sources that can provide cross validation and an improved representation of prediction uncertainty.

5. Recent advances in both new sensors and improved observational techniques, such as space-borne solar-induced chlorophyll fluorescence (SIF) (Jiao et al., 2019a; Sun et al., 2015), light detection and ranging (LiDAR) and hyperspectral sensors (Asner et al., 2016; Brodrick

et al., 2019; Zhu et al., 2019) offer complementary information that can be integrated into multi-sensor drought studies to better understand the mechanisms of drought development and impacts (Aubrecht et al., 2016; Smith et al., 2019b; Yang et al., 2018a; Yang et al., 2018b).

To advocate and encourage on-going exploration and integration of multi-sensor remote sensing for drought studies, we provide an overview of the role of multi-sensor remote sensing for addressing knowledge gaps and driving advances in drought studies. To this end, we provide a systematic review of multi-sensor remote sensing drought studies from a number of critical aspects, including datasets, phenomena, mechanisms, and modeling. We first present a comprehensive summary of large-scale drought-related remote sensing datasets that could be used for multi-sensor drought studies (section 2). We then discuss the role of multi-sensor remote sensing for characterizing important drought related mechanisms, including evaluating mechanisms of vegetation response to drought (section 3.1) and monitoring land-atmosphere feedbacks (section 3.2). We follow this with a review of the role of multi-sensor remote sensing for identifying important drought related phenomena, including drought-induced tree mortality (section 3.3), ecosystem fires (section 3.4), post-drought recovery and drought legacy effects (section 3.5), flash drought (section 3.6), and drought trends under global warming (section 3.7). Recent modeling advances for developing integrated multi-sensor remote sensing drought indices are reviewed in section 4, followed by a discussion on some of the challenges (section 5) and a potential road map for the future (section 6). In combination, we seek to establish the important role that multi-sensor remote sensing can play in bridging spatiotemporal divides, in improving our understanding of the underlying mechanisms and processes, as well as in

196 advancing our ability to proactively monitor and predict drought events as they occur and
197 develop.

198 **2. Satellite-based products for multi-sensor drought characterization**

199 Dataset selection is fundamental to multi-sensor remote sensing of drought (Zhang et al., 2017a).
200 Benefitting from an increasingly wide array of available satellite-based observations, remote
201 sensing provides a capacity to characterize drought from a range of perspectives, including
202 precipitation, temperature, soil moisture, terrestrial water storage, evaporation, snow, vegetation
203 response and plant function. **Table 1** collates a comprehensive overview of datasets that could be
204 incorporated into multi-sensor drought studies. In the following paragraphs, we use this as a
205 basis to explore the characteristics, strengths and constraints of major drought related remote
206 sensing datasets.

207 **[Insert Table 1 here]**

208 **2.1 Remote sensing based precipitation**

209 Precipitation measurements are perhaps the most fundamental element for calibrating drought
210 models (Orville, 1990; Wilhite and Glantz, 1985), and most certainly the principal variable in
211 identifying and defining meteorological drought (Palmer, 1965). The challenges of single-sensor
212 satellite precipitation data have been well recognized by the community for many years, with
213 multi-product and multi-sensor ensembles receiving much attention over the last decade (Beck et
214 al., 2019; Martinaitis et al., 2017; Prakash et al., 2018; Sorooshian et al., 2011; Zhang et al.,
215 2016a). The lack of consistency between different satellite precipitation datasets – even those
216 from the same sensors – further complicate dataset selection (Tapiador et al., 2017). **Table 1**
217 identifies the commonly used large scale satellite based precipitation datasets, with each having
218 their own spatial, temporal, and regional coverages. A series of studies have attempted to inter-

compare these various precipitation datasets at regional to global scales, with most finding that multi-sensor/multi-source ensemble products provide the highest quality (Beck et al., 2020; Derin and Yilmaz, 2014; Gehne et al., 2016; Sun et al., 2014; Sun et al., 2018a; Zeng et al., 2018; Zhu et al., 2015). Some recent studies have focused inter-comparisons on drought monitoring using different precipitation products (Zhong et al., 2019), with the authors highlighting the benefit of integrated precipitation data (e.g., Multi-Satellite Precipitation Analysis, TMPA 3B42V7).

2.2 Remote sensing based land surface temperature

Land surface temperature (LST) is another key parameter for integrated drought monitoring, since it provides an indirect measure of the surface energy balance (Tomlinson et al., 2011). Thermal stress (or thermal inertia), which can be obtained from land surface temperature and air temperature, has also been shown to be a good indicator of drought condition (Anderson et al., 2008; Otkin et al., 2013; Seyednasrollah et al., 2019). Drought monitoring based on thermal stress has been shown to be capable of monitoring drought at early stages (Seyednasrollah et al., 2019). The combination of LST with vegetation indicators such as NDVI, which can reflect the vegetation response to drought, provides an excellent example of multi-sensor strategies (Orhan et al., 2014; Patel et al., 2012; Son et al., 2012; Sruthi and Aslam, 2015). The triangle space relationship between LST and vegetation index (Ts-VI) (Goward et al., 1985) has been successfully applied to study soil water content and drought monitoring (Nemani et al., 1993; Nishida et al., 2003; Running et al., 1994). Various Ts-VI drought indices, including the Temperature–Vegetation Dryness Index (TVDI) (Sandholt et al., 2002), Vegetation Temperature Condition Index (VTCI) (McVicar and Bierwirth, 2001), Microwave Temperature Vegetation Drought Index (MTVDI) (Liu et al., 2017a), and the Temperature Vegetation Precipitation

242 Dryness Index (TVPDI) (Wei et al., 2020) have been developed to leverage this relationship. In
243 addition, the combination of LST with other metrics (e.g. soil moisture; see section 2.3) has also
244 been explored and shown to have potential for improved drought monitoring (Hao et al., 2015;
245 Jiao et al., 2019b).

246 There are numerous remote sensing LST datasets from different satellite platforms that
247 can be used for multi-sensor integrated drought monitoring (see **Table 1)**. The listed datasets
248 present different observation periods, temporal and spatial resolutions, overpass times, and
249 accuracies, and as a result, have differing strengths. Several factors, such as difficulties in
250 atmospheric correction and emissivity estimation, the accessibility of data or having restrictions
251 on its use (e.g., ASTER LST and other GOES datasets) (Tomlinson et al., 2011), may have
252 limited wider application of LST data (Gutman, 1999; Li et al., 2014). Although a number of
253 efforts have sought to overcome these constraints (Pinheiro et al., 2004; Pouliot et al., 2009),
254 widely used datasets (e.g., MODIS and AVHRR LST datasets) offer a compromise between
255 regular satellite revisit time and a reasonable spatial resolution. Higher-resolution Landsat data,
256 as well as the improved spatio-temporal insights of the exploratory ECOSTRESS mission (Fisher
257 et al., 2020), highlight the added value of thermal data for a range of hydrological studies,
258 including drought monitoring.

259 **2.3 Remote sensing based soil moisture**

260 Soil moisture is a key variable for agricultural planning and water resources management, and
261 remote sensing based products have seen extensive application to define and identify agricultural
262 drought (Keshavarz et al., 2014; Vicente-Serrano et al., 2019; Wang and Qu, 2009). Soil
263 moisture also plays a key role in the climate system, since its deficit can trigger changes in
264 precipitation and energy storage within the soil-vegetation-atmosphere system, resulting in local

to regional scale impacts (Seneviratne et al., 2010). As such, drought detection using soil moisture data not only benefits agricultural related systems, but also broadly enhances our understanding of land-atmosphere interactions for weather and climate predictions. Remotely sensed datasets can be obtained from at least four different types of sensors, comprising optical, thermal, passive microwave and active microwave systems (Wang and Qu, 2009), with each type having its relative advantages and limitations. The most commonly used remote sensing based soil moisture products are listed in **Table 1**. Numerous studies have evaluated the utility of remotely sensed soil moisture products for drought characterization (Bolten et al., 2009; Martínez-Fernández et al., 2016; Nicolai-Shaw et al., 2017). However, quantitative soil moisture estimation remains difficult, especially under vegetation cover (Dorigo et al., 2017; Wang and Qu, 2009). Moreover, any non-linear relationship between soil moisture and drought indices makes the application of soil moisture data more complicated (Sims et al., 2002). Development of soil moisture from multi-sensor remote sensing data show clear advantages, especially in terms of developing long-term datasets. As part of the European Space Agencies (ESA) Climate Change Initiative (CCI), Gruber et al. (2019) developed one of the longest temporal sequences of global soil moisture, providing the opportunity to explore a range of related process.

2.4 Remote sensing based groundwater and surface water storage

Groundwater, streamflow and surface water storage are key variables to identify and define hydrological drought (Tallaksen and Van Lanen, 2004; Van Loon, 2015; West et al., 2019). Hydrological drought (i.e., deficit of groundwater and/or surface water storage) can have longer and broader impacts than meteorological and agricultural drought, particularly in terms of drinking water supply, irrigation, and even electricity production via hydropower (Van Loon, 2015). Frappart and Ramillien (2018) presented a detailed discussion on the potential for

288 groundwater monitoring from satellite remote sensing, highlighting the potential to measure
289 groundwater potential, storage, and fluxes when combined with numerical modeling and ground-
290 based measurements. A number of recent studies have illustrated that terrestrial water storage
291 observations derived from NASA's Gravity Recovery and Climate Experiment (GRACE)
292 satellite can provide important insights into drought behavior (Bhanja et al., 2016; Feng et al.,
293 2013; Thomas et al., 2017). Interferometric Synthetic Aperture Radar (InSAR) sensors have also
294 been used for groundwater and terrestrial water studies (Bell et al., 2008; Castellazzi et al., 2018;
295 Normand and Heggy, 2015). These systems are able to precisely determine the magnitude of
296 surface deformation and subsidence, even under challenging atmospheric conditions, and
297 represent a cost-efficient approach for large scale monitoring (Galloway and Hoffmann, 2007).
298 However, both GRACE and InSAR data have their limitations. The coarse spatial resolution (i.e.,
299 pixel sizes of roughly 300-400 km) and post-processing demands of GRACE, present
300 considerable constraints (Chen et al., 2016). In addition, GRACE based terrestrial water storage
301 estimates were found to have larger bias in humid regions, due to large seasonal water storage
302 changes and propagation uncertainty of signal from all hydrological processes (Shamsudduha et
303 al., 2012). While several novel strategies have been proposed to improve the spatial resolution
304 (Bruinsma et al., 2010; Save et al., 2012), ongoing research is needed to address the issues,
305 including algorithmic improvements, noise reduction and signal decomposition. InSAR presents
306 its own limitations in terms of the signal coherence in areas with dense vegetation or regions
307 with existing surface disturbance (e.g., agricultural areas) (Castellazzi et al., 2016). Recent
308 efforts to combine GRACE and InSAR data have illustrated the benefit of multi-sensor
309 approaches for both resolution improvements and for necessary monitoring of groundwater
310 depletion (Castellazzi et al., 2018).

311 **2.5 Remote sensing based snow data**

312 Similar to soil moisture and precipitation data, remote sensing of snow can be broadly classified
313 into optical and microwave approaches, and those that combine the two (Frei et al., 2012).
314 Monitoring changes in snow coverage, depth, and duration are important for characterizing
315 drought in areas where snow provides a substantial contribution to the hydrological cycle (Chang
316 et al., 2019; Mote et al., 2005; Pederson et al., 2011; Stewart, 2009). It is worth noting that
317 drought events (e.g., 2014/15 drought event in the state of Washington in the United States (Fosu
318 et al., 2016)) can occur under normal precipitation, but deficiency of the winter snowpack.
319 Deficit of snow cover in winter can cause severe hydrological and agricultural drought in
320 summer, making the incorporation of snow cover information into integrated drought monitoring
321 an important task (Hamlet et al., 2005; Kalra et al., 2008; Margulis et al., 2016). Drought indices
322 accounting for snow (e.g., Standardized Snow Melt and Rain Index (SMRI) (Staudinger et al.,
323 2014)) have been shown to provide enhancements relative to traditional meteorological drought
324 indices. Snowpack data has also been used in combination with soil moisture information to
325 show improved indicators for drought estimation and disaster risk prediction (Kumar et al., 2014;
326 Tachiiri et al., 2008). It is also important to note that global warming causes changes of
327 snowpack in many regions and changes the sensitivity of snowpack to climate (Flanner and
328 Zender, 2006; Mote et al., 2005; Stewart, 2009), so incorporating snow data into drought studies
329 is likely to be an aspect of increasing importance.

330 **2.6 Remote sensing based evaporation**

331 Given its central role as a linking mechanism between the water and energy cycles, evaporation
332 presents as an important metric for drought monitoring and estimation. Determining evaporation
333 dynamics from satellite observations is complicated, since it is not directly observable from any

sensor, but rather inferred through combining meteorological, radiation, vegetation and other data with an interpretive model. Evaporation also represents the integration of a range of water loss processes, from direct soil and canopy evaporation, as well as the transpiration deriving from plants, making its accurate modeling a challenging task (Anderson et al., 2011b; Mu et al., 2011; Su et al., 2005). Numerous models and algorithms have been developed to infer evaporation from remote sensing observations, and the readers are referred to some of the extensive reviews undertaken by Kustas and Norman (1996), Kalma et al. (2008), Li et al. (2009), Wang and Dickinson (2012) and Fisher et al. (2017) for further details. Drought monitoring studies have used evaporation as a parameter to develop drought indices, with the most recognized being the Palmer Drought Severity Index (PDSI) (Palmer, 1965), Standardized Precipitation Evapotranspiration Index (SPEI) (Vicente-Serrano et al., 2010) and the Evaporative Stress Index (ESI) (Anderson et al., 2011a; Anderson et al., 2016). However, most of the commonly used long-term ET based drought monitoring indices are derived from coarse spatial resolution (e.g., 0.5^{o} grid cell size for SPEI, 2.5^{o} grid cell size for PDSI) with monthly temporal resolution, which limit their applicability for drought monitoring. Given the important role that evaporation plays, not just in drought studies, but also in monitoring ecosystem function, understanding water and carbon cycles (Wilkinson et al., 2020), and food and water security studies (López Valencia et al., 2020), the need for ongoing and improved satellite missions dedicated to its measurement is a critical requirement (Fisher et al., 2017; Wang et al., 2012). Efforts exploring the recently commissioned ECOsystem Spaceborne Thermal Radiometer Experiment on Space Station (ECOSTRESS) (Fisher et al., 2020) provide an example of current capabilities for multi-sensor high spatiotemporal observations of evaporation. Future multi-instrument satellite systems, such as the Hyperspectral Infrared Imager mission (HyspIRI), may

provide the combination of spectral, spatial and temporal resolution needed for global evaporation derivation (Lee et al., 2015).

2.7 Remote sensing based vegetation vigor

Vegetation plays the most active role in modulating the water and carbon cycles of most ecosystems (Jasechko et al., 2013; Lanning et al., 2020; Lanning et al., 2019; Wang et al., 2014). Plants respond quickly and dynamically to hydrologic stress and control the land-atmosphere exchanges of water and energy (Novick et al., 2016). Over the past few decades, remote sensing based vegetation observations have explored the optical and microwave domains of the electromagnetic spectrum, with a large number of available multi- and hyperspectral sensors at ground-, air- and space-borne level. An historical overview of vegetation estimation based on leaf spectral properties can go back to the 1970s (Ryu et al., 2019). With the launch of Landsat in 1972, pioneering studies sought to explore drought impacts on vegetation growth at the landscape to regional scales (e.g., Thompson and Wehmanen 1977; Short 1976). The launch of active and passive microwave and hyperspectral sensors (e.g., Hyperion data from Earth Observing-1 (EO-1) satellite, launched November 21, 2000), provided further data to study drought impacts on vegetation beyond more traditional observations from broad-band optical sensors. In more recent times, active light detection and ranging (LiDAR), especially in combination with Unmanned Aerial System (UAS) platforms (Sankey et al., 2018) have dramatically expanded the fine-scale application of remote sensing vegetation monitoring (Xue and Su, 2017).

Vegetation indices are the primary approach towards monitoring vegetation greenness, with changes in the spectral characteristics of plant leaves and canopy being used to provide insights into health and condition (Bannari et al., 1995; Zargar et al., 2011). One of the most

widely used remote sensing based vegetation indices is the Normalized Difference Vegetation Index (NDVI) (Rouse et al., 1974). However, as with many such indices, NDVI has a range of limitations related to its sensitivity to background factors, such as shading and soil brightness, atmospheric effects, as well as saturation issues (Huete, 1988; Richardson and Wiegand, 1990). A suite of other NDVI type indices were subsequently developed in an attempt to improve such limitations, or to provide a more focused retrieval of plant physiological features. For example, the Soil-Adjusted Vegetation Index (SAVI) (Huete, 1988), modified SAVI (MSAVI) (Qi et al., 1994), or the Global Environment Monitoring Index (GEMI) (Xue and Su, 2017) were all developed to eliminate the soil background effect of vegetation indices, while the enhanced vegetation index (EVI) was developed to simultaneously correct soil and atmospheric effects (Huete et al., 2002). More recently, Badgley et al. (2017) developed near-infrared reflectance of vegetation (NIR_V) with the aim of minimizing both the effects of soil contamination and variable viewing geometry from satellite observations.

While broad-band based indices have provided numerous opportunities for vegetation sensing, hyperspectral sensors can provide an order of magnitude increase in spectral information relative to multispectral systems. Hyperspectral reflectance derived indices such as the Photochemical Reflectance Index (PRI) (Thenot et al., 2002) or the MERIS terrestrial chlorophyll index (MTCI) (Dash and Curran, 2007), were shown to have good performance in monitoring early plant water stress by reflecting drought-induced vegetation physiological and biochemical processes change (He et al., 2016; Suárez et al., 2008).

The main advantage of microwave sensors is that they have higher penetration ability and are less affected by weather and atmospheric influences. While the value of microwave remote sensing has been well detailed in the context of oceanographic applications and soil moisture

403 estimation, an increasing number of recent studies have explored its sensitivity to plant water
404 content (Konings et al., 2019; Liu et al., 2011), particularly via examination of the vegetation
405 optical depth (VOD). However, the drawbacks of passive microwave observations include the
406 relatively low spatial resolution and the sensitivity to both temperature and single-scattering
407 albedo, which can affect the derivation of VOD accuracy (Vreugdenhil et al., 2019).

408 Besides vegetation indices, other variables that are more directly linked to vegetation
409 photosynthesis have been used to estimate drought impacts. Vegetation Gross Primary
410 Productivity (GPP) is one of the most commonly used photosynthesis proxies that can be
411 employed to infer drought impact and prediction (Meng et al., 2014; Zhao and Running, 2010).
412 Current satellite GPP can be generally estimated from four types of modeling: process-based
413 model (Farquhar et al., 1980), light use efficiency (LUE) models (Zhao et al., 2005), machine
414 learning techniques based on eddy covariance measurements (Tramontana et al., 2016), and solar
415 induced chlorophyll fluorescence (SIF) based statistical model (Guanter et al., 2014). However,
416 there remain considerable uncertainties in using GPP datasets for drought studies. For example,
417 Stocker et al. (2019) found that satellite GPP data underestimated the drought impact on
418 terrestrial primary production due to the lack of consideration of soil moisture information.
419 Studies also indicate the divergent ability of reflecting drought impact among different GPP
420 models and products (Chang et al., 2020; Li and Xiao, 2020). Remote sensing based solar
421 induced chlorophyll fluorescence (SIF) is a rapidly advancing research front in studies of global
422 vegetation (Guan et al., 2016; Guanter et al., 2007; Joiner et al., 2013), with recent research
423 indicating its potential to monitor the drought impact on vegetation dynamics (Jiao et al., 2019a;
424 Sun et al., 2015; Yoshida et al., 2015). Although there have yet to be any satellites specifically
425 designed to measure SIF, the planned FLuorescence EXplorer (FLEX) (scheduled to launch in

2022) will be the first (Mohammed et al., 2019). Remote sensing based SIF retrieval mechanisms have been studied for decades, with detailed reviews provided by Mohammed et al. (2019), Ni et al. (2019), Aasen et al. (2019), and Bandopadhyay et al. (2020). Several satellite-based SIF datasets have been compiled from other satellite missions and directed towards the study of drought. SIF products derived from the Greenhouse gases Observing Satellite (GOSAT) provided regional to global scale availability (Frankenberg et al., 2011; Joiner et al., 2011). Datasets from other satellite sensors such as the SCanning Imaging Absorption spectroMeter for Atmospheric CartograpHY (SCIAMACHY) (Joiner et al., 2012), the Global Monitoring Ozone Experiment 2 (GOME-2) (Joiner et al., 2013), Orbiting Carbon Observatory-2 (OCO-2) (Sun et al., 2018b; Taylor et al., 2020), the TROPOspheric Monitoring Instrument (TROPOMI) (Köhler et al., 2018), and Orbiting Carbon Observatory-3 (OCO-3) (Taylor et al., 2020) have also provided global SIF retrievals. The use of recent TROPOMI observations for providing relatively high spatiotemporal resolutions revolutionized satellite-based SIF application for drought studies (Köhler et al., 2018). However, current SIF data also have a number of limitations, including noise from clouds and aerosols, coarse spatial resolution and sensor degradation (Mohammed et al., 2019), all of which may introduce uncertainties for drought study. Despite such uncertainties, SIF presents several key advantages over other vegetation proxies and may provide an alternative perspective to study the impact of drought on vegetation photosynthesis. Indeed, SIF has been shown to track the seasonality of photosynthesis and be more consistent with site-observed GPP variability than vegetation indices such as EVI and photochemical reflectivity index (PRI) (Magney et al., 2019; Smith et al., 2018; Verma et al., 2017). Incorporating satellite SIF could also improve global estimates of important plant traits, such as GPP and photosynthetic capacity (He et al., 2019; Smith et al., 2018; Zuromski et al.,

2018). Recent studies have indicated that SIF is more sensitive to drought related water and heat stress than greenness indices (Qiu et al., 2020; Song et al., 2018), highlighting this potential.

3. The role of multi-sensor remote sensing for drought related phenomena and mechanisms

Drought can substantially impact global and regional carbon cycling and cause irreversible damage to ecosystem function in a warming climate (Anderegg, 2015; Dai, 2011; Garcia et al., 2014; Hao et al., 2017; Seddon et al., 2016; Sippel et al., 2018; Willis et al., 2018). Recent research suggests that drought associated with extreme high temperatures are leading to negative impacts on carbon uptake, slowing down carbon dioxide and nitrogen fertilization effects on terrestrial ecosystem vegetation (Peñuelas et al., 2017). In addition, drought has been reported to have increasing impacts on ecosystem carbon uptake. In a related study, Yuan et al. (2019a) indicated an increasing impact of drought related vapor pressure deficit on vegetation growth over the past three decades. However, drought impact on ecosystems is complex and many uncertainties and questions remain unresolved (Trnka et al., 2018). Due to the complexity of drought interactions within ecosystems, single sensor remote sensing observation are unlikely to provide a comprehensive and convincing accounting of their characterization. On the other hand, multi-sensor based evaluations can offer deeper insights across a range of drought-related research. For instance, multi-sensor based evaluations can improve the understanding of drought related phenomena such as drought-induced tree mortality, drought-related ecosystem fire, and developing trends under climate change. Multi-sensor based evaluations can also enhance the understanding of drought related mechanisms, including those behind vegetation response and land-atmospheric feedbacks during drought. Here we provide a review of these research aspects as well as identify some of the current gaps in drought research that could benefit from multi-sensor observations.

3.1 Monitoring mechanisms of vegetation response to drought using remote sensing

Drought can have a direct impact on the terrestrial carbon sink, with vegetation response being a key indicator of this influence (Piao et al., 2019). Drought impact on the terrestrial carbon cycle has been evaluated using remote sensing observations (AghaKouchak et al., 2015), with decreases in vegetation productivity acting to reduce CO_2 uptake (Chen et al., 2013; Ciais et al., 2005; Donohue et al., 2013). However, vegetation response to drought can vary considerably, both physiologically and structurally across leaf to canopy levels, let alone for different biome types and species (Zhang et al., 2013). The structural and physiological responses of plants to droughts are not well understood at large scales (Van der Molen et al., 2011). Physiological responses vary depending on the photosynthesis related enzymatic activities and stomatal closure, which act to prevent water loss (Chang et al., 2020; Meir et al., 2008; Meir and Woodward, 2010). Two contrasting stomatal closure strategies for water use under drought have been identified: isohydric, where species decrease stomatal conductance to prevent reducing leaf water potential; and anisohydric, where species exert little or no stomatal control in response to drought (Klein, 2014; Lanning et al., 2020; Roman et al., 2015). Due to the different stomatal closure strategies under drought, isohydric species are generally expected to experience a larger reduction of short-term gross primary productivity (GPP) than anisohydric species (Van der Molen et al., 2011). A recent multi-sensor approach by Hwang et al. (2017) indicated that photochemical reflectance index (PRI), derived from Moderate Resolution Imaging Spectroradiometer (MODIS) observations and field spectroradiometer data, can capture the divergent isohydric and anisohydric behavior under drought stress at both leaf and canopy scales, from sunlit and shaded portions of the canopy. Their study provided a theoretical framework for observing the vegetation physiological response to drought at large scales. GPP reduction caused

by drought can also be determined from structural changes in the vegetation canopy (Van der Molen et al., 2011).

Structural change under drought stress can include reductions in leaf area, leaf shed, and the alteration of leaf angle distribution within the canopy (Kull et al., 1999). Such change has often been inferred via remote sensing based leaf area index (LAI) measurements (Zhang et al., 2013). However, accurate LAI estimation at regional to global scales remains a longstanding challenge (Richardson et al., 2009). Remote sensing of LAI can be determined from passive optical sensors, microwave sensors, and active light detection and ranging (LiDAR) instruments, with each method having its relative strengths and limitations (Fang et al., 2019; Zheng and Moskal, 2009). For example, passive optical sensors can provide multispectral imagery, which is beneficial to object discrimination (Chen et al., 2004). However, passive optical sensor based LAI estimations can be affected by multiple factors, such as saturation of vegetation index based derivation of LAI, sensor degradation, mitigating leaf pigment effects, and atmospheric contaminations (Xie et al., 2018; Yan et al., 2019). Microwave based LAI estimation has the potential to overcome the impacts from cloud and other atmospheric influences (Fang et al., 2019). However, few microwave based LAI estimations are based on radar physical models, and the accuracy of large regional scale microwave based LAI retrievals need further evaluations (Fang et al., 2019; Tao et al., 2016). LiDAR based LAI can be estimated by separating canopy woody and foliage components (Zhao et al., 2011). In addition, LiDAR observations are have the potential to characterize the vertical vegetation structure at different heights, and provide accurate three-dimensional (3D) point cloud data (Liu et al., 2017b). Such data provides new opportunities for detailed assessments of drought impact on canopy structure. For example, a recent study by Smith et al. (2019a) indicated that LiDAR showed great potential in capturing

canopy structural heterogeneity in response to drought and seasonality. However, limitations such as the uncertainty of LiDAR based LAI estimation models, and the issue of converting effective LAI (LAI_{eff}) to LAI can also hamper the applications of LiDAR based LAI. (Fang et al., 2019). More generally, the combined use of multi-sensor information from LiDAR and optical observation (Ma et al., 2014), tend to show capacity for a more comprehensive description of the biophysical characteristics of forest ecosystems, making for a promising opportunity for further exploration in multi-senor drought studies. Besides remote sensing LAI data, multi-angle reflectance based observations have been linked to canopy structure characteristics such as canopy roughness (Strahler, 1997), foliage clumping (Chen et al., 2005), and leaf angle distribution (Roujean and Lacaze, 2002). Recent multi-angle approaches such as MODIS derived Multi-Angle Implementation of Atmospheric Correction (MAIAC) has identified anomalies in Amazon forest canopy structure under drought (De Moura et al., 2015).

Species composition could change in response to drought, and multi-sensor based evaluations have the capacity to capture such changes. Recent studies indicate that ecosystems tend to change species composition towards deeper rooted varieties in order to stabilize ecosystem primary production under drying conditions (Griffin‐Nolan et al., 2019; Liu et al., 2018a; Luo et al., 2019). Ecosystem with more species exhibiting lower productivity declines during droughts, tend to recover faster after extreme droughts (Anderegg et al., 2019; Anderegg et al., 2018). The reason is that different species can have different drought tolerances, and although some species may die during prolonged droughts, other species are able to persist. For example, Coates et al. (2015) used hyperspectral and thermal observations to study the impacts of the 2013-2014 drought on Southern California chaparral species and established that

Ceanothus were the least well-adapted species, while deeply rooted species were the least impacted.

Drought impacts on an ecosystems carbon cycle can be examined via multi-sensor observations of vegetation greenness and other biophysical variables. Due to the complexity of drought response and the inherent uncertainties in any single remote sensing product, attempting to answer the same question using different remote sensing observations and platforms has the potential to produce conflicting (and sometime erroneous) conclusions. For example, a number of early studies exploring the impacts of the 2005 Amazon drought used observed LAI and spectral reflectance data in the near infrared region (NIR) to suggest that severe drought caused reductions in LAI and carbon storage (Brando et al., 2008). Another study based on MODIS EVI proposed a finding that the Amazon forest showed a greening-up, even during a severe drought, and indicated that Amazon forests might be more resilient to severe drought than previously thought (Saleska et al., 2007). However, a later study by Samanta et al. (2010) indicated that Amazon forests did not green up during 2005 drought. In another later study exploring the Amazon's response to drought, Liu et al. (2018c) used AMSR-E derived vegetation optical depth (VOD), MODIS based LAI, EVI, aerosol optical depth (AOD) and cloud optical thickness (COT), CERES derived photosynthetically active radiation (PAR), GRACE based terrestrial water storage (TWS), and AIRS based surface skin temperature, air temperature and relative humidity data. Multiple lines of evidence from the change of VOD, LAI, and EVI indicated that during the early drought stage, sufficient soil moisture enhanced leaf development and ecosystem photosynthesis, while prolonged intense drought in the dry season negatively impacted forest growth (Liu et al., 2018c). The divergent results highlight the challenges in using single sensor observations that cannot always resolve the inherent uncertainties of complex

563 interactions (Asner and Alencar, 2010) and the importance of exploiting multiple lines of
564 evidence.

565 Indeed, multi-sensor observation strategies allow for the introduction of alternative and
566 complementary sources of information to help disentangle complex phenomena. For example,
567 SIF has been used to provide insight beyond more standard greenness approaches, with a number
568 of studies exploring its potential for drought impact monitoring (Sun et al., 2015; Yoshida et al.,
569 2015). Other studies have evaluated the SIF sensitivity to drought under various conditions. For
570 example, Liu et al. (2018b) showed that SIF is better than NDVI for early drought detection,
571 although NDVI remains useful in reflecting long lasting droughts. Multi-sensor observations
572 have also been used to examine drought impact on carbon uptake. Wigneron et al. (2020) used
573 MODIS based EVI and GOME-2 based SIF data to test the robustness of spatial patterns of
574 anomalies in aboveground biomass carbon (AGC) to indicate that tropical forests did not recover
575 from the 2015–2016 El Niño event. Other studies have employed multi-platform and multi-
576 sensor approaches. For example, Zhou et al. (2014) conducted a comprehensive evaluation of
577 the impacts of chronic drought on the Congo rainforest, using multi-sensor satellite products of
578 EVI, VOD, backscatter anomaly, photosynthetically active radiation (PAR), terrestrial water
579 storage (TWS), aerosol optical thickness (AOD), cloud optical thickness (COT), and land surface
580 temperature (LST) to show the widespread decline of Congo rainforest greenness due to the
581 long-term drying trend over the past decade. In another case, Wang et al. (2016a) used MODIS
582 LST, NDVI, fire count, fire radiative power, fire density, atmospheric water vapor, cloud
583 fraction, and TRMM accumulated rainfall to study the characteristics of the 2012 Central Plains
584 drought. Li et al. (2019) used MODIS NDVI, EVI, and GIMMS NDVI3g to provide robust
585 analysis of the impact of the 2009/2010 South China drought on vegetation growth and terrestrial

586 carbon balance. Park et al. (2020) used multi-sensor based Scaled Drought Condition Index
587 (SDCI) and Evaporative Stress Index (ESI) to explore the influence of El Nino-Southern
588 Oscillation (ENSO) on East African drought during rainy seasons. More recently, a study from
589 Jiao et al. (2020) used multiple sensors to examine the drought responses of biophysical
590 variables including fraction of absorbed photosynthetic active radiation (fPAR), canopy density,
591 photosynthetic vegetation cover, and aboveground biomass carbon, with all showing increased
592 sensitivity during Australia's millennium drought.

593 **3.2 Monitoring land-atmospheric feedbacks mechanisms**

594 Land–atmospheric feedbacks play an important role in water and carbon cycles during droughts
595 (Baldocchi et al., 2001; Roundy and Santanello, 2017). It is generally acknowledged that severe
596 droughts dry out soils and vegetation and reduce land evaporation, hence making the near-
597 surface air even drier, which may in turn decrease the likelihood of rainfall and further
598 exacerbate the occurrence of droughts (Roundy et al., 2014; Seneviratne et al., 2010; Zaitchik et
599 al., 2013). However, our knowledge of how droughts start and evolve, and how climate change
600 will affect their occurrence, remains incomplete (Miralles et al., 2019). There has been a strong
601 focus on climate modeling of large scale land–atmospheric feedback during droughts over the
602 last decade (Fischer et al., 2007; Stegehuis et al., 2015). One particular challenge of these studies
603 is the degree of variability in modeling the strength of the land-atmosphere coupling, which has a
604 strong impact on accurately forecasting and predicting climate extremes such as drought. Multi-
605 sensor remote sensing provides large-scale observational variables and parameters for land–
606 atmospheric feedbacks that can be used to reduce such uncertainties. For example, evaporation is
607 a key linking mechanism in land–atmosphere feedback studies and is a direct modulator of
608 climates trends and hydro-meteorological extremes through a series of feedbacks acting on air

609 temperature, precipitation, cloud cover, and photosynthesis (Douville et al., 2013; Miralles et al.,
610 2014; Seneviratne et al., 2006; Teuling et al., 2010). To date, global climate model based land
611 evaporation estimates remain unreliable (Dolman et al., 2014; Jimenez et al., 2011; Mueller et al.,
612 2011; Wang and Dickinson, 2012), making their use as diagnostic tools challenging. On the
613 other hand, multi-sensor based remote sensing approaches have been applied to provide more
614 realistic observationally-based estimates of evaporation (Martens et al., 2017), offering the
615 capacity for new insights into land-atmosphere behavior. A number of recent efforts have
616 evaluated multi-sensor remote sensing data in land-atmosphere coupling studies exploring
617 drought, and illustrated their considerable advantages (Hao et al., 2018b; Roundy and Santanello,
618 2017; Santanello Jr et al., 2018). Further work is required, but with the advent of an increasing
619 number of sensors and complementary platforms, additional insights and clearer identification of
620 patterns and trends in land–atmospheric feedbacks during droughts are anticipated.

621 **3.3 Exploring drought-induced tree mortality**

622 Severe drought acts not only to reduce vegetation productivity, but may also cause large-scale
623 plant mortality (Allen et al., 2015). Myriad studies on the mechanisms of plant response to
624 drought may not necessarily involve drought-induced tree mortality, which can also lead to
625 ecosystem recession and impact ecosystem water and carbon cycles (Huang et al., 2019; Piao et
626 al., 2019). Hydraulic failure and carbon starvation have been widely reported as two
627 nonexclusive mechanisms of drought-induced tree mortality (Anderegg et al., 2012; Hartmann,
628 2015; McDowell et al., 2018). Hydraulic failure occurs when drought-caused embolisms block
629 xylem cells and impair hydraulic transport systems (Huang et al., 2019). Carbon starvation
630 occurs when isohydric species close stomata to avoid excessive water loss. However, the closure
631 of stomata not only avoids water loss, but also forgoes access to atmospheric carbon dioxide, and

632 if respiratory consumption of the needed carbon exceeds stored resources, tree mortality may
633 occur (Adams et al., 2010). One of the main approaches for studying drought-induced tree
634 mortality is to estimate the plant water content (Huang et al., 2019; McDowell and Sevanto,
635 2010). Historically, satellite multispectral sensors were used to extract vegetation water status
636 (Kokaly et al., 2009; Zarco-Tejada et al., 2003). However, it is challenging to accurately extract
637 canopy water content for forest regions via traditional remote sensing observations, due to the
638 cloud cover and the fact that those observations primarily sense the top of the canopy only
639 (Asner et al., 2004; Konings et al., 2019). New large-scale datasets such as satellite-based VOD
640 are emerging (Rao et al., 2019) and can be used as indicators of drought-induced tree mortality.
641 Currently, high spatial resolution images are the most commonly used datasets to monitor
642 regional forest health (Huang et al., 2019). Recent integrations of multi-sensor airborne
643 hyperspectral and LiDAR have shown potential to provide accurate estimation of leaf water
644 content at regional scales. Stovall et al. (2019) combined airborne LiDAR and optical data to
645 track tree mortality rates and indicated that higher trees are more vulnerable than small trees
646 during extreme droughts. Zhu et al. (2019) combined LiDAR and hyperspectral data using
647 radiative transfer models (RTM) and an invertible forest reflectance model to address the effects
648 of canopy structure variation, and to estimate leaf water content over the Bavarian Forest
649 National Park in southeastern Germany. Related studies show that the integrated use of airborne
650 high-fidelity imaging spectroscopy (HiFIS) and LiDAR scanning improves the ability for
651 monitoring forest canopy water content (Shugart et al., 2015). The integrated application of
652 HiFIS and LiDAR provides three dimensional forest measurements and allows for excluding
653 non-forest covers, such as grass, bare ground and rock cover, which could affect the analysis
654 (Asner et al., 2007). Recently, Asner et al. (2016) provided a multi-sensor remote sensing canopy

water content observation strategy by fusing HiFIS and LiDAR with Landsat data, and illustrated a progressive canopy water loss across California forests during 2012-2015 that allowed improved predictions of tree mortality. Research from Brodrick and Asner (2017) used a similar strategy to monitor progressive canopy water content loss to tree mortality during the 2015-2016 Sierra Nevada mountain drought in California. The NASA Global Ecosystem Dynamics Investigation (GEDI) LiDAR, which launched to the International Space Station in December 2018 and has been collecting observation data since March 2019 (Hancock et al., 2019), serves as an exploratory mission to study tree mortality from canopy structure measurements (Qi et al., 2019). The combination of simulated GEDI with other measurements such as TerraSAR-X add-on for Digital Elevation Measurement (Tandem-X) InSAR (Lee et al., 2018; Qi and Dubayah, 2016) and Ice, cloud, and land elevation satellite-2 (ICESat-2) and NASA-ISRO Synthetic Aperture Radar (NISAR) (Fatoyinbo et al., 2017; Silva et al., 2018) highlights the potential of mapping tree health from a forest structure perspective.

3.4 Investigating drought-related ecosystem fires

Drought may cause an increase in the frequency of ecosystem fires, which is an important factor in the decline of ecosystem carbon uptake (Brando et al., 2014). Remote sensing may be the only technology that can provide for drought-induced wildfire observations at regional to global scales. Thermal remote sensing has been widely used to establish the location of active fires (Asner and Alencar, 2010). However, due to the spatial resolution and observation period, it is challenging for single sensor based remote sensing observations to provide long time period and accurate detection, and thus integrated use of multi-sensor remote sensing observations has often been applied to improve long-term fire detection. Van Der Werf et al. (2004) combined multi-sensor satellite observations of global fire activity over the 1997 to 2001 El Niño/La Niña period

678 from TRMM, European Remote Sensing Satellite–Along Track Scanning Radiometer (ERS-
679 ATSR), and MODIS Terra satellite sensors, showing increases in tropical fires during droughts
680 associated with ENSO. For datasets related to global fires, the widely used Global Fire
681 Emissions Database (GFED) was developed based on the integrated use of fire products from
682 Terra and Aqua MODIS and the ATSR-based World Fire Atlas, to provide global daily, monthly,
683 and annual burned area from 1995 onwards (Giglio et al., 2013). A particular challenge for single
684 sensor observations for drought-induced fire studies is to detect ground-covering fires from space,
685 since a moist and highly foliated canopy could block the fire signal on the ground (Goetz et al.,
686 2006; Meng et al., 2017; Yi et al., 2013). Integrated use of multi-sensor satellite products by
687 overlying fire detections (e.g., TRMM fire detections) on satellite deforestation maps (e.g.,
688 multi-sensor remote sensing based Brazilian National Institute of Space Research, INPE
689 deforestation map) was shown to provide good indications for detecting ground-covering fire
690 signals above the moist and highly foliated canopy (Asner and Alencar, 2010; Asner et al., 2005).
691 In addition, the integrated use of multi-sensor observations from airborne imaging spectroscopy
692 and LiDAR was tested to quantify the post-fire forest recovery rate and demonstrated that
693 integrated multi-sensor observation can separate canopy recovery from understory recovery,
694 providing reliable information of post-fire forest recovery over large scales (Meng et al., 2018).
695 Apart from reliable detection of burned areas, satellite estimation of fire-induced CO and CO_2
696 emission measurements are useful for understanding the impact of drought-induced wildfire to
697 ecosystem carbon and water cycles. The combination of satellite-derived burned areas with
698 atmospheric CO and CO_2 measurements is likely to assist in quantitatively estimating the impact
699 of drought-induced fires on ecosystem carbon cycle (Piao et al., 2019).

700 Live fuel moisture content (LFMC), which is defined as the mass of water contained
701 within vegetation in relation to the total dry mass, is another primary variable that has been
702 widely used in drought-related fire prediction and fire risk models (Yebra et al., 2013). Remote
703 sensing observations could provide the opportunity of frequent monitoring of LFMC over large
704 areas. However, there are a number of challenges for existing estimations of LFMC from remote
705 sensing, with the retrieval of LFMC influenced by multiple factors. The physical basis for remote
706 sensing based estimation of LFMC is via the different absorption and reflectance of radiation in
707 NIR and SWIR spectral regions due to water content within vegetation (Tucker, 1980). As such,
708 traditional indices such as the Normalized Difference Infrared Index (NDII) (Hardisky et al.,
709 1983), Normalized Difference Water Index (NDWI) (Gao, 1996), and Normalized Difference
710 Vegetation Index (NDVI) (Rouse et al., 1974) have all been applied to estimate the LFMC over
711 large regions. Indices based on the optical and thermal bands provide important information on
712 LFMC estimation via vegetation vigor and water content. However, observations from optical
713 regions are limited in their ability to provide accurate estimation of LFMC. First, the optical and
714 thermal wavelengths are affected by contamination such as clouds, smoke, and atmospheric
715 aerosols. In addition, remote sensing based retrieval of LFMC are affected by confounding
716 factors such as canopy structure and biomass (Yebra et al., 2013). Apart from observations
717 across optical wavelengths, signals from the microwave portion of the electromagnetic spectrum
718 have been explored as alternatives for monitoring LFMC (Fan et al., 2018) due to the advantage
719 that they can detect changes in canopy structure, biomass, soil and vegetation water content,
720 while being less sensitive to atmospheric and cloud contamination (Al-Yaari et al., 2016). As
721 such, exploiting multi-sensor remote sensing to estimate LFMC can offer multiple advantages.
722 First, the multi-sensor approach can provide insights into the many complementary sensitives to

723 needed parameters (such as vegetation water content, greenness, canopy structure) required by
724 LFMC retrievals. Second, multi-sensor observations alleviate individual limitations from any
725 specific sensor. Third, multi-sensor observations can provide high temporal and spatial LFMC
726 estimations needed for fire risk and prediction. One recent example of multi-sensor remote
727 sensing based LFMC estimation is the study of Rao et al. (2020), which presents an improved
728 LFMC estimation every 15 days at 250 m resolution.

729 **3.5 Identifying post-drought recovery and drought legacy effects**

730 Drought extremes not only have immediate impacts on ecosystem functioning, but can also
731 impart long-lasting lagged effects, hindering a comprehensive understanding of terrestrial
732 ecosystem response to drought (Anderegg et al., 2015). Our understanding of drought legacy is
733 challenged by the fact that such effects can be highly variable for species, ecosystems, climate
734 conditions, and can even have both positive or negative impacts on plants (Kannenberg et al.,
735 2020; Wu et al., 2018; Xu et al., 2010). A number of recent studies have examined drought
736 recovery and legacy effects from organism to ecosystem scales based on tree ring chronologies,
737 flux towers, and remote sensing datasets (Kannenberg et al., 2020). Compared with flux towers
738 and tree ring observations, remote sensing has been widely used for drought recovery and legacy
739 effects at both ecosystem and global scales due to the large spatial support scales (Schwalm et al.,
740 2017; Wu et al., 2018). However, due to the complexity of ecosystem drought legacy impacts
741 and difficulties in quantifying drought recovery time, large uncertainties still exist for regional to
742 global drought recovery and legacy effect studies (Liu et al., 2019a). Multi-sensor remote
743 sensing can provide drought identification from various aspects that enhance our understanding
744 of these drought recovery and legacy effects. For example, the recovery of photosynthetic
745 capacity can be relatively quick and can be quantified via greenness indices. The combination of

optical/NIR sensors with airborne SAR may be useful for quantifying the canopy recovery, and the recovery of below canopy structure in forests can be extracted by LiDAR and microwave imagery, since they are sensitive to properties of the below canopy (Frolking et al., 2009). Characterization of drought recovery legacy effects can be further complicated, since droughts not only have legacy impacts on vegetation structure and photosynthetic capacity, but also on other aspects such as phenology. Recent studies such as Peng et al. (2019), indicated that drought has both lagged and cumulative impacts on autumn leaf senescence over the Northern Hemisphere. Yuan et al. (2020) found that pre-season drought could impact vegetation spring phenology. Buermann et al. (2018) highlighted the growing adverse negative lagged effect of spring warmth on northern hemisphere vegetation productivity. Shi et al. (2019) examined the legacy effects of precipitation and evaporation changes during the 2005 Amazon drought based on multiple satellite observations of precipitation and evaporation, and found that the drought effect induced evaporation reductions, triggering a delay of the wet season onset. Gonçalves et al. (2020) confirmed the 2005 Amazon drought legacy effects on tropical forest leaf phenology using multi-sensor observations of near-surface and satellite remote sensing. Overall, like many of the other aspects explored herein, observations from multi-sensor remote sensing provide multiple lines of evidence for the study of drought recovery and legacy effects.

3.6 Capturing and monitoring flash droughts

While drought is generally described as a slowly evolving phenomena (Wilhite et al., 2007), recent rapidly developing drought events (e.g., 2012 United States summer drought) have caused a growing interests in the study of so-called “flash drought” within the scientific community. Flash droughts are generally defined as a short term but severe drought with rapid onset and evolving processes (Ford and Labosier, 2017; Otkin et al., 2018; Senay et al., 2008). Flash

droughts can cause severe environmental and agricultural impacts in a short time period, and since they have a sudden onset and rapid intensification, can bring particular challenges for drought monitoring, forecasting, and mitigation (Christian et al., 2019; Ford and Labosier, 2017; Pendergrass et al., 2020). The identification of flash droughts is of great importance. Distinct from conventional droughts, high evaporation rates are usually found before their developments (Chen et al., 2019). Thus, remote sensing based evaporation products have been used to identify these events. A good example is the satellite-based evaporative stress index (ESI) (Anderson et al., 2016), which was shown to provide early warning of flash drought impacts on agricultural system. More recently, a series of ESI based drought indices, including the rapid change index (RCI) (Otkin et al., 2014), evaporative demand drought index (EDDI) (Hobbins et al., 2016), and standardized evaporative stress ratio (SESR) (Christian et al., 2019) were developed for flash drought characterization. Studies have also identified that other drought characteristics, such as rapid declines in precipitation, soil moisture and abnormally high temperature, were also important to identify flash droughts (Haile et al., 2020; Mo and Lettenmaier, 2015). The combined information of soil moisture, temperature, and evaporation was applied by Wang et al. (2016b) to identify a flash drought in China and indicated an increasing number of flash droughts from 1979 to 2010 due to global warming. Other multi-sensor remote sensing based integrated drought indices have also been developed for characterizing flash droughts. For example, the Quick Drought Response Index (QuickDRI) (Svoboda et al., 2017), which integrated satellite based ESI and Standardized Vegetation Index (SVI) (Peters et al., 2002) with climate indicators such as SPEI, Standardized Precipitation Index (SPI), and North American Land Data Assimilation System-2 (NLDAS-2) based soil moisture data, was developed to characterize shorter-term and quickly evolving droughts. Although a relatively new drought classification, the

characteristics of flash droughts, including sudden onset, rapid evolution, and severe impacts on ecosystem (Mo and Lettenmaier, 2015; Yuan et al., 2019b), make their further study and description of considerable importance. Multi-sensor remote sensing observations provide a unique platform for providing the needed high spatial-temporal resolutions for flash droughts, and will undoubtedly play a key role in enhancing aspects of their description.

3.7 Drought trends under climate change

There is ongoing scientific debate on whether climate change will cause global drying, and how drought will evolve under such conditions (Vicente‐Serrano et al., 2020). Climate metrics such as the self-calibrated Palmer drought severity index (scPDSI), PDSI with potential evapotranspiration estimated using the Penman-Monteith equation (sc_PDSI_pm) and climate model predictions themselves, suggest a likely strong increase of drought severity and severe drought impacts in the future (Baig et al., 2020; Dai, 2013; Trenberth et al., 2014; Xu et al., 2019). However, other research providing a retrospective assessment has indicated that relatively little change in global drought has occurred over the past 60 years (Sheffield et al., 2012). Some climate model simulations suggest that global drying may not happen due to predicted increases in runoff, and that the effect of an increase in evaporation could be offset by a decrease in evaporation driven by increased surface resistance responding to elevated CO_2 (Berg and Sheffield, 2019; Yang et al., 2019). However, other studies have indicated that vegetation will reduce future runoff despite the increased surface resistance to evaporation, due to increasing canopy water demands and freshwater availability that will be reduced due to climate change (Mankin et al., 2019).

Studies of global drought trends based on multi-sensor remote sensing can provide a range of informative metrics, including their use as signals to evaluate climate model output.

Damberg and AghaKouchak (2014) indicated that there was no significant drying trend from 1980-2012 by combining multi-sensor satellite precipitation data from the Global Precipitation Climatology Project (GPCP), Multi-satellite Precipitation Analysis – Near Real Time (TMPA) (TMPA-RT), and Precipitation Estimation from Remotely Sensed Information using Artificial Neural Networks (PERSIANN) satellite data. Dorigo et al. (2012) analyzed the global trend in a multi-sensor soil moisture product from 1988-2010, which indicated a strong tendency towards drying soil moisture. They also found that the drying soil moisture trends were not consistent with the patterns of precipitation, which indicated that even though precipitation is the main driver of variations in soil moisture, other factors such as evaporation, soil type, and vegetation cannot be neglected (Dorigo et al., 2012). Recently, a drought trend study over the United States using multi-sensor satellite data from the Scanning Multi-channel Microwave Radiometer (SMMR), the Special Sensor Microwave Imager (SSM/I), the Advanced Scatterometer (ASCAT), MODIS, AMSR-E, AMSR-2, and SMOS and SMAP soil moisture data (Kumar et al., 2019), indicated a trend of longer and more severe droughts over parts of the Western United States. Despite these and related studies, the complexity of spatially heterogeneous trends, limited coverage periods of individual satellite data, and inherent uncertainties from single satellite datasets, all suggest that further integration of multi-sensor observations are needed to disentangle the development of global scale drought trends under a changing climate.

4. Recent modeling advances for developing integrated multi-sensor remote sensing drought indices

Drought indices integrate various drought related variables (e.g., precipitation, temperature, evaporation, snow, groundwater, and soil moisture) to monitor and assess physical characteristics such as onset, duration, severity, and spatial extent (Hao and Singh, 2015; Hayes et al., 2007;

838 Mishra and Singh, 2010). Drought has multiple aspects, examples of which might be high
839 temperature with low soil moisture along with declines in plant function: all of which can occur
840 independently or simultaneously (Wilhite, 2000). As such, a single drought index that is
841 developed based on one particular element is unlikely to capture many complex processes and
842 diverse impacts (Jiao et al., 2019b). For example, a precipitation based drought index may fail to
843 characterize plant water stress linked to rising vapor pressure deficit (VPD) during a heat wave,
844 since drought can have independent impacts on both meteorology and plant function (Novick et
845 al., 2016; Stocker et al., 2018). Not surprisingly, multivariate drought indices developed using
846 multiple models and indices, and including drought properties such as severity and duration or
847 alternative data sources, have proved to better and more comprehensively characterize drought
848 than any single index (Andreadis et al., 2005; Hao and AghaKouchak, 2013; Touma et al., 2015).
849
850 Many studies have sought to develop multivariate indices by combining observations
851 from *in-situ* observations, gridded climate datasets, and single-sensor remote sensing dataset
852 (AghaKouchak, 2015; Brown et al., 2008; Hao and AghaKouchak, 2013; Hao and AghaKouchak,
853 2014; Huang et al., 2016; Kao and Govindaraju, 2010; Niemeyer, 2008; Sepulcre-Canto et al.,
854 2012; Tabari et al., 2013; Vasiliades et al., 2011; Waseem et al., 2015; Westra et al., 2007).
855 Integrated drought indices that only exploit multi-sensor remote sensing data is an emerging
856 research topic (AghaKouchak et al., 2015; West et al., 2019). While a number of multi-variable
857 drought indices have been developed, few have been applied using multi-sensor remote sensing
858 observations. One reason is the relatively short length of satellite records (AghaKouchak et al.,
859 2015; Lettenmaier et al., 2015). On the other hand, numerous recent efforts have been made
860 towards integrated multi-sensor drought indices based on multiple models. These multi-sensor

based drought indices can generally be divided into three categories: data-driven models, water balance models, and process-based models. Here we provide an overview of these and related studies, with **Table 2** providing a summary of some of the core research efforts.

4.1 Data-driven models

Data-driven models are the most commonly used models for multi-sensor integrated drought indices development. The primary strategy of data-driven models is combining the input variables using a set of statistical models, and often with limited knowledge about the physical mechanism of the system (Solomatine, 2002). Some recent examples can be summarized through their use of simple linear combination models, principal component analysis (PCA) combination models, machine learning models, and fuzzy weighting models, and all of which are described below.

4.1.1 Simple linear combination models

One of the most commonly employed statistical models to integrate drought variables from multiple sensors is simple linear combination. Several multi-sensor integrated drought indices were developed by linearly assigning weights to single drought variables. For example, the Microwave Integrated Drought Index (MIDI) (Zhang and Jia, 2013) combines the Soil Moisture Condition Index (SMCI) from AMSR-E data, the Precipitation Condition Index (PCI) using TRMM, and the Temperature Condition Index (TCI) from MODIS LST data. Similarly, the Scaled Drought Condition Index (SDCI), Optimized Meteorological Drought Index (OMDI) and Optimized Vegetation Drought Index (OVDI) integrate drought variables including precipitation, soil moisture, vegetation indices, and LST, also using linear weighting (Hao et al., 2015; Rhee et al., 2010). The advantage of simple linear combination models is that they are relatively easy to calculate and straightforward to implement. While they have been shown to present good

884 performance for drought monitoring at local scales (Zhang et al., 2017a), simple linear
885 combination model have limitations for large scale implementation. For instance, they often
886 assume that the sub-areas of a particular study area contribute the same weight for a particular
887 single variable. Also, assigned weights for each drought variable are likely to vary in different
888 climate regions, and may thus lead to poor performance when applied to diverse climate
889 conditions (Hao and Singh, 2015; Jiao et al., 2019b).

890 **4.1.2 Principal component analysis models**

891 Since the basic purpose of principal component analysis (PCA) is to distill a large number of
892 variables into a new data set with low dimensionality (Wold et al., 1987), it is no surprise that it
893 has been commonly used to develop drought indices from multi-variables. Numerous studies
894 have developed integrated drought indices based on site observation data using PCA (Arabzadeh
895 et al., 2016; Barua et al., 2011; Bazrafshan et al., 2014; Bazrafshan et al., 2015; Keyantash and
896 Dracup, 2004; Liu et al., 2019b), while others have also applied PCA to develop multi-sensor
897 remote sensing based drought indices. Du et al. (2013) developed a synthesized drought index
898 (SDI) using PCA to combine vegetation, temperature, and precipitation variables from TRMM
899 and MODIS data. PCA has also been combined with other models to developed integrated multi-
900 sensor based drought indices. For example, PCA was applied with a partial least squares
901 regression (PLSR) model to assess agricultural drought in East Africa (Agutu et al., 2017), while
902 Jiao et al. (2019c) used PCA with a geographically weighted regression (GWR) model to
903 developed a station-enabled Geographically Independent Integrated Drought Index
904 (GIIDI_station), which showed good performance under diverse climate regions. One of the
905 main limitations of the PCA based indices is the linearity assumption of the input variables and
906 the assumption that the maximum information of the input variables is oriented along the

907 direction of maximum variance of data transformation (Wold et al., 1987). However, the
908 Gaussianity of input variables and their linearity may not always be met in reality (Azmi et al.,
909 2016; Hao and Singh, 2015). To avoid those limitations, it may be helpful to explore other
910 feature extraction models, such as kernel entropy component analysis (KECA), kernel PCA, and
911 sparse KPCA (SKPCA), which have recently been developed as modified PCA models to
912 overcome the linearity assumption (Rajsekhar et al., 2015; Waseem et al., 2015).

913 **4.1.3 Machine learning models**

914 Big data is a term that is well associated with the collection and storage of vast amounts of
915 remote sensing data (Ma et al., 2015). Recent studies have used multiple machine learning
916 algorithms to incorporate multi-sensor remote sensing information for drought assessment at
917 regional scales. Park et al. (2016) monitored meteorological and agricultural drought in the arid
918 region of Arizona and New Mexico and the humid region of North Carolina and South Carolina
919 by incorporating sixteen remote sensing based drought factors from MODIS and TRMM satellite
920 sensors using random forest, boosted regression trees, and Cubist models. Similarly, Park et al.
921 (2017) developed the High resolution Soil Moisture Drought Index (HSMDI) for meteorological,
922 agricultural, and hydrological droughts over the Korean peninsula using Random Forest, Cubist,
923 and Boosted Regression Trees based on AMSR-E soil moisture, MODIS NDVI, ET, albedo and
924 LST data. Han et al. (2019) developed the combined drought monitoring index (CDMI) in
925 Shaanxi province in China by combining MODIS LST, NDVI and ET data with TRMM
926 precipitation data using a random forest model. Feng et al. (2019) adopted a bias-corrected
927 random forest, support vector machine, and multi-layer perceptron neural network using thirty
928 remotely sensed drought factors from the TRMM and the MODIS satellite sensors to reproduce
929 drought conditions in South-Eastern Australia. Their results indicated strong correlation between

930 machine learning based satellite drought observations and ground-based crop yield and drought
931 indices (Feng et al., 2019). Similar to the development of the Vegetation Drought Response
932 Index (VegDRI) (Brown et al., 2008), Wu et al. (2015) developed an Integrated Surface Drought
933 Index (ISDI) using a classification and regression tree (CART) approach based on MODIS
934 NDVI and LST and climate data in China. Rahmati et al. (2020) mapped agricultural drought
935 using CART, boosted regression trees (BRT), random forests (RF), multivariate adaptive
936 regression splines (MARS), flexible discriminant analysis (FDA) and support vector machines
937 (SVM) in the south-east region of Queensland Australia. Son et al. (2021) developed a Vector
938 Projection Index of Drought (VPID) based on Vector Projection Analysis (VPA) by integrating
939 site observation based SPI, SPEI, PDSI, and Z-index with multi-sensor satellite based
940 precipitation, evaporation, vegetation, and soil moisture data.

941 Of course, the advantage of using machine learning models for integrated drought
942 monitoring is that such models are good at handling multi-dimensional and multi-variable data in
943 different environments and without human intervention (Lary et al., 2016; Ma et al., 2015).
944 However, machine learning based integrated drought monitoring relies heavily on the selection
945 of training data. They also require massive data sets to train on, and are highly susceptible to
946 errors that often exist when a training set is not representative of diverse environmental
947 conditions or climate states (Ali et al., 2015; Lary et al., 2016). The transferability issue means
948 that for regions with limited available ground observation, machine learning models may have
949 limited application. Whether this can be overcome with the availability of spatiotemporal remote
950 sensing records is a topic of ongoing research.

4.1.4 Fuzzy weighting models

The lack of a widely accepted drought definition is one of the primary obstacles to effectively investigate drought events (Lloyd-Hughes, 2014). The majority of research divides drought into different types: meteorological, agricultural, hydrological, and social-economic (Wilhite and Glantz, 1985). However, the boundaries separating these drought conceptions are vague, and it is difficult to set a specific boundary for drought impacts of certain rates to meteorology, agriculture, hydrology, and social-economic (Pesti et al., 1996). To address these concerns, fuzzy analysis methods have been used to monitor drought based on multi-sensor remote sensing observations. Alizadeh and Nikoo (2018) applied an Ordered Weighted Averaged approach using multi-sensor data from CHOMPS, GPCP, CMAP, PERSIANN-CD, TRMM, GLDAS-2, MERRA-2, with results indicating that the model significantly improved drought estimation. Jiao et al. (2019b) proposed a framework for developing a Geographically Independent Integrated Drought Index (GIIDI), based on local OWA models and multi-sensor data from MODIS NDVI, TRMM precipitation, and AMSR-E soil moisture data, which could have applicability for various climate regions. Huang et al. (2015) developed the Integrated Drought Index (IDI), combining meteorological, hydrological, and agricultural factors across the Yellow River basin in North China based on variable fuzzy set theory. In another approach, Nasab et al. (2018) developed a Fuzzy Integrated Drought Index (FIDI) based on an entropy weighting fuzzy model, utilizing the Anomaly Percentage Index of precipitation, runoff, actual ET, and soil moisture in the Neyshabour basin, Iran. Fuzzy weighting models are widely used in the multi-criteria decision making field (Aruldoss et al., 2013). These models aim to address the uncertainty and interior related relationship between the single variables (Jiang and Eastman, 2000; Yager, 1996). However, the limitation of weights determined by fuzzy weighting algorithms are not

974 straightforward and the development of fuzzy models is often tedious (Grabisch, 1996;
975 Reshmidevi et al., 2009; Velasquez and Hester, 2013). In addition, other studies argue that the
976 min-max ordered rule of fuzzy weighting models may not be able to best reflect the conjunctive
977 and disjunctive reasoning, and integrated fuzzy models should be applied in the real world
978 (Simić et al., 2017).

979 **4.2 Process based models**

980 Drought is a complex natural hazard with gradual dynamic transition between drought and non-
981 drought conditions (Rulinda et al., 2012). Different stages of drought, cumulative impacts, or
982 even different drought timings, can all affect the environment differently (Fukai and Cooper,
983 1995; Pasho et al., 2011; Peng et al., 2019; Sippel et al., 2018). Drought monitoring indices that
984 are based on the evolution of the drought process may better reflect the dynamic of drought
985 severity changes. Zhang et al. (2017b) recently proposed an Evolution Process-based Multi-
986 sensor Collaboration (EPMC) framework and developed the Process-based Accumulated
987 Drought Index (PADI) based on multi-sensor data that included GPCC precipitation data,
988 GLDAS soil moisture data, and AVHRR NDVI data. The various phases of drought latency,
989 onset, development, and recovery were quantified differently by the authors, and their results
990 showed that the process based drought monitoring framework could provide robust multi-sensor
991 remote sensing based agricultural drought monitoring analysis (Zhang et al., 2017b).

992 **4.3 Water balance models**

993 While there are various definitions of drought and different classification types, it is a well-
994 accepted theme that drought is a condition of insufficient water to meet needs (Redmond, 2002).
995 A range of water budget based drought indices have been developed and widely used for a
996 number of decades. One of the most widely employed indices is the PDSI, which is based on a

997 water balance model of soil moisture supply and water demand of evaporation, with the input
998 data including precipitation, temperature, and soil water content (Palmer, 1965). The Palmer
999 Hydrologic Drought Index (PHDI) (Karl et al., 1987) and Surface Water Supply Index (SWSI)
1000 (Shafer and Dezman, 1982) are other examples of widely used water budget models for
1001 monitoring drought. Similarly, the standardized precipitation evapotranspiration index (SPEI)
1002 monitors drought by estimating the water balance using the difference between precipitation and
1003 PET (Vicente-Serrano et al., 2010). Remote sensing based water balance models offer an
1004 important means to monitor droughts, since they are able to map the physical mechanisms
1005 behind ecosystem water supply and demand at regional to global scales, and previous multi-
1006 sensor remote sensing studies have shown the potential for the estimation of regional terrestrial
1007 water cycles (Pan et al., 2008; Sheffield et al., 2009). In related efforts, Zhang et al. (2019b)
1008 developed the Standardized Moisture Anomaly Index (SZI) using a water-energy balance
1009 approach that combined remote sensing estimates of precipitation, potential evaporation, and
1010 runoff. A global evaluation of SZI indicated that it has strong performance for drought
1011 monitoring in different climate regions and could physically capture surface water-energy
1012 balances (Zhang et al., 2019a). However, while effectively capturing natural water balance
1013 behavior is important, there are other elements that effect budget calculations. Anthropogenic
1014 effects associated with land use change, irrigation efficiency, and rapid increases in population
1015 can all effect the physical consistency of hydrological processes, yet the vast majority of water
1016 budget based drought indices fail to consider these (Mukherjee et al., 2018). If truly integrated
1017 approaches are to be developed, incorporation of the anthropogenic effects into multi-sensor
1018 drought index approaches are required.

5. Challenges

While there is general recognition that multi-sensor remote sensing presents a great opportunity for integrated drought studies, it remains very much in its infancy, and multiple challenges to effective implementation remain. Foremost amongst these is the inconsistency between variables derived from different sensors, which may lead to uncertainties in multi-sensor integration efforts. Differences arising from spatial, temporal, and spectral resolution, spatial extent, overpass time, and length of record all contribute to complicate data synthesis. The recent advances in new satellite data acquisition such as SIF serve as a notable example of the future need for more focused efforts on data fusion techniques. For example, current methods for observing SIF require the exploitation of different features of the electromagnetic spectrum, resulting in SIF observation across different platforms that are specific to different wavelengths (Cendrero-Mateo et al., 2019; Mohammed et al., 2019), challenging data fusion techniques. Additionally, SIF varies considerably with time, and thus moving from instantaneous to daily SIF, together with any associated data fusion across platforms, may prove to be challenging. For SIF, as well as other land surface variables including LST, observations at different times of the day are critically needed (e.g., OCO3 and ECOSTRESS), as are geostationary missions (e.g., GeoCarb and GOES). However, this is not a problem unique to drought studies. Indeed, it is an area that is being actively explored in topics such as the development of remote sensing based climate records and essential climate variables (Hamaguchi et al., 2018; McCabe et al., 2008; Zhang, 2010), so much can be learned from these efforts. Related advances in data fusion and merging approaches provide a natural pathway for progress in this area.

Another challenge relates to what precisely "drought severity" might mean for multi-sensor remote sensing based drought indices. Drought indices such as SPI and SPEI (McKee et

al., 1993; Vicente-Serrano et al., 2010) define severity using drought frequency based on probability distributions (e.g., gamma and log-logistic distribution) from long-term observations. Other indices arbitrarily define drought severity based on the abnormal degree of the current state compared with an historical calendric "normal" status over a period of years (without calculating probability distributions). For instance, the vegetation condition index (VCI), temperature condition index (TCI), and precipitation condition index (PCI) are widely used in multi-sensor integrated drought index models, and are all based on the similar standardization method, i.e., $\frac{V_{i,j}-V_{i,min}}{V_{i,max}-V_{i,min}}$, where $V_{i,j}$ represents the monthly PCI, TCI, and VCI for month i in year j, and $V_{i,max}$ and $V_{i,min}$ denote the multiyear minimum and maximum PCI, TCI, and VCI, respectively, for month i in year j. The arbitrary definition that VCI is less than 0.1 for extreme drought may not be accurate. In addition, the same value of VCI, TCI, and PCI may not reflect the same degree of drought anomaly, since the relationships between vegetation indices, soil moisture, precipitation and temperature are rarely linear. The problem is also exacerbated by the fact that remote sensing observations do not generally extend beyond 5-10 years of continuous observation (sometimes, much less), meaning that anomaly records must be developed based on multi-sensor integrations, which can introduce biases. Future multi-sensor remote sensing drought monitoring studies may need to develop more objective, rather than arbitrary, definitions of drought severity.

In addition, there is still a lack of cause-and-effect based drought monitoring studies. Most current multi-sensor drought monitoring strategies are based on data-driven models, which lack mechanisms detailing how droughts impact ecosystems. For example, few current drought indices can directly reflect vegetation water stress. Due to the complexity of the Earth system, there are multiple factors other than drought (e.g., insects, disease, and hail damage) that could

cause ecosystem anomalies (Brown et al., 2008). The compound feature of hazards (e.g., drought and heat waves) makes cause-and-effect studies even more needed in order to explicitly understand drought characteristics and their underlying features (AghaKouchak et al., 2020; Hao et al., 2018a; Zscheischler et al., 2020). Causal models based on multi-sensor remote sensing data are needed to augment widely used linear correlation studies, since correlations do not impart causality.

6. A road map for the future

6.1 Integrating new and emerging sensors/platforms into physical models

With an increasing level of both remote sensing and *in-situ* data availability (McCabe et al., 2017b), there are new and emerging opportunities that have the potential to further advance multi-sensor remote sensing drought characterization. Physical models that integrate such data are likely to improve our understanding of the complex mechanisms of immediate and lagged drought effects across spatial, spectral and temporal scales. For example, hyperspectral remote sensing presents an opportunity to more directly detect the plant physiological and biochemical changes under water stress than traditional broad optical wavelengths. Hyperspectral remote sensing missions under operation or development, including the Hyperspectral Imager Suite (HISUI) (Iwasaki et al., 2011), High-resolution Temperature and Spectral Emissivity Mapping (HiTeSEM) (Udelhoven et al., 2017), hyperspectral infrared imager (HyspIRI) (Abrams and Hook, 2013), Environmental Mapping And Analysis Program (EnMAP) (Kaufmann et al., 2008), Precursore Iperspettrale Della Missione Applicativa (PRISMA) (Labate et al., 2009), and FLuorescence EXplorer (FLEX) (Mohammed et al., 2019) offer possibilities for regional to global hyperspectral remote sensing for future multi-sensor drought studies.

As noted in Section 2.7, hyperspectral based approaches offer just one of the pathways for improving our drought observation capacity. Leveraging LiDAR observations also provides opportunities for future multi-sensor drought characterization since LiDAR data have advantages in mapping canopy vertical change and 3-D reproduction. The LiDAR on the Global Ecosystem Dynamics Investigation (GEDI) instrument (Coyle et al., 2015), provides global LiDAR data availability that is suitable for use in multi-sensor drought studies. Recent studies synergizing LiDAR with hyperspectral data at regional scales have shown potential for multi-sensor early warning of plant water stress (Degerickx et al., 2018; Sankey et al., 2018; Shivers et al., 2019; Sobejano-Paz et al., 2020).

Drought studies based on Unmanned Aerial Systems (UAS) also present new opportunities to improve our understanding of the underlying mechanisms and processes, as well as in advancing our ability to proactively monitor and predict drought events as they occur and develop. The benefits of incorporating UAS observations into multi-sensor drought studies include the relatively low costs, sensor agnostic capability, and the on-demand capability combined with high spatial resolution. These UAS-based advantages make it possible to detect local-to-regional scale water deficit before they become widespread and this is particularly useful for agriculture and forest management applications.

Likewise, leveraging geostationary satellite systems provides another opportunity for advancing multi-sensor drought studies. The high temporal frequency of geostationary satellites affords a unique platform for monitoring rapid-development in drought response (i.e., flash droughts) (Otkin et al., 2013). Studies indicate that geostationary satellite systems such as Himawari-8/9 showed great insight for agricultural drought monitoring (e.g., Hu et al. 2020b). The upcoming Geostationary Carbon Cycle Observatory (GeoCarb) mission will provide CO_2

and SIF measurement at higher than 3-hour temporal resolution (Moore III et al., 2018), which makes it possible to study large-scale drought impacts on carbon cycles and vegetation photosynthesis at sub-daily scales. Fusing geostationary satellite observations with polar-orbiting sensors would provide a pathway towards high spatiotemporal resolution of drought related variables, following similar efforts with evaporation and land surface temperature (Smith et al., 2019b).

6.2 Establishing the spatiotemporal resolution needed to deliver effective drought monitoring

Effective drought monitoring often require both high spatial and temporal resolution observations (e.g., flash drought and vegetation photosynthesis dynamics under droughts). Over the last decade, there have been a number of major international efforts to address both model development and inter-comparison activities across various hydrological variables (McCabe et al., 2016; Miralles et al., 2016) with an assessment of both limitations and advantages forming key areas of focus (Chen et al., 2014; Liou and Kar, 2014; Yang et al., 2015; Zhang et al., 2016b). One of the major limitations identified in many of those studies relates to the trade-off between spatial resolution and temporal frequency: that is, a compromise is routinely required, whereby you can have one, but only at the expense of the other (McCabe et al., 2017a). Observations with both high spatial resolution and temporal frequency are urgently needed for a range of applications. Emerging constellations of space-based data offer an enhanced observation capacity for drought characterization that can overcome such constraints. For example, the application of constellations such as ASCAT onboard the Metop-A, B, and C platforms can provide sub-daily microwave soil moisture products, which are capable of leading the next generation high spatiotemporal soil moisture observation (Peng et al., 2020). New opportunities

1133 such as the Multi-Radar Multi-Sensor (MRMS) system, which integrated about 180 operational
1134 radars to provide a three dimensional radar mosaic with both high spatial (1km) and high
1135 temporal (2 min) resolution is another good example, although the current MRMS only covers
1136 the United States and Canada (Zhang et al., 2016a). New approaches exploiting constellations of
1137 small CubeSat systems, provide an enhanced capacity that also collapses this spatiotemporal
1138 constraint (Aragon et al., 2018). **Figure 2** shows an example of the competing resolution of
1139 CubeSat imagery alongside Sentinel-2 and Landsat, illustrating the spatial advantage. With its
1140 fleet of more than 170 CubeSats, Planet is able to provide multi-spectral reflectance data at ~3 m
1141 spatial and daily resolution (Houborg and McCabe, 2018b). While presenting clear
1142 spatiotemporal advantages, the commercial-off-the-shelf sensors have lower radiometric quality
1143 compared to more traditional satellite platforms (McCabe et al., 2017a; Ryu et al., 2019).
1144 However, sensor harmonization strategies, such as the CubeSat Enabled Spatiotemporal
1145 Enhancement Method (CESTEM) of Houborg and McCabe (2018a) have overcome such sensor
1146 limitations, offering an analysis ready product comparable to Sentinel-2 and Landsat systems.
1147 The approach has enabled atmospherically corrected high-spatiotemporal surface reflectance and
1148 vegetation variables such as LAI and NDVI to be developed at unprecedented resolutions
1149 (Houborg and McCabe, 2018a; Houborg and McCabe, 2018b). Such sensor fusion and
1150 harmonization approaches offer much potential for drought studies and characterization in the
1151 future. Geostationary platforms such as the Geostationary Operational Environmental Satellites
1152 (GOES) also provide multi-sensor data opportunities for drought characterizations. The GOES
1153 series of satellites (R, S, T, and U), which cover the western hemisphere (from the west coast of
1154 Africa to New Zealand) could provide both multichannel passive imaging and near-infrared
1155 optical observations with up to 1-min imagery research request (Goodman, 2020), making it

possible for nearly continuous monitoring of drought impacts (e.g., vegetation photosynthesis) for the covered regions.

[Insert Figure 2 here]

6.3 Retrospective assessment of long-term multi-sensor remote sensing record

As noted in section 2, a suite of regional to global satellite observations of drought-related variables have been collected from as early as the 1970s. However, those satellite observations for drought-related variables often suffer from various uncertainties (e.g., data contamination, sensor degradation, and model retrieval uncertainties) and result in data inconsistency (e.g., GPP inconsistency revealed by O'Sullivan et al. (2020)). Such uncertainties may cause overestimation or underestimation of drought impacts (Stocker et al., 2019; Zhang et al., 2017c). Retrospective assessment of long-term remote sensing record for multi-sensor drought studies provide opportunities to more accurately evaluate the drought impacts. In addition, the development of multi-sensor remote sensing data fusion models has the potential to curate long-term remote sensing records with high spatiotemporal resolutions. Retrospective drought studies based on the long-term multi-sensor remote sensing record present opportunities to better evaluate the underlying drought mechanisms and improving modelling accuracy.

6.4 Exploiting the new multi-sensor capabilities based on existing sensors

Together with new and emerging sensors/platforms (as noted in section 6.1), exploring novel applications of existing sensor records also provides new opportunities for drought characterization. Many remote sensing sensors originally designed for a specific application have been subsequently utilized to produce new capabilities (so-called "signals of opportunity" as in McCabe et al. (2017b)). For example, several atmospheric satellite sensors have been shown to have the capability to measure vegetation SIF (Mohammed et al., 2019). Likewise, many of the

existing microwave vegetation water content observations are a by-product of microwave soil moisture retrievals, with a good example of the development of a long-term global multi-sensor based VOD dataset (Liu et al. 2011). Likewise, other existing sensors also provide opportunities for new multi-sensor capabilities of drought studies. The Global Navigation Satellite System (GNSS), which was originally designed for navigation and communication, has illustrated the potential for constellation-based precipitation monitoring and prediction (Asgarimehr et al., 2018; Cardellach et al., 2019), with further studies exploring its capability for soil moisture retrieval. Leveraging our existing networks of both *in-situ* and space-based sensors for such purposes offers further data and needed insights to better understand drought.

6.5 Identifying the capabilities of drought prediction and early warning through target experiments

Drought prediction and early warning are effective approaches to mitigate drought impacts. Current drought prediction methods can be generally divided into statistical drought prediction models, dynamical drought prediction approaches, or combinations of both (Hao et al., 2017). All need multi-sensor remote sensing observations to improve large-scale drought prediction reliabilities. For the statistical approaches, predictions require a long-term observation records to build reliable historical relationship between predictors and observations. The dynamical method is based on climate/hydrologic models linked to the physical processes of land-atmospheric interactions (Hao et al., 2018b). Multi-sensor remote sensing can not only provide long-term record for statistical prediction but also multiple components of observations for the land, ocean, and atmospheric for better simulation of description of linked processes. Target experiments can be performed to evaluate drought prediction models, providing evidence-based assessment of drought-climate links and confidence in the chosen prediction approach. Indeed, establishing the

physical basis and/or empirical links between drought extent, severity and duration and changing features of the climate system remains one of the outstanding questions where multi-sensor methods may play an important role. Moreover, identifying the interlinked variables responsible for driving the initiation, prolongation and completion of drought events may only be possible through such studies.

6.6 Identifying the missing elements in drought assessment

Given the complexity of the various direct and indirect elements of drought impacts, drought characterization demands interdisciplinary expertise. Over the decades of remote sensing-based drought studies, some drought features have been relatively well studied, while other elements remain less studied or even missing. For example, much of our understanding of remote sensing-based drought characterization has focused on natural ecosystems, while drought impacts on social-hydrological systems (Sivapalan et al., 2012) remain less studied. Multi-sensor drought studies that include human interventions (e.g., irrigation and water pumping to mitigate agriculture drought) will provide opportunities to physically improve water budget models for multi-sensor drought monitoring, providing capacity to not just monitor, but also manage the water resource systems under drought conditions. Incorporating key aspects of socio-economic impacts, social response, needs of governments, business/insurance companies is a much needed future objective to translate the science into actionable response.

6.7 Leveraging new strategies of data processing

Relative to single sensor drought studies, one of the obvious differences for multi-sensor drought studies is the increased data volumes with high dimensionality and metadata. Indeed, this is true not just for future multi-sensor drought studies, but for future remote sensing applications in general, due to the exponential increases in remote sensing data being produced. The data

volume and velocity comes with particular challenges for data storage, management, transfer and processing. In this regard, efficient drought identification and characterization strategies that significantly reduce data redundancy and improve generality and transferability are critically needed. Leveraging high-performance computing (HPC) and cloud-based resources (e.g., Google Earth Engine, GEE) provide an obvious path to deal with the such storage and processing challenges.

7. Conclusions

Leveraging advances in our capacity to monitor and characterize droughts not only improves our understanding of their initiation and development, but also provides a pathway for improved conceptual understanding and physical description of the underlying process. Likewise, enhancing our understanding and description of key vegetation-water-carbon interactions, which is becoming increasingly viable due to opportunities provided by multi-sensor remote sensing, may not only drive these needed improvements, but also provide a path towards developing mechanism-based drought prediction. Exploiting the expanding array of remote sensing platforms, whether *in-situ*, airborne or satellite-based, and recognizing that each system provides independent insights and supporting evidence, is an obvious way to drive these needed developments in process understanding. The expanding capacity of multi-sensor observations also increases our capacity to develop the mechanistic descriptions required to deliver improved drought monitoring, early warning and prediction systems in the coming decades. Such knowledge will be central to disentangling the complex interplays that define the drought process. Importantly, these knowledge advances are not just key to resolving the influences and fingerprints of climate change on drought occurrence, severity and duration, but also in

developing the socio-economic links that are desperately needed for drought monitoring and prediction systems that can be applied towards planning, management and mitigation efforts.

Acknowledgments: We greatly appreciate the comparison of Landsat 8, Sentinel-2A and Planet images of an agricultural area along the Nile River near Banha, Egypt provided by Bruno Aragon (King Abdullah University of Science and Technology, KAUST). We acknowledge support from the Division of Earth Sciences of National Science Foundation (NSF EAR - 1554894) and from the Agriculture and Food Research Initiative program (201767013 - 26191) of the USDA National Institute of Food and Agriculture. Matthew McCabe is supported by funding from KAUST. We would like to thank the editors and three anonymous reviewers for their constructive comments and suggestions, which we believe significantly strengthened our manuscript.

References

Aasen, H. et al., 2019. Sun-induced chlorophyll fluorescence II: Review of passive measurement setups, protocols, and their application at the leaf to canopy level. Remote Sensing, 11(8): 927.

Abdelwahab, S., Hamdaoui, B., Guizani, M. and Rayes, A., 2014. Enabling smart cloud services through remote sensing: An internet of everything enabler. IEEE Internet of Things Journal, 1(3): 276-288.

Abrams, M.J. and Hook, S.J., 2013. NASA's hyperspectral infrared imager (HyspIRI), Thermal infrared remote sensing. Springer, pp. 117-130.

Adams, H.D. et al., 2010. Climate-induced tree mortality: Earth system consequences. Eos, Transactions American Geophysical Union, 91(17): 153-154.

Adler, R.F. et al., 2003. The version-2 global precipitation climatology project (GPCP) monthly precipitation analysis (1979–present). Journal of Hydrometeorology, 4(6): 1147-1167.

AghaKouchak, A., 2015. A multivariate approach for persistence-based drought prediction: Application to the 2010–2011 East Africa drought, Journal of Hydrology, pp. 127-135.

AghaKouchak, A. et al., 2020. Climate Extremes and Compound Hazards in a Warming World. Annual Review of Earth and Planetary Sciences, 48.

AghaKouchak, A. et al., 2015. Remote sensing of drought: Progress, challenges and opportunities. Reviews of Geophysics, 53(2): 452-480.

Agutu, N. et al., 2017. Assessing multi-satellite remote sensing, reanalysis, and land surface models' products in characterizing agricultural drought in East Africa. Remote Sensing of Environment, 194: 287-302.

1283 Al-Yaari, A. et al., 2016. Testing regression equations to derive long-term global soil moisture
1284 datasets from passive microwave observations. Remote Sensing of Environment, 180:
1285 453-464.
1286 Ali, I., Greifeneder, F., Stamenkovic, J., Neumann, M. and Notarnicola, C., 2015. Review of
1287 machine learning approaches for biomass and soil moisture retrievals from remote
1288 sensing data. Remote Sensing, 7(12): 16398-16421.
1289 Alizadeh, M.R. and Nikoo, M.R., 2018. A fusion-based methodology for meteorological drought
1290 estimation using remote sensing data. Remote Sensing of Environment, 211: 229-247.
1291 Allen, C.D., Breshears, D.D. and McDowell, N.G., 2015. On underestimation of global
1292 vulnerability to tree mortality and forest die-off from hotter drought in the Anthropocene.
1293 Ecosphere, 6(8): 1-55.
1294 Allen, C.D. et al., 2010. A global overview of drought and heat-induced tree mortality reveals
1295 emerging climate change risks for forests. Forest Ecology and Management, 259(4): 660-
1296 684.
1297 Allen, R.G., Tasumi, M. and Trezza, R., 2007. Satellite-based energy balance for mapping
1298 evapotranspiration with internalized calibration (METRIC)—Model. Journal of Irrigation
1299 and Drainage Engineering, 133(4): 380-394.
1300 Anderegg, W.R., 2015. Spatial and temporal variation in plant hydraulic traits and their
1301 relevance for climate change impacts on vegetation. New Phytologist, 205(3): 1008-1014.
1302 Anderegg, W.R., Anderegg, L.D., Kerr, K.L. and Trugman, A.T., 2019. Widespread drought-
1303 induced tree mortality at dry range edges indicates that climate stress exceeds species'
1304 compensating mechanisms. Global Change Biology, 25(11): 3793-3802.

1305 Anderegg, W.R., Berry, J.A. and Field, C.B., 2012. Linking definitions, mechanisms, and
1306 modeling of drought-induced tree death. Trends in Plant Science, 17(12): 693-700.
1307 Anderegg, W.R. et al., 2018. Hydraulic diversity of forests regulates ecosystem resilience during
1308 drought. Nature, 561(7724): 538.
1309 Anderegg, W.R. et al., 2015. Pervasive drought legacies in forest ecosystems and their
1310 implications for carbon cycle models. Science, 349(6247): 528-532.
1311 Anderson, M. et al., 2008. A thermal-based remote sensing technique for routine mapping of
1312 land-surface carbon, water and energy fluxes from field to regional scales. Remote
1313 Sensing of Environment, 112(12): 4227-4241.
1314 Anderson, M.C. et al., 2011a. Evaluation of drought indices based on thermal remote sensing of
1315 evapotranspiration over the continental United States. Journal of Climate, 24(8): 2025-
1316 2044.
1317 Anderson, M.C. et al., 2011b. Mapping daily evapotranspiration at field to continental scales
1318 using geostationary and polar orbiting satellite imagery. Hydrology and Earth System
1319 Sciences, 15: 223-239.
1320 Anderson, M.C. et al., 2016. The Evaporative Stress Index as an indicator of agricultural drought
1321 in Brazil: An assessment based on crop yield impacts. Remote Sensing of Environment,
1322 174: 82-99.
1323 Andreadis, K.M., Clark, E.A., Wood, A.W., Hamlet, A.F. and Lettenmaier, D.P., 2005.
1324 Twentieth-century drought in the conterminous United States. Journal of
1325 Hydrometeorology, 6(6): 985-1001.

1326 Arabzadeh, R., Kholoosi, M.M. and Bazrafshan, J., 2016. Regional hydrological drought
1327 monitoring using principal components analysis. Journal of Irrigation and Drainage
1328 Engineering, 142(1): 04015029.
1329 Aragon, B., Houborg, R., Tu, K., Fisher, J.B. and McCabe, M., 2018. CubeSats enable high
1330 spatiotemporal retrievals of crop-water use for precision agriculture. Remote Sensing,
1331 10(12): 1867.
1332 Aruldoss, M., Lakshmi, T.M. and Venkatesan, V.P., 2013. A survey on multi criteria decision
1333 making methods and its applications. American Journal of Information Systems, 1(1): 31-
1334 43.
1335 Asgarimehr, M., Zavorotny, V., Wickert, J. and Reich, S., 2018. Can GNSS reflectometry detect
1336 precipitation over oceans? Geophysical Research Letters, 45(22): 12,585-12,592.
1337 Ashouri, H. et al., 2015. PERSIANN-CDR: Daily precipitation climate data record from
1338 multisatellite observations for hydrological and climate studies. Bulletin of the American
1339 Meteorological Society, 96(1): 69-83.
1340 Asner, G.P. and Alencar, A., 2010. Drought impacts on the Amazon forest: the remote sensing
1341 perspective. New phytologist, 187(3): 569-578.
1342 Asner, G.P. et al., 2016. Progressive forest canopy water loss during the 2012–2015 California
1343 drought. Proceedings of the National Academy of Sciences, 113(2): E249-E255.
1344 Asner, G.P. et al., 2005. Selective logging in the Brazilian Amazon. Science, 310(5747): 480-
1345 482.
1346 Asner, G.P. et al., 2007. Carnegie airborne observatory: in-flight fusion of hyperspectral imaging
1347 and waveform light detection and ranging for three-dimensional studies of ecosystems.
1348 Journal of Applied Remote Sensing, 1(1): 013536.

1349 Asner, G.P., Nepstad, D., Cardinot, G. and Ray, D., 2004. Drought stress and carbon uptake in
1350 an Amazon forest measured with spaceborne imaging spectroscopy. Proceedings of the
1351 National Academy of Sciences, 101(16): 6039-6044.
1352 Aubrecht, D.M. et al., 2016. Continuous, long-term, high-frequency thermal imaging of
1353 vegetation: Uncertainties and recommended best practices. Agricultural and forest
1354 Meteorology, 228: 315-326.
1355 Azmi, M., Rüdiger, C. and Walker, J.P., 2016. A data fusion-based drought index. Water
1356 Resources Research, 52(3): 2222-2239.
1357 Badgley, G., Field, C.B. and Berry, J.A., 2017. Canopy near-infrared reflectance and terrestrial
1358 photosynthesis. Science Advances, 3(3): e1602244.
1359 Baig, M.H.A. et al., 2020. Assessing Meteorological and Agricultural Drought in Chitral Kabul
1360 River Basin Using Multiple Drought Indices. Remote Sensing, 12(9): 1417.
1361 Baldocchi, D. et al., 2001. FLUXNET: A new tool to study the temporal and spatial variability of
1362 ecosystem-scale carbon dioxide, water vapor, and energy flux densities. Bulletin of the
1363 American Meteorological Society, 82(11): 2415-2434.
1364 Bandopadhyay, S., Rastogi, A. and Juszczak, R., 2020. Review of Top-of-Canopy Sun-Induced
1365 Fluorescence (SIF) studies from ground, UAV, airborne to spaceborne observations.
1366 Sensors, 20(4): 1144.
1367 Bannari, A., Morin, D., Bonn, F. and Huete, A., 1995. A review of vegetation indices. Remote
1368 Sensing Reviews, 13(1-2): 95-120.
1369 Barua, S., Ng, A. and Perera, B., 2011. Comparative evaluation of drought indexes: case study
1370 on the Yarra River catchment in Australia. Journal of Water Resources Planning and
1371 Management, 137(2): 215-226.

1372 Bazrafshan, J., Hejabi, S. and Rahimi, J., 2014. Drought monitoring using the multivariate
1373 standardized precipitation index (MSPI). Water Resources Management, 28(4): 1045-
1374 1060.
1375 Bazrafshan, J., Nadi, M. and Ghorbani, K., 2015. Comparison of empirical copula-based joint
1376 deficit index (JDI) and multivariate standardized precipitation index (MSPI) for drought
1377 monitoring in Iran. Water Resources Management, 29(6): 2027-2044.
1378 Beck, H.E. et al., 2011. Global evaluation of four AVHRR–NDVI data sets: Intercomparison and
1379 assessment against Landsat imagery. Remote Sensing of Environment, 115(10): 2547-
1380 2563.
1381 Beck, H.E. et al., 2020. Global-scale evaluation of 22 precipitation datasets using gauge
1382 observations and hydrological modeling, Satellite Precipitation Measurement. Springer,
1383 pp. 625-653.
1384 Beck, H.E. et al., 2019. MSWEP V2 global 3-hourly 0.1 precipitation: methodology and
1385 quantitative assessment. Bulletin of the American Meteorological Society, 100(3): 473-
1386 500.
1387 Beck, P.S., Atzberger, C., Høgda, K.A., Johansen, B. and Skidmore, A.K., 2006. Improved
1388 monitoring of vegetation dynamics at very high latitudes: A new method using MODIS
1389 NDVI. Remote Sensing of Environment, 100(3): 321-334.
1390 Bell, J.W., Amelung, F., Ferretti, A., Bianchi, M. and Novali, F., 2008. Permanent scatterer
1391 InSAR reveals seasonal and long-term aquifer-system response to groundwater pumping
1392 and artificial recharge. Water Resources Research, 44(2).
1393 Berg, A. and Sheffield, J., 2019. Historic and projected changes in coupling between soil
1394 moisture and evapotranspiration (ET) in CMIP5 models confounded by the role of

different ET components. Journal of Geophysical Research: Atmospheres, 124(11): 5791-5806.

Bhanja, S.N., Mukherjee, A., Saha, D., Velicogna, I. and Famiglietti, J.S., 2016. Validation of GRACE based groundwater storage anomaly using in-situ groundwater level measurements in India. Journal of Hydrology, 543: 729-738.

Bolten, J.D., Crow, W.T., Zhan, X., Jackson, T.J. and Reynolds, C.A., 2009. Evaluating the utility of remotely sensed soil moisture retrievals for operational agricultural drought monitoring. IEEE Journal of Selected Topics in Applied Earth Observations and Remote Sensing, 3(1): 57-66.

Brando, P.M. et al., 2014. Abrupt increases in Amazonian tree mortality due to drought–fire interactions. Proceedings of the National Academy of Sciences, 111(17): 6347-6352.

Brando, P.M. et al., 2008. Drought effects on litterfall, wood production and belowground carbon cycling in an Amazon forest: results of a throughfall reduction experiment. Philosophical Transactions of the Royal Society B: Biological Sciences, 363(1498): 1839-1848.

Brocca, L. et al., 2011. Soil moisture estimation through ASCAT and AMSR-E sensors: An intercomparison and validation study across Europe. Remote Sensing of Environment, 115(12): 3390-3408.

Brodrick, P., Anderegg, L. and Asner, G., 2019. Forest drought resistance at large geographic scales. Geophysical Research Letters, 46(5): 2752-2760.

Brodrick, P. and Asner, G., 2017. Remotely sensed predictors of conifer tree mortality during severe drought. Environmental Research Letters, 12(11): 115013.

1417 Brown, J.F., Wardlow, B.D., Tadesse, T., Hayes, M.J. and Reed, B.C., 2008. The Vegetation
1418 Drought Response Index (VegDRI): A new integrated approach for monitoring drought
1419 stress in vegetation. GIScience & Remote Sensing, 45(1): 16-46.
1420 Brown, R.D., Brasnett, B. and Robinson, D., 2003. Gridded North American monthly snow
1421 depth and snow water equivalent for GCM evaluation. Atmosphere-Ocean, 41(1): 1-14.
1422 Bruinsma, S., Lemoine, J.-M., Biancale, R. and Valès, N., 2010. CNES/GRGS 10-day gravity
1423 field models (release 2) and their evaluation. Advances in Space Research, 45(4): 587-
1424 601.
1425 Buermann, W. et al., 2018. Widespread seasonal compensation effects of spring warming on
1426 northern plant productivity. Nature, 562(7725): 110-114.
1427 Cardellach, E. et al., 2019. Sensing heavy precipitation with GNSS polarimetric radio
1428 occultations. Geophysical Research Letters, 46(2): 1024-1031.
1429 Castellazzi, P. et al., 2018. Quantitative mapping of groundwater depletion at the water
1430 management scale using a combined GRACE/InSAR approach. Remote Sensing of
1431 Environment, 205: 408-418.
1432 Castellazzi, P., Martel, R., Galloway, D.L., Longuevergne, L. and Rivera, A., 2016. Assessing
1433 groundwater depletion and dynamics using GRACE and InSAR: potential and limitations.
1434 Groundwater, 54(6): 768-780.
1435 Cendrero-Mateo, M.P. et al., 2019. Sun-induced chlorophyll fluorescence III: Benchmarking
1436 retrieval methods and sensor characteristics for proximal sensing. Remote Sensing, 11(8):
1437 962.
1438 Chang, A. and Rango, A., 2000. Algorithm theoretical basis document (ATBD) for the AMSR-E
1439 snow water equivalent algorithm. NASA/GSFC, Nov.

1440 Chang, Q. et al., 2019. Assessing consistency of spring phenology of snow-covered forests as
1441 estimated by vegetation indices, gross primary production, and solar-induced chlorophyll
1442 fluorescence. Agricultural and Forest Meteorology, 275: 305-316.
1443 Chang, Q. et al., 2020. Estimating site-specific optimum air temperature and assessing its effect
1444 on the photosynthesis of grasslands in mid-to high-latitudes. Environmental Research
1445 Letters, 15(3): 034064.
1446 Chen, J., Famigliett, J.S., Scanlon, B.R. and Rodell, M., 2016. Groundwater storage changes:
1447 present status from GRACE observations, Remote Sensing and Water Resources.
1448 Springer, pp. 207-227.
1449 Chen, J., Menges, C. and Leblanc, S., 2005. Global mapping of foliage clumping index using
1450 multi-angular satellite data. Remote Sensing of Environment, 97(4): 447-457.
1451 Chen, L.-C., Teo, T.-A., Shao, Y.-C., Lai, Y.-C. and Rau, J.-Y., 2004. Fusion of LIDAR data and
1452 optical imagery for building modeling. International Archives of Photogrammetry and
1453 Remote Sensing, 35(B4): 732-737.
1454 Chen, L.G. et al., 2019. Flash drought characteristics based on US Drought Monitor. Atmosphere,
1455 10(9): 498.
1456 Chen, T., Van der Werf, G., De Jeu, R., Wang, G. and Dolman, A., 2013. A global analysis of
1457 the impact of drought on net primary productivity. Hydrology and Earth System Sciences,
1458 17: 3885-3894.
1459 Chen, Y. et al., 2014. Comparison of satellite-based evapotranspiration models over terrestrial
1460 ecosystems in China. Remote Sensing of Environment, 140: 279-293.

1461 Christian, J.I. et al., 2019. A methodology for flash drought identification: Application of flash
1462 drought frequency across the United States. Journal of Hydrometeorology, 20(5): 833-
1463 846.
1464 Ciais, P. et al., 2005. Europe-wide reduction in primary productivity caused by the heat and
1465 drought in 2003. Nature, 437(7058): 529.
1466 Claverie, M. et al., 2018. The Harmonized Landsat and Sentinel-2 surface reflectance data set.
1467 Remote Sensing of Environment, 219: 145-161.
1468 Coates, A.R., Dennison, P.E., Roberts, D.A. and Roth, K.L., 2015. Monitoring the impacts of
1469 severe drought on southern California chaparral species using hyperspectral and thermal
1470 infrared imagery. Remote Sensing, 7(11): 14276-14291.
1471 Coyle, D.B., Stysley, P.R., Poulios, D., Clarke, G.B. and Kay, R.B., 2015. Laser transmitter
1472 development for NASA's Global Ecosystem Dynamics Investigation (GEDI) lidar, Lidar
1473 Remote Sensing for Environmental Monitoring XV. International Society for Optics and
1474 Photonics, pp. 961208.
1475 Crausbay, S.D. et al., 2017. Defining ecological drought for the twenty-first century. Bulletin of
1476 the American Meteorological Society, 98(12): 2543-2550.
1477 Dai, A., 2011. Drought under global warming: a review. Wiley Interdisciplinary Reviews:
1478 Climate Change, 2(1): 45-65.
1479 Dai, A., 2013. Increasing drought under global warming in observations and models. Nature
1480 Climate Change, 3(1): 52.
1481 Damberg, L. and AghaKouchak, A., 2014. Global trends and patterns of drought from space.
1482 Theoretical and Applied Climatology, 117(3-4): 441-448.

1483 Daryanto, S., Wang, L. and Jacinthe, P.-A., 2015. Global synthesis of drought effects on food
1484 legume production. PloS one, 10(6): e0127401.
1485 Daryanto, S., Wang, L. and Jacinthe, P.-A., 2016. Global synthesis of drought effects on maize
1486 and wheat production. PloS one, 11(5): e0156362.
1487 Das, N.N., Entekhabi, D. and Njoku, E.G., 2010. An algorithm for merging SMAP radiometer
1488 and radar data for high-resolution soil-moisture retrieval. IEEE Transactions on
1489 Geoscience and Remote Sensing, 49(5): 1504-1512.
1490 Dash, J. and Curran, P., 2007. Evaluation of the MERIS terrestrial chlorophyll index (MTCI).
1491 Advances in Space Research, 39(1): 100-104.
1492 De Moura, Y.M. et al., 2015. Seasonality and drought effects of Amazonian forests observed
1493 from multi-angle satellite data. Remote Sensing of Environment, 171: 278-290.
1494 Degerickx, J., Roberts, D.A., McFadden, J.P., Hermy, M. and Somers, B., 2018. Urban tree
1495 health assessment using airborne hyperspectral and LiDAR imagery. International
1496 Journal of Applied Earth Observation and Geoinformation, 73: 26-38.
1497 Derin, Y. and Yilmaz, K.K., 2014. Evaluation of multiple satellite-based precipitation products
1498 over complex topography. Journal of Hydrometeorology, 15(4): 1498-1516.
1499 Dolman, A.J., Miralles, D.G. and de Jeu, R.A., 2014. Fifty years since Monteith's 1965 seminal
1500 paper: the emergence of global ecohydrology. Ecohydrology, 7(3): 897-902.
1501 Donohue, I. et al., 2013. On the dimensionality of ecological stability. Ecology Letters, 16(4):
1502 421-429.
1503 Dorigo, W. et al., 2012. Evaluating global trends (1988–2010) in harmonized multi-satellite
1504 surface soil moisture. Geophysical Research Letters, 39(18).

1505 Dorigo, W. et al., 2017. ESA CCI Soil Moisture for improved Earth system understanding: State-
1506 of-the art and future directions. Remote Sensing of Environment, 203: 185-215.
1507 Douville, H., Ribes, A., Decharme, B., Alkama, R. and Sheffield, J., 2013. Anthropogenic
1508 influence on multidecadal changes in reconstructed global evapotranspiration. Nature
1509 Climate Change, 3(1): 59-62.
1510 Du, L. et al., 2013. A comprehensive drought monitoring method integrating MODIS and
1511 TRMM data. International Journal of Applied Earth Observation and Geoinformation, 23:
1512 245-253.
1513 Faghmous, J.H. and Kumar, V., 2014. A big data guide to understanding climate change: The
1514 case for theory-guided data science. Big Data, 2(3): 155-163.
1515 Fan, L. et al., 2018. Evaluation of microwave remote sensing for monitoring live fuel moisture
1516 content in the Mediterranean region. Remote Sensing of Environment, 205: 210-223.
1517 Fang, H., Baret, F., Plummer, S. and Schaepman-Strub, G., 2019. An overview of global leaf
1518 area index (LAI): Methods, products, validation, and applications. Reviews of
1519 Geophysics, 57(3): 739-799.
1520 Farquhar, G.D., von Caemmerer, S.v. and Berry, J.A., 1980. A biochemical model of
1521 photosynthetic CO 2 assimilation in leaves of C 3 species. Planta, 149(1): 78-90.
1522 Fatoyinbo, L. et al., 2017. The 2016 NASA AfriSAR campaign: Airborne SAR and Lidar
1523 measurements of tropical forest structure and biomass in support of future satellite
1524 missions, 2017 IEEE International Geoscience and Remote Sensing Symposium
1525 (IGARSS). IEEE, pp. 4286-4287.

1526 Feng, G., Masek, J., Schwaller, M. and Hall, F., 2006. On the blending of the Landsat and
1527 MODIS surface reflectance: predicting daily Landsat surface reflectance. IEEE
1528 Transactions on Geoscience and Remote Sensing, 44(8): 2207-2218.
1529 Feng, P., Wang, B., Li Liu, D. and Yu, Q., 2019. Machine learning-based integration of
1530 remotely-sensed drought factors can improve the estimation of agricultural drought in
1531 South-Eastern Australia. Agricultural Systems, 173: 303-316.
1532 Feng, W. et al., 2013. Evaluation of groundwater depletion in North China using the Gravity
1533 Recovery and Climate Experiment (GRACE) data and ground-based measurements.
1534 Water Resources Research, 49(4): 2110-2118.
1535 Fischer, E.M., Seneviratne, S.I., Lüthi, D. and Schär, C., 2007. Contribution of land-atmosphere
1536 coupling to recent European summer heat waves. Geophysical Research Letters, 34(6).
1537 Fisher, J.B. et al., 2020. ECOSTRESS: NASA's next generation mission to measure
1538 evapotranspiration from the International Space Station. Water Resources Research,
1539 56(4).
1540 Fisher, J.B. et al., 2017. The future of evapotranspiration: Global requirements for ecosystem
1541 functioning, carbon and climate feedbacks, agricultural management, and water resources.
1542 Water Resources Research, 53(4): 2618-2626.
1543 Flanner, M.G. and Zender, C.S., 2006. Linking snowpack microphysics and albedo evolution.
1544 Journal of Geophysical Research: Atmospheres, 111(D12).
1545 Flechtner, F. et al., 2016. What can be expected from the GRACE-FO laser ranging
1546 interferometer for Earth science applications?, Remote Sensing and Water Resources.
1547 Springer, pp. 263-280.

1548 Ford, T.W. and Labosier, C.F., 2017. Meteorological conditions associated with the onset of
1549 flash drought in the eastern United States. Agricultural and Forest Meteorology, 247:
1550 414-423.
1551 Fosu, B.O., Simon Wang, S.-Y. and Yoon, J.-H., 2016. The 2014/15 snowpack drought in
1552 Washington State and its climate forcing. Bulletin of the American Meteorological
1553 Society, 97(12): S19-S24.
1554 Frankenberg, C. et al., 2011. New global observations of the terrestrial carbon cycle from
1555 GOSAT: Patterns of plant fluorescence with gross primary productivity. Geophysical
1556 Research Letters, 38(17).
1557 Frankenberg, C. et al., 2014. Prospects for chlorophyll fluorescence remote sensing from the
1558 Orbiting Carbon Observatory-2. Remote Sensing of Environment, 147: 1-12.
1559 Frappart, F. and Ramillien, G., 2018. Monitoring groundwater storage changes using the Gravity
1560 Recovery and Climate Experiment (GRACE) satellite mission: A review. Remote
1561 Sensing, 10(6): 829.
1562 Frei, A. et al., 2012. A review of global satellite-derived snow products. Advances in Space
1563 Research, 50(8): 1007-1029.
1564 Frolking, S. et al., 2009. Forest disturbance and recovery: A general review in the context of
1565 spaceborne remote sensing of impacts on aboveground biomass and canopy structure.
1566 Journal of Geophysical Research: Biogeosciences, 114(G2).
1567 Fukai, S. and Cooper, M., 1995. Development of drought-resistant cultivars using
1568 physiomorphological traits in rice. Field Crops Research, 40(2): 67-86.

1569 Galloway, D.L. and Hoffmann, J., 2007. The application of satellite differential SAR
1570 interferometry-derived ground displacements in hydrogeology. Hydrogeology Journal,
1571 15(1): 133-154.
1572 Gao, B., 1996. NDWI—A normalized difference water index for remote sensing of vegetation
1573 liquid water from space. Remote Sensing of Environment, 58(3): 257-266.
1574 Garcia, R.A., Cabeza, M., Rahbek, C. and Araújo, M.B., 2014. Multiple dimensions of climate
1575 change and their implications for biodiversity. Science, 344(6183): 1247579.
1576 Gehne, M., Hamill, T.M., Kiladis, G.N. and Trenberth, K.E., 2016. Comparison of global
1577 precipitation estimates across a range of temporal and spatial scales. Journal of Climate,
1578 29(21): 7773-7795.
1579 Giglio, L., Randerson, J.T. and van der Werf, G.R., 2013. Analysis of daily, monthly, and annual
1580 burned area using the fourth-generation global fire emissions database (GFED4). Journal
1581 of Geophysical Research: Biogeosciences, 118(1): 317-328.
1582 Godfray, H.C.J. et al., 2010. Food security: the challenge of feeding 9 billion people. Science,
1583 327(5967): 812-818.
1584 Goetz, S.J., Fiske, G.J. and Bunn, A.G., 2006. Using satellite time-series data sets to analyze fire
1585 disturbance and forest recovery across Canada. Remote Sensing of Environment, 101(3):
1586 352-365.
1587 Gonçalves, N.B. et al., 2020. Both near-surface and satellite remote sensing confirm drought
1588 legacy effect on tropical forest leaf phenology after 2015/2016 ENSO drought. Remote
1589 Sensing of Environment, 237: 111489.
1590 Goodman, S.J., 2020. GOES-R series introduction, The GOES-R Series. Elsevier, pp. 1-3.

1591 Goward, S.N., Cruickshanks, G.D. and Hope, A.S., 1985. Observed relation between thermal
1592 emission and reflected spectral radiance of a complex vegetated landscape. Remote
1593 Sensing of Environment, 18(2): 137-146.
1594 Grabisch, M., 1996. The application of fuzzy integrals in multicriteria decision making.
1595 European Journal of Operational Research, 89(3): 445-456.
1596 Griffin-Nolan, R.J. et al., 2019. Shifts in plant functional composition following long-term
1597 drought in grasslands. Journal of Ecology, 107(5): 2133-2148.
1598 Gruber, A., Scanlon, T., van der Schalie, R., Wagner, W. and Dorigo, W., 2019. Evolution of the
1599 ESA CCI Soil Moisture climate data records and their underlying merging methodology.
1600 Earth System Science Data: 1-37.
1601 Guan, K. et al., 2016. Improving the monitoring of crop productivity using spaceborne solar-
1602 induced fluorescence. Global Change Biology, 22(2): 716-726.
1603 Guanter, L. et al., 2007. Estimation of solar-induced vegetation fluorescence from space
1604 measurements. Geophysical Research Letters, 34(8).
1605 Guanter, L. et al., 2014. Global and time-resolved monitoring of crop photosynthesis with
1606 chlorophyll fluorescence. Proceedings of the National Academy of Sciences, 111(14):
1607 E1327-E1333.
1608 Guo, H. et al., 2019. Determining variable weights for an Optimal Scaled Drought Condition
1609 Index (OSDCI): Evaluation in Central Asia. Remote Sensing of Environment, 231:
1610 111220.
1611 Gutman, G., 1999. On the monitoring of land surface temperatures with the NOAA/AVHRR:
1612 removing the effect of satellite orbit drift. International Journal of Remote Sensing,
1613 20(17): 3407-3413.

1614 Haile, G.G., Tang, Q., Li, W., Liu, X. and Zhang, X., 2020. Drought: Progress in broadening its
1615 understanding. Wiley Interdisciplinary Reviews: Water, 7(2): e1407.
1616 Hall, D.K., Riggs, G.A., Salomonson, V.V., DiGirolamo, N.E. and Bayr, K.J., 2002. MODIS
1617 snow-cover products. Remote Sensing of Environment, 83(1-2): 181-194.
1618 Hamaguchi, R., Fujita, A., Nemoto, K., Imaizumi, T. and Hikosaka, S., 2018. Effective use of
1619 dilated convolutions for segmenting small object instances in remote sensing imagery,
1620 2018 IEEE winter conference on applications of computer vision (WACV). IEEE, pp.
1621 1442-1450.
1622 Hamlet, A.F., Mote, P.W., Clark, M.P. and Lettenmaier, D.P., 2005. Effects of temperature and
1623 precipitation variability on snowpack trends in the western United States. Journal of
1624 Climate, 18(21): 4545-4561.
1625 Han, H., Bai, J., Yan, J., Yang, H. and Ma, G., 2019. A combined drought monitoring index
1626 based on multi-sensor remote sensing data and machine learning. Geocarto International:
1627 1-16.
1628 Hancock, S. et al., 2019. The GEDI simulator: A large-footprint waveform lidar simulator for
1629 calibration and validation of spaceborne missions. Earth and Space Science, 6(2): 294-
1630 310.
1631 Hao, C., Zhang, J. and Yao, F., 2015. Combination of multi-sensor remote sensing data for
1632 drought monitoring over Southwest China. International Journal of Applied Earth
1633 Observation and Geoinformation, 35: 270-283.
1634 Hao, Z. and AghaKouchak, A., 2013. Multivariate standardized drought index: a parametric
1635 multi-index model. Advances in Water Resources, 57: 12-18.

1636 Hao, Z. and AghaKouchak, A., 2014. A nonparametric multivariate multi-index drought
1637 monitoring framework. Journal of Hydrometeorology, 15(1): 89-101.
1638 Hao, Z. and Singh, V.P., 2015. Drought characterization from a multivariate perspective: A
1639 review. Journal of Hydrology, 527: 668-678.
1640 Hao, Z., Singh, V.P. and Hao, F., 2018a. Compound extremes in hydroclimatology: a review.
1641 Water, 10(6): 718.
1642 Hao, Z., Singh, V.P. and Xia, Y., 2018b. Seasonal drought prediction: advances, challenges, and
1643 future prospects. Reviews of Geophysics, 56(1): 108-141.
1644 Hao, Z., Yuan, X., Xia, Y., Hao, F. and Singh, V.P., 2017. An overview of drought monitoring
1645 and prediction systems at regional and global scales. Bulletin of the American
1646 Meteorological Society.
1647 Hardisky, M.A., Klemas, V. and Smart, R.M., 1983. The influence of soil salinity, growth form,
1648 and leaf moisture on the spectral radiance of Spartina alterniflora canopies.
1649 Photogrammetric Engineering & Remote Sensing, 49(1): 77-83.
1650 Hartmann, H., 2015. Carbon starvation during drought-induced tree mortality–are we chasing a
1651 myth?
1652 Hayes, M.J., Alvord, C. and Lowrey, J., 2007. Drought indices. Intermountain West Climate
1653 Summary, 3(6): 2-6.
1654 He, L. et al., 2019. Diverse photosynthetic capacity of global ecosystems mapped by satellite
1655 chlorophyll fluorescence measurements. Remote Sensing of Environment, 232: 111344.
1656 He, M. et al., 2016. Satellite detection of soil moisture related water stress impacts on ecosystem
1657 productivity using the MODIS-based photochemical reflectance index. Remote Sensing
1658 of Environment, 186: 173-183.

1659 Helfrich, S.R., McNamara, D., Ramsay, B.H., Baldwin, T. and Kasheta, T., 2007. Enhancements
1660 to, and forthcoming developments in the Interactive Multisensor Snow and Ice Mapping
1661 System (IMS). Hydrological Processes: An International Journal, 21(12): 1576-1586.
1662 Hobbins, M.T. et al., 2016. The evaporative demand drought index. Part I: Linking drought
1663 evolution to variations in evaporative demand. Journal of Hydrometeorology, 17(6):
1664 1745-1761.
1665 Hou, A.Y. et al., 2014. The global precipitation measurement mission. Bulletin of the American
1666 Meteorological Society, 95(5): 701-722.
1667 Hou, A.Y., Skofronick-Jackson, G., Kummerow, C.D. and Shepherd, J.M., 2008. Global
1668 precipitation measurement, Precipitation: Advances in Measurement, Estimation and
1669 Prediction. Springer, pp. 131-169.
1670 Houborg, R. and McCabe, M.F., 2018a. A cubesat enabled spatio-temporal enhancement method
1671 (cestem) utilizing planet, landsat and modis data. Remote Sensing of Environment, 209:
1672 211-226.
1673 Houborg, R. and McCabe, M.F., 2018b. Daily Retrieval of NDVI and LAI at 3 m Resolution via
1674 the Fusion of CubeSat, Landsat, and MODIS Data. Remote Sensing, 10(6): 890.
1675 Hu, T. et al., 2020a. Monitoring agricultural drought in Australia using MTSAT-2 land surface
1676 temperature retrievals. Remote Sensing of Environment, 236: 111419.
1677 Hu, T. et al., 2020b. On agricultural drought monitoring in Australia using Himawari-8
1678 geostationary thermal infrared observations. International Journal of Applied Earth
1679 Observation and Geoinformation, 91: 102153.

1680 Huang, C., Anderegg, W.R. and Asner, G.P., 2019. Remote sensing of forest die-off in the
1681 Anthropocene: From plant ecophysiology to canopy structure. Remote Sensing of
1682 Environment, 231: 111233.
1683 Huang, S., Chang, J., Leng, G. and Huang, Q., 2015. Integrated index for drought assessment
1684 based on variable fuzzy set theory: a case study in the Yellow River basin, China. Journal
1685 of Hydrology, 527: 608-618.
1686 Huang, S., Huang, Q., Leng, G. and Chang, J., 2016. A hybrid index for characterizing drought
1687 based on a nonparametric kernel estimator. Journal of Applied Meteorology and
1688 Climatology, 55(6): 1377-1389.
1689 Huete, A., 1988. Huete, AR A soil-adjusted vegetation index (SAVI). Remote Sensing of
1690 Environment. Remote Sensing of Environment, 25: 295-309.
1691 Huete, A. et al., 2002. Overview of the radiometric and biophysical performance of the MODIS
1692 vegetation indices. Remote Sensing of Environment, 83(1-2): 195-213.
1693 Huffman, G.J. et al., 2007. The TRMM multisatellite precipitation analysis (TMPA): Quasi-
1694 global, multiyear, combined-sensor precipitation estimates at fine scales. Journal of
1695 Hydrometeorology, 8(1): 38-55.
1696 Huntington, J.L. et al., 2017. Climate Engine: cloud computing and visualization of climate and
1697 remote sensing data for advanced natural resource monitoring and process understanding.
1698 Bulletin of the American Meteorological Society, 98(11): 2397-2410.
1699 Hwang, T. et al., 2017. Capturing species-level drought responses in a temperate deciduous
1700 forest using ratios of photochemical reflectance indices between sunlit and shaded
1701 canopies. Remote Sensing of Environment, 199: 350-359.

1702 Iwasaki, A., Ohgi, N., Tanii, J., Kawashima, T. and Inada, H., 2011. Hyperspectral Imager Suite
1703 (HISUI)-Japanese hyper-multi spectral radiometer, 2011 IEEE International Geoscience
1704 and Remote Sensing Symposium. IEEE, pp. 1025-1028.
1705 Jasechko, S. et al., 2013. Terrestrial water fluxes dominated by transpiration. Nature, 496(7445):
1706 347-350.
1707 Jiang, H. and Eastman, J.R., 2000. Application of fuzzy measures in multi-criteria evaluation in
1708 GIS. International Journal of Geographical Information Science, 14(2): 173-184.
1709 Jiao, T., Williams, C.A., Rogan, J., De Kauwe, M.G. and Medlyn, B.E., 2020. Drought impacts
1710 on Australian vegetation during the Millennium drought measured with multisource
1711 spaceborne remote sensing. Journal of Geophysical Research: Biogeosciences, 125(2).
1712 Jiao, W., Chang, Q. and Wang, L., 2019a. The Sensitivity of Satellite Solar-Induced Chlorophyll
1713 Fluorescence to Meteorological Drought. Earth's Future, 7(5): 558-573.
1714 Jiao, W., Tian, C., Chang, Q., Novick, K.A. and Wang, L., 2019b. A new multi-sensor integrated
1715 index for drought monitoring. Agricultural and Forest Meteorology, 268: 74-85.
1716 Jiao, W., Wang, L., Novick, K.A. and Chang, Q., 2019c. A new station-enabled multi-sensor
1717 integrated index for drought monitoring. Journal of Hydrology, 574: 169-180.
1718 Jiménez-Muñoz, J.C. and Sobrino, J.A., 2009. A single-channel algorithm for land-surface
1719 temperature retrieval from ASTER data. IEEE Geoscience and Remote Sensing Letters,
1720 7(1): 176-179.
1721 Jimenez, C. et al., 2011. Global intercomparison of 12 land surface heat flux estimates. Journal
1722 of Geophysical Research: Atmospheres, 116(D2).

1723 Joiner, J. et al., 2013. Global monitoring of terrestrial chlorophyll fluorescence from moderate
1724 spectral resolution near-infrared satellite measurements: Methodology, simulations, and
1725 application to GOME-2. Atmospheric Measurement Techniques, 6(2): 2803-2823.
1726 Joiner, J., Yoshida, Y., Vasilkov, A. and Middleton, E., 2011. First observations of global and
1727 seasonal terrestrial chlorophyll fluorescence from space. Biogeosciences, 8(3): 637-651.
1728 Joiner, J. et al., 2012. Filling-in of near-infrared solar lines by terrestrial fluorescence and other
1729 geophysical effects: simulations and space-based observations from SCIAMACHY and
1730 GOSAT. Atmospheric Measurement Techniques, 5(4): 809-829.
1731 Kalma, J.D., McVicar, T.R. and McCabe, M.F., 2008. Estimating land surface evaporation: A
1732 review of methods using remotely sensed surface temperature data. Surveys in
1733 Geophysics, 29(4-5): 421-469.
1734 Kalra, A., Piechota, T.C., Davies, R. and Tootle, G.A., 2008. Changes in US streamflow and
1735 western US snowpack. Journal of Hydrologic Engineering, 13(3): 156-163.
1736 Kannenberg, S.A., Schwalm, C.R. and Anderegg, W.R., 2020. Ghosts of the past: how drought
1737 legacy effects shape forest functioning and carbon cycling. Ecology Letters, 23(5): 891-
1738 901.
1739 Kao, S.-C. and Govindaraju, R.S., 2010. A copula-based joint deficit index for droughts. Journal
1740 of Hydrology, 380(1-2): 121-134.
1741 Karl, T., Quinlan, F. and Ezell, D., 1987. Drought termination and amelioration: Its
1742 climatological probability. Journal of Climate and Applied Meteorology, 26(9): 1198-
1743 1209.

1744 Kaufmann, H. et al., 2008. Environmental mapping and analysis program (EnMAP)-Recent
1745 advances and status, IGARSS 2008-2008 IEEE International Geoscience and Remote
1746 Sensing Symposium. IEEE, pp. IV-109-IV-112.
1747 Kerr, Y.H., Lagouarde, J.P. and Imbernon, J., 1992. Accurate land surface temperature retrieval
1748 from AVHRR data with use of an improved split window algorithm. Remote Sensing of
1749 Environment, 41(2-3): 197-209.
1750 Kerr, Y.H. et al., 2012. The SMOS soil moisture retrieval algorithm. IEEE Transactions on
1751 Geoscience and Remote Sensing, 50(5): 1384-1403.
1752 Keshavarz, M.R., Vazifedoust, M. and Alizadeh, A., 2014. Drought monitoring using a Soil
1753 Wetness Deficit Index (SWDI) derived from MODIS satellite data. Agricultural Water
1754 Management, 132: 37-45.
1755 Keyantash, J.A. and Dracup, J.A., 2004. An aggregate drought index: Assessing drought severity
1756 based on fluctuations in the hydrologic cycle and surface water storage. Water Resources
1757 Research, 40(9).
1758 Kim, S., Liu, Y.Y., Johnson, F.M., Parinussa, R.M. and Sharma, A., 2015. A global comparison
1759 of alternate AMSR2 soil moisture products: Why do they differ? Remote Sensing of
1760 Environment, 161: 43-62.
1761 Klein, T., 2014. The variability of stomatal sensitivity to leaf water potential across tree species
1762 indicates a continuum between isohydric and anisohydric behaviours. Functional Ecology,
1763 28(6): 1313-1320.
1764 Köhler, P. et al., 2018. Global retrievals of solar-induced chlorophyll fluorescence with
1765 TROPOMI: First results and intersensor comparison to OCO-2. Geophysical Research
1766 Letters, 45(19): 10,456-10,463.

1767 Köhler, P., Guanter, L. and Joiner, J., 2014. A linear method for the retrieval of sun-induced
1768 chlorophyll fluorescence from GOME-2 and SCIAMACHY data. Atmospheric
1769 Measurement Techniques, 7(12): 12,173-12,217.
1770 Kokaly, R.F., Asner, G.P., Ollinger, S.V., Martin, M.E. and Wessman, C.A., 2009.
1771 Characterizing canopy biochemistry from imaging spectroscopy and its application to
1772 ecosystem studies. Remote Sensing of Environment, 113: S78-S91.
1773 Konings, A.G., Rao, K. and Steele-Dunne, S.C., 2019. Macro to micro: microwave remote
1774 sensing of plant water content for physiology and ecology. New Phytologist, 223(3):
1775 1166-1172.
1776 Kubota, T. et al., 2007. Global precipitation map using satellite-borne microwave radiometers by
1777 the GSMaP project: Production and validation. IEEE Transactions on Geoscience and
1778 Remote Sensing, 45(7): 2259-2275.
1779 Kull, O., Broadmeadow, M., Kruijt, B. and Meir, P., 1999. Light distribution and foliage
1780 structure in an oak canopy. Trees, 14(2): 55-64.
1781 Kumar, S.V. et al., 2019. NCA-LDAS land analysis: Development and performance of a
1782 multisensor, multivariate land data assimilation system for the National Climate
1783 Assessment. Journal of Hydrometeorology, 20(8): 1571-1593.
1784 Kumar, S.V. et al., 2014. Assimilation of remotely sensed soil moisture and snow depth
1785 retrievals for drought estimation. Journal of Hydrometeorology, 15(6): 2446-2469.
1786 Kustas, W. and Norman, J., 1996. Use of remote sensing for evapotranspiration monitoring over
1787 land surfaces. Hydrological Sciences Journal, 41(4): 495-516.
1788 Labate, D. et al., 2009. The PRISMA payload optomechanical design, a high performance
1789 instrument for a new hyperspectral mission. Acta Astronautica, 65(9-10): 1429-1436.

1790 Lanning, M., Wang, L. and Novick, K.A., 2020. The importance of cuticular permeance in
1791 assessing plant water–use strategies. Tree Physiology, 40(4): 425-432.
1792 Lanning, M. et al., 2019. Intensified vegetation water use under acid deposition. Science
1793 Advances, 5(7): eaav5168.
1794 Lary, D.J., Alavi, A.H., Gandomi, A.H. and Walker, A.L., 2016. Machine learning in
1795 geosciences and remote sensing. Geoscience Frontiers, 7(1): 3-10.
1796 Lee, C.M. et al., 2015. An introduction to the NASA Hyperspectral InfraRed Imager (HyspIRI)
1797 mission and preparatory activities. Remote Sensing of Environment, 167: 6-19.
1798 Lee, S.-K. et al., 2018. GEDI and TanDEM-X fusion for 3D forest structure parameter retrieval,
1799 IGARSS 2018-2018 IEEE International Geoscience and Remote Sensing Symposium.
1800 IEEE, pp. 380-382.
1801 Lettenmaier, D.P. et al., 2015. Inroads of remote sensing into hydrologic science during the
1802 WRR era. Water Resources Research, 51(9): 7309-7342.
1803 Li, H. et al., 2014. Evaluation of the VIIRS and MODIS LST products in an arid area of
1804 Northwest China. Remote Sensing of Environment, 142: 111-121.
1805 Li, X. et al., 2019. The impact of the 2009/2010 drought on vegetation growth and terrestrial
1806 carbon balance in Southwest China. Agricultural and Forest Meteorology, 269: 239-248.
1807 Li, X. and Xiao, J., 2020. Global climatic controls on interannual variability of ecosystem
1808 productivity: Similarities and differences inferred from solar-induced chlorophyll
1809 fluorescence and enhanced vegetation index. Agricultural and Forest Meteorology:
1810 108018.
1811 Li, Z.-L. et al., 2009. A review of current methodologies for regional evapotranspiration
1812 estimation from remotely sensed data. Sensors, 9(5): 3801-3853.

1813 Liou, Y.-A. and Kar, S.K., 2014. Evapotranspiration estimation with remote sensing and various
1814 surface energy balance algorithms—A review. Energies, 7(5): 2821-2849.
1815 Liu, H. et al., 2018a. Shifting plant species composition in response to climate change stabilizes
1816 grassland primary production. Proceedings of the National Academy of Sciences, 115(16):
1817 4051-4056.
1818 Liu, L. et al., 2019a. Revisiting assessments of ecosystem drought recovery. Environmental
1819 Research Letters, 14(11): 114028.
1820 Liu, L. et al., 2017a. The Microwave Temperature Vegetation Drought Index (MTVDI) based on
1821 AMSR-E brightness temperatures for long-term drought assessment across China (2003–
1822 2010). Remote Sensing of Environment, 199: 302-320.
1823 Liu, L. et al., 2018b. Evaluating the utility of solar-induced chlorophyll fluorescence for drought
1824 monitoring by comparison with NDVI derived from wheat canopy. Science of The Total
1825 Environment, 625: 1208-1217.
1826 Liu, S. et al., 2017b. Estimating wheat green area index from ground-based LiDAR measurement
1827 using a 3D canopy structure model. Agricultural and Forest Meteorology, 247: 12-20.
1828 Liu, W. et al., 2016a. A worldwide evaluation of basin-scale evapotranspiration estimates against
1829 the water balance method. Journal of Hydrology, 538: 82-95.
1830 Liu, X. et al., 2016b. Agricultural drought monitoring: Progress, challenges, and prospects.
1831 Journal of Geographical Sciences, 26(6): 750-767.
1832 Liu, Y. et al., 2019b. On the mechanisms of two composite methods for construction of
1833 multivariate drought indices. Science of the Total Environment, 647: 981-991.

1834 Liu, Y.Y., de Jeu, R.A., McCabe, M.F., Evans, J.P. and van Dijk, A.I., 2011. Global long-term
1835 passive microwave satellite-based retrievals of vegetation optical depth. Geophysical
1836 Research Letters, 38(18).
1837 Liu, Y.Y. et al., 2018c. Enhanced canopy growth precedes senescence in 2005 and 2010
1838 Amazonian droughts. Remote Sensing of Environment, 211: 26-37.
1839 Lloyd-Hughes, B., 2014. The impracticality of a universal drought definition. Theoretical and
1840 Applied Climatology, 117(3-4): 607-611.
1841 López Valencia, O.M. et al., 2020. Mapping groundwater abstractions from irrigated agriculture:
1842 big data, inverse modeling, and a satellite–model fusion approach. Hydrology and Earth
1843 System Sciences, 24(11): 5251-5277.
1844 Luo, W. et al., 2019. Long term experimental drought alters community plant trait variation, not
1845 trait means, across three semiarid grasslands. Plant and Soil, 442(1-2): 343-353.
1846 Ma, H., Song, J., Wang, J., Xiao, Z. and Fu, Z., 2014. Improvement of spatially continuous forest
1847 LAI retrieval by integration of discrete airborne LiDAR and remote sensing multi-angle
1848 optical data. Agricultural and Forest Meteorology, 189: 60-70.
1849 Ma, Y. et al., 2015. Remote sensing big data computing: Challenges and opportunities. Future
1850 Generation Computer Systems, 51: 47-60.
1851 Magney, T.S. et al., 2019. Mechanistic evidence for tracking the seasonality of photosynthesis
1852 with solar-induced fluorescence. Proceedings of the National Academy of Sciences,
1853 116(24): 11640-11645.
1854 Mankin, J.S., Seager, R., Smerdon, J.E., Cook, B.I. and Williams, A.P., 2019. Mid-latitude
1855 freshwater availability reduced by projected vegetation responses to climate change.
1856 Nature Geoscience: 1-6.

1857 Margulis, S.A. et al., 2016. Characterizing the extreme 2015 snowpack deficit in the Sierra
1858 Nevada (USA) and the implications for drought recovery. Geophysical Research Letters,
1859 43(12): 6341-6349.
1860 Martens, B. et al., 2017. GLEAM v3: Satellite-based land evaporation and root-zone soil
1861 moisture. Geoscientific Model Development, 10(5): 1903-1925.
1862 Martinaitis, S.M. et al., 2017. The HMT multi-radar multi-sensor hydro experiment. Bulletin of
1863 the American Meteorological Society, 98(2): 347-359.
1864 Martínez-Fernández, J., González-Zamora, A., Sánchez, N., Gumuzzio, A. and Herrero-Jiménez,
1865 C., 2016. Satellite soil moisture for agricultural drought monitoring: Assessment of the
1866 SMOS derived Soil Water Deficit Index. Remote Sensing of Environment, 177: 277-286.
1867 McCabe, M., Aragon, B., Houborg, R. and Mascaro, J., 2017a. CubeSats in hydrology:
1868 Ultrahigh-resolution insights into vegetation dynamics and terrestrial evaporation. Water
1869 Resources Research, 53(12): 10017-10024.
1870 McCabe, M. et al., 2008. Hydrological consistency using multi-sensor remote sensing data for
1871 water and energy cycle studies. Remote Sensing of Environment, 112(2): 430-444.
1872 McCabe, M.F. et al., 2016. The GEWEX LandFlux project: Evaluation of model evaporation
1873 using tower-based and globally gridded forcing data. Geoscientific Model Development,
1874 9(1): 283-305.
1875 McCabe, M.F. et al., 2017b. The future of Earth observation in hydrology. Hydrology and Earth
1876 System Sciences, 21(7): 3879.
1877 McDowell, N. et al., 2018. Drivers and mechanisms of tree mortality in moist tropical forests.
1878 New Phytologist, 219(3): 851-869.

McDowell, N.G. and Sevanto, S., 2010. The mechanisms of carbon starvation: how, when, or does it even occur at all? New Phytologist, 186(2): 264-266.

McKee, T.B., Doesken, N.J. and Kleist, J., 1993. The relationship of drought frequency and duration to time scales, Proceedings of the 8th Conference on Applied Climatology. American Meteorological Society Boston, MA, pp. 179-183.

McVicar, T. and Bierwirth, P., 2001. Rapidly assessing the 1997 drought in Papua New Guinea using composite AVHRR imagery. International Journal of Remote Sensing, 22(11): 2109-2128.

Meir, P., Metcalfe, D.B., Costa, A. and Fisher, R.A., 2008. The fate of assimilated carbon during drought: impacts on respiration in Amazon rainforests. Philosophical Transactions of the Royal Society B: Biological Sciences, 363(1498): 1849-1855.

Meir, P. and Woodward, F.I., 2010. Amazonian rain forests and drought: response and vulnerability. New Phytologist, 187(3): 553-557.

Meng, L., Dong, T. and Zhang, W., 2016. Drought monitoring using an Integrated Drought Condition Index (IDCI) derived from multi-sensor remote sensing data. Natural Hazards, 80(2): 1135-1152.

Meng, R. et al., 2017. Using high spatial resolution satellite imagery to map forest burn severity across spatial scales in a Pine Barrens ecosystem. Remote Sensing of Environment, 191: 95-109.

Meng, R. et al., 2018. Measuring short-term post-fire forest recovery across a burn severity gradient in a mixed pine-oak forest using multi-sensor remote sensing techniques. Remote Sensing of Environment, 210: 282-296.

1901 Meng, X.H., Evans, J.P. and McCabe, M.F., 2014. The Impact of Observed Vegetation Changes
1902 on Land–Atmosphere Feedbacks During Drought. Journal of Hydrometeorology, 15(2):
1903 759-776.
1904 Miralles, D., De Jeu, R., Gash, J., Holmes, T. and Dolman, A., 2011. Magnitude and variability
1905 of land evaporation and its componentsat the global scale. Hydrology and Earth System
1906 Sciences, 15(3): 967-981.
1907 Miralles, D.G., Gentine, P., Seneviratne, S.I. and Teuling, A.J., 2019. Land–atmospheric
1908 feedbacks during droughts and heatwaves: state of the science and current challenges.
1909 Annals of the New York Academy of Sciences, 1436(1): 19.
1910 Miralles, D.G. et al., 2016. The WACMOS-ET project-Part 2: Evaluation of global terrestrial
1911 evaporation data sets. Hydrology and Earth System Sciences, 20(2): 823-842.
1912 Miralles, D.G., Teuling, A.J., Van Heerwaarden, C.C. and De Arellano, J.V.-G., 2014. Mega-
1913 heatwave temperatures due to combined soil desiccation and atmospheric heat
1914 accumulation. Nature Geoscience, 7(5): 345-349.
1915 Mishra, A.K. and Singh, V.P., 2010. A review of drought concepts. Journal of Hydrology, 391(1):
1916 202-216.
1917 Mo, K.C. and Lettenmaier, D.P., 2015. Heat wave flash droughts in decline. Geophysical
1918 Research Letters, 42(8): 2823-2829.
1919 Mohammed, G.H. et al., 2019. Remote sensing of solar-induced chlorophyll fluorescence (SIF)
1920 in vegetation: 50 years of progress. Remote Sensing of Environment, 231: 111177.
1921 Moore III, B. et al., 2018. The potential of the geostationary Carbon Cycle Observatory
1922 (GeoCarb) to provide multi-scale constraints on the carbon cycle in the Americas.
1923 Frontiers in Environmental Science, 6: 109.

1924 Mote, P.W., Hamlet, A.F., Clark, M.P. and Lettenmaier, D.P., 2005. Declining mountain
1925 snowpack in western North America. Bulletin of the American Meteorological Society,
1926 86(1): 39-50.
1927 Mu, Q., Zhao, M. and Running, S.W., 2011. Improvements to a MODIS global terrestrial
1928 evapotranspiration algorithm. Remote Sensing of Environment, 115(8): 1781-1800.
1929 Mueller, B. et al., 2011. Evaluation of global observations-based evapotranspiration datasets and
1930 IPCC AR4 simulations. Geophysical Research Letters, 38(6).
1931 Mukherjee, S., Mishra, A. and Trenberth, K.E., 2018. Climate change and drought: a perspective
1932 on drought indices. Current Climate Change Reports, 4(2): 145-163.
1933 Myneni, R.B. et al., 2002. Global products of vegetation leaf area and fraction absorbed PAR
1934 from year one of MODIS data. Remote Sensing of Environment, 83(1-2): 214-231.
1935 Nasab, A.H., Ansary, H. and Sanaei-Nejad, S.H., 2018. Analyzing drought history using Fuzzy
1936 Integrated Drought Index (FIDI): a case study in the Neyshabour basin, Iran. Arabian
1937 Journal of Geosciences, 11(14): 390.
1938 Nemani, R., Pierce, L., Running, S. and Goward, S., 1993. Developing satellite-derived estimates
1939 of surface moisture status. Journal of Applied Meteorology, 32(3): 548-557.
1940 Ni, Z., Lu, Q., Huo, H. and Zhang, H., 2019. Estimation of chlorophyll fluorescence at different
1941 scales: A review. Sensors, 19(13): 3000.
1942 Nicolai-Shaw, N., Zscheischler, J., Hirschi, M., Gudmundsson, L. and Seneviratne, S.I., 2017. A
1943 drought event composite analysis using satellite remote-sensing based soil moisture.
1944 Remote Sensing of Environment, 203: 216-225.
1945 Niemeyer, S., 2008. New drought indices. Options Méditerranéennes. Série A: Séminaires
1946 Méditerranéens, 80: 267-274.

1947 Nishida, K., Nemani, R.R., Running, S.W. and Glassy, J.M., 2003. An operational remote
1948 sensing algorithm of land surface evaporation. Journal of Geophysical Research:
1949 Atmospheres, 108(D9).
1950 Normand, J.C. and Heggy, E., 2015. InSAR assessment of surface deformations in urban coastal
1951 terrains associated with groundwater dynamics. IEEE Transactions on Geoscience and
1952 Remote Sensing, 53(12): 6356-6371.
1953 Novick, K.A. et al., 2016. The increasing importance of atmospheric demand for ecosystem
1954 water and carbon fluxes. Nature Climate Change, 6(11): 1023-1027.
1955 O'Sullivan, M. et al., 2020. Climate-driven variability and trends in plant productivity over
1956 recent decades based on three global products. Global Biogeochemical Cycles:
1957 e2020GB006613.
1958 Orhan, O., Ekercin, S. and Dadaser-Celik, F., 2014. Use of landsat land surface temperature and
1959 vegetation indices for monitoring drought in the Salt Lake Basin Area, Turkey. The
1960 Scientific World Journal, 2014.
1961 Orville, H.D., 1990. AMS statement on meteorological drought. Bulletin of the American
1962 Meteorological Society, 71(7): 1021-1025.
1963 Otkin, J.A. et al., 2013. Examining rapid onset drought development using the thermal infrared–
1964 based evaporative stress index. Journal of Hydrometeorology, 14(4): 1057-1074.
1965 Otkin, J.A., Anderson, M.C., Hain, C. and Svoboda, M., 2014. Examining the relationship
1966 between drought development and rapid changes in the evaporative stress index. Journal
1967 of Hydrometeorology, 15(3): 938-956.

1968 Otkin, J.A. et al., 2018. Flash droughts: a review and assessment of the challenges imposed by
1969 rapid-onset droughts in the United States. Bulletin of the American Meteorological
1970 Society, 99(5): 911-919.
1971 Pachauri, R.K. et al., 2014. Climate change 2014: synthesis report. Contribution of Working
1972 Groups I, II and III to the fifth assessment report of the Intergovernmental Panel on
1973 Climate Change. IPCC.
1974 Palmer, W.C., 1965. Meteorological drought, 30. Citeseer.
1975 Paloscia, S., Macelloni, G. and Santi, E., 2006. Soil moisture estimates from AMSR-E brightness
1976 temperatures by using a dual-frequency algorithm. IEEE Transactions on Geoscience and
1977 Remote Sensing, 44(11): 3135-3144.
1978 Paloscia, S., Macelloni, G., Santi, E. and Koike, T., 2001. A multifrequency algorithm for the
1979 retrieval of soil moisture on a large scale using microwave data from SMMR and SSM/I
1980 satellites. IEEE Transactions on Geoscience and Remote Sensing, 39(8): 1655-1661.
1981 Pan, M., Wood, E.F., Wójcik, R. and McCabe, M.F., 2008. Estimation of regional terrestrial
1982 water cycle using multi-sensor remote sensing observations and data assimilation.
1983 Remote Sensing of Environment, 112(4): 1282-1294.
1984 Pandey, S., Bhandari, H.S. and Hardy, B., 2007. Economic costs of drought and rice farmers'
1985 coping mechanisms: a cross-country comparative analysis. International Rice Research
1986 Institute, 203 pp.
1987 Park, S., Im, J., Jang, E. and Rhee, J., 2016. Drought assessment and monitoring through
1988 blending of multi-sensor indices using machine learning approaches for different climate
1989 regions. Agricultural and Forest Meteorology, 216: 157-169.

1990 Park, S., Im, J., Park, S. and Rhee, J., 2017. Drought monitoring using high resolution soil
1991 moisture through multi-sensor satellite data fusion over the Korean peninsula.
1992 Agricultural and Forest Meteorology, 237: 257-269.
1993 Park, S., Kang, D., Yoo, C., Im, J. and Lee, M.-I., 2020. Recent ENSO influence on East African
1994 drought during rainy seasons through the synergistic use of satellite and reanalysis data.
1995 ISPRS Journal of Photogrammetry and Remote Sensing, 162: 17-26.
1996 Pasho, E., Camarero, J.J., de Luis, M. and Vicente-Serrano, S.M., 2011. Impacts of drought at
1997 different time scales on forest growth across a wide climatic gradient in north-eastern
1998 Spain. Agricultural and Forest Meteorology, 151(12): 1800-1811.
1999 Patel, N., Parida, B., Venus, V., Saha, S. and Dadhwal, V., 2012. Analysis of agricultural
2000 drought using vegetation temperature condition index (VTCI) from Terra/MODIS
2001 satellite data. Environmental Monitoring and Assessment, 184(12): 7153-7163.
2002 Pederson, G.T. et al., 2011. The unusual nature of recent snowpack declines in the North
2003 American Cordillera. Science, 333(6040): 332-335.
2004 Pendergrass, A.G. et al., 2020. Flash droughts present a new challenge for subseasonal-to-
2005 seasonal prediction. Nature Climate Change, 10(3): 191-199.
2006 Peng, J. et al., 2020. A roadmap for high-resolution satellite soil moisture applications –
2007 confronting product characteristics with user requirements. Remote Sensing of
2008 Environment: 112162.
2009 Peng, J., Wu, C., Zhang, X., Wang, X. and Gonsamo, A., 2019. Satellite detection of cumulative
2010 and lagged effects of drought on autumn leaf senescence over the Northern Hemisphere.
2011 Global Change Biology, 25(6): 2174-2188.

2012 Peñuelas, J. et al., 2017. Shifting from a fertilization-dominated to a warming-dominated period.
2013 Nature Ecology & Evolution, 1(10): 1438-1445.
2014 Pesti, G., Shrestha, B.P., Duckstein, L. and Bogárdi, I., 1996. A fuzzy rule-based approach to
2015 drought assessment. Water Resources Research, 32(6): 1741-1747.
2016 Peters, A.J. et al., 2002. Drought monitoring with NDVI-based standardized vegetation index.
2017 Photogrammetric Engineering and Remote Sensing, 68(1): 71-75.
2018 Piao, S. et al., 2019. The impacts of climate extremes on the terrestrial carbon cycle: A review.
2019 Science China Earth Sciences: 1-13.
2020 Pinheiro, A.C., Privette, J.L., Mahoney, R. and Tucker, C.J., 2004. Directional effects in a daily
2021 AVHRR land surface temperature dataset over Africa. IEEE Transactions on Geoscience
2022 and Remote Sensing, 42(9): 1941-1954.
2023 Pohl, C. and Van Genderen, J.L., 1998. Review article multisensor image fusion in remote
2024 sensing: concepts, methods and applications. International Journal of Remote Sensing,
2025 19(5): 823-854.
2026 Pouliot, D., Latifovic, R. and Olthof, I., 2009. Trends in vegetation NDVI from 1 km AVHRR
2027 data over Canada for the period 1985–2006. International Journal of Remote Sensing,
2028 30(1): 149-168.
2029 Prakash, S. et al., 2018. A preliminary assessment of GPM-based multi-satellite precipitation
2030 estimates over a monsoon dominated region. Journal of Hydrology, 556: 865-876.
2031 Prata, A., 2002. Land surface temperature measurement from space: AATSR algorithm
2032 theoretical basis document. Contract Report to ESA, CSIRO Atmospheric Research,
2033 Aspendale, Victoria, Australia, 2002: 1-34.

2034 Price, J.C., 1994. How unique are spectral signatures? Remote Sensing of Environment, 49(3):
2035 181-186.
2036 Pulliainen, J. and Hallikainen, M., 2001. Retrieval of regional snow water equivalent from space-
2037 borne passive microwave observations. Remote Sensing of Environment, 75(1): 76-85.
2038 Qi, J., Chehbouni, A., Huete, A.R., Kerr, Y.H. and Sorooshian, S., 1994. A modified soil
2039 adjusted vegetation index. Remote Sensing of Environment, 48(2): 119-122.
2040 Qi, W. and Dubayah, R.O., 2016. Combining Tandem-X InSAR and simulated GEDI lidar
2041 observations for forest structure mapping. Remote Sensing of Environment, 187: 253-266.
2042 Qi, W., Saarela, S., Armston, J., Ståhl, G. and Dubayah, R., 2019. Forest biomass estimation
2043 over three distinct forest types using TanDEM-X InSAR data and simulated GEDI lidar
2044 data. Remote Sensing of Environment, 232: 111283.
2045 Qiu, B., Ge, J., Guo, W., Pitman, A.J. and Mu, M., 2020. Responses of Australian Dryland
2046 Vegetation to the 2019 Heat Wave at a Subdaily Scale. Geophysical Research Letters,
2047 47(4).
2048 Rahmat-Samii, Y., Manohar, V. and Kovitz, J.M., 2017. For Satellites, Think Small, Dream Big:
2049 A review of recent antenna developments for CubeSats. IEEE Antennas and Propagation
2050 Magazine, 59(2): 22-30.
2051 Rahmati, O. et al., 2020. Machine learning approaches for spatial modeling of agricultural
2052 droughts in the south-east region of Queensland Australia. Science of the Total
2053 Environment, 699: 134230.
2054 Rajsekhar, D., Singh, V.P. and Mishra, A.K., 2015. Multivariate drought index: An information
2055 theory based approach for integrated drought assessment. Journal of Hydrology, 526:
2056 164-182.

2057 Rao, K., Anderegg, W.R., Sala, A., Martínez-Vilalta, J. and Konings, A.G., 2019. Satellite-based
2058 vegetation optical depth as an indicator of drought-driven tree mortality. Remote Sensing
2059 of Environment, 227: 125-136.
2060 Rao, K., Williams, A.P., Flefil, J.F. and Konings, A.G., 2020. SAR-enhanced mapping of live
2061 fuel moisture content. Remote Sensing of Environment, 245: 111797.
2062 Redmond, K.T., 2002. The depiction of drought: A commentary. Bulletin of the American
2063 Meteorological Society, 83(8): 1143-1148.
2064 Reshmidevi, T., Eldho, T. and Jana, R., 2009. A GIS-integrated fuzzy rule-based inference
2065 system for land suitability evaluation in agricultural watersheds. Agricultural Systems,
2066 101(1-2): 101-109.
2067 Rhee, J., Im, J. and Carbone, G.J., 2010. Monitoring agricultural drought for arid and humid
2068 regions using multi-sensor remote sensing data. Remote Sensing of Environment,
2069 114(12): 2875-2887.
2070 Richardson, A.J. and Wiegand, C.L., 1990. Comparison of two models for simulating the soil-
2071 vegetation composite reflectance of a developing cotton canopy. Remote Sensing, 11(3):
2072 447-459.
2073 Richardson, J.J., Moskal, L.M. and Kim, S.-H., 2009. Modeling approaches to estimate effective
2074 leaf area index from aerial discrete-return LIDAR. Agricultural and Forest Meteorology,
2075 149(6-7): 1152-1160.
2076 Roman, D. et al., 2015. The role of isohydric and anisohydric species in determining ecosystem-
2077 scale response to severe drought. Oecologia, 179(3): 641-654.
2078 Roujean, J.L. and Lacaze, R., 2002. Global mapping of vegetation parameters from POLDER
2079 multiangular measurements for studies of surface-atmosphere interactions: A pragmatic

2080 method and its validation. Journal of Geophysical Research: Atmospheres, 107(D12):
2081 ACL 6-1-ACL 6-14.
2082 Roundy, J.K., Ferguson, C.R. and Wood, E.F., 2014. Impact of land-atmospheric coupling in
2083 CFSv2 on drought prediction. Climate Dynamics, 43(1-2): 421-434.
2084 Roundy, J.K. and Santanello, J.A., 2017. Utility of satellite remote sensing for land–atmosphere
2085 coupling and drought metrics. Journal of Hydrometeorology, 18(3): 863-877.
2086 Rouse, J., Haas, R., Schell, J. and Deering, D., 1974. Monitoring vegetation systems in the Great
2087 Plains with ERTS. NASA special publication, 351: 309.
2088 Rulinda, C.M., Dilo, A., Bijker, W. and Stein, A., 2012. Characterising and quantifying
2089 vegetative drought in East Africa using fuzzy modelling and NDVI data. Journal of Arid
2090 Environments, 78: 169-178.
2091 Running, S.W. et al., 1994. Terrestrial remote sensing science and algorithms planned for
2092 EOS/MODIS. International Journal of Remote sensing, 15(17): 3587-3620.
2093 Ruzmaikin, A., Aumann, H.H. and Manning, E.M., 2014. Relative humidity in the troposphere
2094 with AIRS. Journal of the Atmospheric Sciences, 71(7): 2516-2533.
2095 Ryu, Y., Berry, J.A. and Baldocchi, D.D., 2019. What is global photosynthesis? History,
2096 uncertainties and opportunities. Remote Sensing of Environment, 223: 95-114.
2097 Saleska, S.R., Didan, K., Huete, A.R. and Da Rocha, H.R., 2007. Amazon forests green-up
2098 during 2005 drought. Science, 318(5850): 612-612.
2099 Samanta, A. et al., 2010. Amazon forests did not green-up during the 2005 drought. Geophysical
2100 Research Letters, 37(5).

2101 Sandholt, I., Rasmussen, K. and Andersen, J., 2002. A simple interpretation of the surface
2102 temperature/vegetation index space for assessment of surface moisture status. Remote
2103 Sensing of Environment, 79(2-3): 213-224.
2104 Sankey, T.T. et al., 2018. UAV hyperspectral and lidar data and their fusion for arid and semi-
2105 arid land vegetation monitoring. Remote Sensing in Ecology and Conservation, 4(1): 20-
2106 33.
2107 Santanello Jr, J.A. et al., 2018. Land–atmosphere interactions: the LoCo perspective. Bulletin of
2108 the American Meteorological Society, 99(6): 1253-1272.
2109 Save, H., Bettadpur, S. and Tapley, B.D., 2012. Reducing errors in the GRACE gravity solutions
2110 using regularization. Journal of Geodesy, 86(9): 695-711.
2111 Schwalm, C.R. et al., 2017. Global patterns of drought recovery. Nature, 548(7666): 202-205.
2112 Schwantes, A.M., Swenson, J.J. and Jackson, R.B., 2016. Quantifying drought-induced tree
2113 mortality in the open canopy woodlands of central Texas. Remote Sensing of
2114 Environment, 181: 54-64.
2115 Seddon, A.W., Macias-Fauria, M., Long, P.R., Benz, D. and Willis, K.J., 2016. Sensitivity of
2116 global terrestrial ecosystems to climate variability. Nature, 531(7593): 229.
2117 Sellars, S. et al., 2013. Computational Earth science: Big data transformed into insight. Eos,
2118 Transactions American Geophysical Union, 94(32): 277-278.
2119 Senay, G.B., Budde, M., Brown, J. and Verdin, J., 2008. Mapping flash drought in the US:
2120 Southern Great Plains, 22nd Conference on Hydrology. American Meteorological
2121 Society New Orleans, LA.
2122 Seneviratne, S.I. et al., 2010. Investigating soil moisture–climate interactions in a changing
2123 climate: A review. Earth-Science Reviews, 99(3-4): 125-161.

2124 Seneviratne, S.I., Lüthi, D., Litschi, M. and Schär, C., 2006. Land–atmosphere coupling and
2125 climate change in Europe. Nature, 443(7108): 205-209.
2126 Sepulcre-Canto, G., Horion, S., Singleton, A., Carrao, H. and Vogt, J., 2012. Development of a
2127 Combined Drought Indicator to detect agricultural drought in Europe. Natural Hazards &
2128 Earth System Sciences, 12(11).
2129 Seyednasrollah, B., Domec, J.-C. and Clark, J.S., 2019. Spatiotemporal sensitivity of thermal
2130 stress for monitoring canopy hydrological stress in near real-time. Agricultural and Forest
2131 Meteorology, 269-270: 220-230.
2132 Shafer, B. and Dezman, L., 1982. Development of surface water supply index (SWSI) to assess
2133 the severity of drought condition in Snowpack runoff areas. Proceding of The Western
2134 Snow Conference.
2135 Shamsudduha, M., Taylor, R. and Longuevergne, L., 2012. Monitoring groundwater storage
2136 changes in the highly seasonal humid tropics: Validation of GRACE measurements in the
2137 Bengal Basin. Water Resources Research, 48(2).
2138 Sheffield, J., Ferguson, C.R., Troy, T.J., Wood, E.F. and McCabe, M.F., 2009. Closing the
2139 terrestrial water budget from satellite remote sensing. Geophysical Research Letters,
2140 36(7).
2141 Sheffield, J., Wood, E.F. and Roderick, M.L., 2012. Little change in global drought over the past
2142 60 years. Nature, 491(7424): 435-438.
2143 Shi, M. et al., 2019. The 2005 Amazon drought legacy effect delayed the 2006 wet season onset.
2144 Geophysical Research Letters, 46(15): 9082-9090.

2145 Shivers, S.W., Roberts, D.A. and McFadden, J.P., 2019. Using paired thermal and hyperspectral
2146 aerial imagery to quantify land surface temperature variability and assess crop stress
2147 within California orchards. Remote Sensing of Environment, 222: 215-231.
2148 Short, N.M., 1976. Mission to Earth: Landsat views the world, 1. Scientific and Technical Office,
2149 National Aeronautics and Space Administration.
2150 Shugart, H.H. et al., 2015. Computer and remote-sensing infrastructure to enhance large-scale
2151 testing of individual-based forest models. Frontiers in Ecology and the Environment,
2152 13(9): 503-511.
2153 Silva, C.A. et al., 2018. Fusing GEDI, ICESat-2 and NISAR data for aboveground biomass
2154 mapping in Sonoma County, California, USA. AGUFM, 2018: B44E-05.
2155 Simić, D., Kovačević, I., Svirčević, V. and Simić, S., 2017. 50 years of fuzzy set theory and
2156 models for supplier assessment and selection: A literature review. Journal of Applied
2157 Logic, 24: 85-96.
2158 Sims, A.P., Niyogi, D.d.S. and Raman, S., 2002. Adopting drought indices for estimating soil
2159 moisture: A North Carolina case study. Geophysical Research Letters, 29(8): 24-1-24-4.
2160 Sippel, S. et al., 2018. Drought, Heat, and the Carbon Cycle: a Review. Current Climate Change
2161 Reports: 1-21.
2162 Sivapalan, M., Savenije, H.H. and Blöschl, G., 2012. Socio-hydrology: A new science of people
2163 and water. Hydrology Process, 26(8): 1270-1276.
2164 Smith, M.N. et al., 2019a. Seasonal and drought-related changes in leaf area profiles depend on
2165 height and light environment in an Amazon forest. New Phytologist, 222(3): 1284-1297.

2166 Smith, W. et al., 2018. Chlorophyll fluorescence better captures seasonal and interannual gross
2167 primary productivity dynamics across dryland ecosystems of southwestern North
2168 America. Geophysical Research Letters, 45(2): 748-757.
2169 Smith, W.K. et al., 2019b. Remote sensing of dryland ecosystem structure and function: Progress,
2170 challenges, and opportunities. Remote Sensing of Environment, 233: 111401.
2171 Smith, W.K. et al., 2016. Large divergence of satellite and Earth system model estimates of
2172 global terrestrial CO_2 fertilization. Nature Climate Change, 6(3): 306.
2173 Sobejano-Paz, V. et al., 2020. Hyperspectral and Thermal Sensing of Stomatal Conductance,
2174 Transpiration, and Photosynthesis for Soybean and Maize under Drought. Remote
2175 Sensing, 12(19): 3182.
2176 Sobrino, J.A., Jiménez-Muñoz, J.C. and Paolini, L., 2004. Land surface temperature retrieval
2177 from LANDSAT TM 5. Remote Sensing of Environment, 90(4): 434-440.
2178 Solomatine, D.P., 2002. Data-driven modelling: paradigm, methods, experiences, Proc. 5th
2179 International Conference on Hydroinformatics, pp. 1-5.
2180 Son, B. et al., 2021. A new drought monitoring approach: Vector Projection Analysis (VPA).
2181 Remote Sensing of Environment, 252: 112145.
2182 Son, N., Chen, C., Chen, C., Chang, L. and Minh, V.Q., 2012. Monitoring agricultural drought in
2183 the Lower Mekong Basin using MODIS NDVI and land surface temperature data.
2184 International Journal of Applied Earth Observation and Geoinformation, 18: 417-427.
2185 Song, L. et al., 2018. Satellite sun-induced chlorophyll fluorescence detects early response of
2186 winter wheat to heat stress in the Indian Indo-Gangetic Plains. Global Change Biology,
2187 24(9): 4023-4037.

2188 Sorooshian, S. et al., 2011. Advanced concepts on remote sensing of precipitation at multiple
2189 scales. Bulletin of the American Meteorological Society, 92(10): 1353-1357.
2190 Sorooshian, S. et al., 2000. Evaluation of PERSIANN system satellite-based estimates of tropical
2191 rainfall. Bulletin of the American Meteorological Society, 81(9): 2035-2046.
2192 Sruthi, S. and Aslam, M.M., 2015. Agricultural drought analysis using the NDVI and land
2193 surface temperature data; a case study of Raichur district. Aquatic Procedia, 4: 1258-1264.
2194 Staudinger, M., Stahl, K. and Seibert, J., 2014. A drought index accounting for snow. Water
2195 Resources Research, 50(10): 7861-7872.
2196 Stegehuis, A. et al., 2015. An observation-constrained multi-physics WRF ensemble for
2197 simulating European mega heat waves. Geoscientific Model Development, 8(7): 2285-
2198 2298.
2199 Stewart, I.T., 2009. Changes in snowpack and snowmelt runoff for key mountain regions.
2200 Hydrological Processes: An International Journal, 23(1): 78-94.
2201 Stocker, B.D. et al., 2018. Quantifying soil moisture impacts on light use efficiency across
2202 biomes. New Phytologist, 218(4): 1430-1449.
2203 Stocker, B.D. et al., 2019. Drought impacts on terrestrial primary production underestimated by
2204 satellite monitoring. Nature Geoscience, 12(4): 264.
2205 Stovall, A.E., Shugart, H. and Yang, X., 2019. Tree height explains mortality risk during an
2206 intense drought. Nature Communications, 10(1): 1-6.
2207 Strahler, A.H., 1997. Vegetation canopy reflectance modeling—Recent developments and
2208 remote sensing perspectives. Remote Sensing Reviews, 15(1-4): 179-194.

2209 Su, H., McCabe, M., Wood, E.F., Su, Z. and Prueger, J., 2005. Modeling evapotranspiration
2210 during SMACEX: Comparing two approaches for local-and regional-scale prediction.
2211 Journal of Hydrometeorology, 6(6): 910-922.
2212 Suárez, L. et al., 2008. Assessing canopy PRI for water stress detection with diurnal airborne
2213 imagery. Remote Sensing of Environment, 112(2): 560-575.
2214 Sun, Q. et al., 2014. Variations in global temperature and precipitation for the period of 1948 to
2215 2010. Environmental Monitoring and Assessment, 186(9): 5663-5679.
2216 Sun, Q. et al., 2018a. A review of global precipitation data sets: Data sources, estimation, and
2217 intercomparisons. Reviews of Geophysics, 56(1): 79-107.
2218 Sun, Y. et al., 2018b. Overview of Solar-Induced chlorophyll Fluorescence (SIF) from the
2219 Orbiting Carbon Observatory-2: Retrieval, cross-mission comparison, and global
2220 monitoring for GPP. Remote Sensing of Environment, 209: 808-823.
2221 Sun, Y. et al., 2017. OCO-2 advances photosynthesis observation from space via solar-induced
2222 chlorophyll fluorescence. Science, 358(6360).
2223 Sun, Y. et al., 2015. Drought onset mechanisms revealed by satellite solar-induced chlorophyll
2224 fluorescence: Insights from two contrasting extreme events. Journal of Geophysical
2225 Research: Biogeosciences, 120(11): 2427-2440.
2226 Svoboda, M. et al., 2002. The drought monitor. Bulletin of the American Meteorological Society,
2227 83(8): 1181-1190.
2228 Svoboda, M. et al., 2017. NDMC Annual Report 2017.
2229 Tabari, H., Nikbakht, J. and Talaee, P.H., 2013. Hydrological drought assessment in
2230 Northwestern Iran based on streamflow drought index (SDI). Water Resources
2231 Management, 27(1): 137-151.

2232 Tachiiri, K., Shinoda, M., Klinkenberg, B. and Morinaga, Y., 2008. Assessing Mongolian snow
2233 disaster risk using livestock and satellite data. Journal of Arid Environments, 72(12):
2234 2251-2263.
2235 Tallaksen, L.M. and Van Lanen, H.A., 2004. Hydrological drought: processes and estimation
2236 methods for streamflow and groundwater, 48. Elsevier.
2237 Tao, L., Li, J., Jiang, J. and Chen, X., 2016. Leaf area index inversion of winter wheat using
2238 modified water-cloud model. IEEE Geoscience and Remote Sensing Letters, 13(6): 816-
2239 820.
2240 Tapiador, F. et al., 2017. Global precipitation measurements for validating climate models.
2241 Atmospheric Research, 197: 1-20.
2242 Taylor, T.E. et al., 2020. OCO-3 early mission operations and initial (vEarly) XCO2 and SIF
2243 retrievals. Remote Sensing of Environment, 251: 112032.
2244 Teuling, A.J. et al., 2010. Contrasting response of European forest and grassland energy
2245 exchange to heatwaves. Nature Geoscience, 3(10): 722-727.
2246 Thenot, F., Méthy, M. and Winkel, T., 2002. The Photochemical Reflectance Index (PRI) as a
2247 water-stress index. International Journal of Remote Sensing, 23(23): 5135-5139.
2248 Thomas, B.F. et al., 2017. GRACE groundwater drought index: Evaluation of California Central
2249 Valley groundwater drought. Remote Sensing of Environment, 198: 384-392.
2250 Thompson, D. and Wehmanen, O., 1977. The use of Landsat digital data to detect and monitor
2251 vegetation water deficiencies.
2252 Tomlinson, C.J., Chapman, L., Thornes, J.E. and Baker, C., 2011. Remote sensing land surface
2253 temperature for meteorology and climatology: a review. Meteorological Applications,
2254 18(3): 296-306.

2255 Touma, D., Ashfaq, M., Nayak, M.A., Kao, S.-C. and Diffenbaugh, N.S., 2015. A multi-model
2256 and multi-index evaluation of drought characteristics in the 21st century. Journal of
2257 Hydrology, 526: 196-207.
2258 Tramontana, G. et al., 2016. Predicting carbon dioxide and energy fluxes across global
2259 FLUXNET sites with regression algorithms. Biogeosciences Discussions, 13(14): 4291-
2260 4313.
2261 Trenberth, K.E. et al., 2014. Global warming and changes in drought. Nature Climate Change,
2262 4(1): 17.
2263 Trnka, M. et al., 2018. Priority questions in multidisciplinary drought research. Climate Research,
2264 75(3): 241-260.
2265 Tucker, C.J., 1980. Remote sensing of leaf water content in the near infrared. Remote Sensing of
2266 Environment, 10(1): 23-32.
2267 Tucker, C.J. et al., 2005. An extended AVHRR 8-km NDVI dataset compatible with MODIS and
2268 SPOT vegetation NDVI data. International Journal of Remote Sensing, 26(20): 4485-
2269 4498.
2270 Udelhoven, T. et al., 2017. A satellite-based imaging instrumentation concept for hyperspectral
2271 thermal remote sensing. Sensors, 17(7): 1542.
2272 Van der Molen, M.K. et al., 2011. Drought and ecosystem carbon cycling. Agricultural and
2273 Forest Meteorology, 151(7): 765-773.
2274 Van Der Werf, G.R. et al., 2004. Continental-scale partitioning of fire emissions during the 1997
2275 to 2001 El Nino/La Nina period. Science, 303(5654): 73-76.

2276 Van Leeuwen, W.J., Orr, B.J., Marsh, S.E. and Herrmann, S.M., 2006. Multi-sensor NDVI data
2277 continuity: Uncertainties and implications for vegetation monitoring applications.
2278 Remote Sensing of Environment, 100(1): 67-81.
2279 Van Loon, A.F., 2015. Hydrological drought explained. Wiley Interdisciplinary Reviews: Water,
2280 2(4): 359-392.
2281 Van Loon, A.F. et al., 2016. Drought in a human-modified world: reframing drought definitions,
2282 understanding, and analysis approaches. Hydrology and Earth System Sciences, 20(9):
2283 3631-3650.
2284 Vasiliades, L., Loukas, A. and Liberis, N., 2011. A water balance derived drought index for
2285 Pinios River Basin, Greece. Water Resources Management, 25(4): 1087-1101.
2286 Velasquez, M. and Hester, P.T., 2013. An analysis of multi-criteria decision making methods.
2287 International Journal of Operations Research, 10(2): 56-66.
2288 Verma, M. et al., 2017. Effect of environmental conditions on the relationship between solar-
2289 induced fluorescence and gross primary productivity at an OzFlux grassland site. Journal
2290 of Geophysical Research: Biogeosciences, 122(3): 716-733.
2291 Vicente-Serrano, S.M., Beguería, S. and López-Moreno, J.I., 2010. A multiscalar drought index
2292 sensitive to global warming: the standardized precipitation evapotranspiration index.
2293 Journal of Climate, 23(7): 1696-1718.
2294 Vicente-Serrano, S.M., Quiring, S.M., Peña-Gallardo, M., Yuan, S. and Domínguez-Castro, F.,
2295 2019. A review of environmental droughts: Increased risk under global warming? Earth-
2296 Science Reviews: 102953.
2297 Vicente-Serrano, S.M. et al., 2020. Global characterization of hydrological and meteorological
2298 droughts under future climate change: The importance of timescales, vegetation-CO2

feedbacks and changes to distribution functions. International Journal of Climatology, 40(5): 2557-2567.

Vittucci, C. et al., 2016. SMOS retrieval over forests: Exploitation of optical depth and tests of soil moisture estimates. Remote Sensing of Environment, 180: 115-127.

Vreugdenhil, M., Hahn, S., Dorigo, W., Steele-Dunne, S. and Wagner, W., 2019. Sentinel-1 backscatter dynamics for vegetation monitoring: Synergies and discordances with Vegetation Optical Depth, Geophysical Research Abstracts.

Wan, Z., 2008. New refinements and validation of the MODIS land-surface temperature/emissivity products. Remote Sensing of Environment, 112(1): 59-74.

Wan, Z. and Li, Z.-L., 1997. A physics-based algorithm for retrieving land-surface emissivity and temperature from EOS/MODIS data. IEEE Transactions on Geoscience and Remote Sensing, 35(4): 980-996.

Wang, J. et al., 2016a. A multi-sensor view of the 2012 central plains drought from space. Frontiers in Environmental Science, 4: 45.

Wang, K. and Dickinson, R.E., 2012. A review of global terrestrial evapotranspiration: Observation, modeling, climatology, and climatic variability. Reviews of Geophysics, 50(2).

Wang, L. et al., 2012. Dryland ecohydrology and climate change: critical issues and technical advances. Hydrology and Earth System Sciences, 16(8): 2585-2603.

Wang, L., Good, S.P. and Caylor, K.K., 2014. Global synthesis of vegetation control on evapotranspiration partitioning. Geophysical Research Letters, 41(19): 6753-6757.

Wang, L. and Qu, J.J., 2009. Satellite remote sensing applications for surface soil moisture monitoring: A review. Frontiers of Earth Science in China, 3(2): 237-247.

2322 Wang, L., Yuan, X., Xie, Z., Wu, P. and Li, Y., 2016b. Increasing flash droughts over China
2323 during the recent global warming hiatus. Scientific Reports, 6: 30571.
2324 Wang, S., Mo, X., Hu, S., Liu, S. and Liu, Z., 2018. Assessment of droughts and wheat yield loss
2325 on the North China Plain with an aggregate drought index (ADI) approach. Ecological
2326 Indicators, 87: 107-116.
2327 Waseem, M., Ajmal, M. and Kim, T.-W., 2015. Development of a new composite drought index
2328 for multivariate drought assessment. Journal of Hydrology, 527: 30-37.
2329 Wei, W. et al., 2020. Temperature Vegetation Precipitation Dryness Index (TVPDI)-based
2330 dryness-wetness monitoring in China. Remote Sensing of Environment, 248: 111957.
2331 West, H., Quinn, N. and Horswell, M., 2019. Remote sensing for drought monitoring & impact
2332 assessment: Progress, past challenges and future opportunities. Remote Sensing of
2333 Environment, 232: 111291.
2334 Westra, S., Brown, C., Lall, U. and Sharma, A., 2007. Modeling multivariable hydrological
2335 series: Principal component analysis or independent component analysis? Water
2336 Resources Research, 43(6).
2337 Wilhite, D.A., 2000. Drought as a natural hazard: concepts and definitions. I: 3-18.
2338 Wilhite, D.A. and Glantz, M.H., 1985. Understanding: the drought phenomenon: the role of
2339 definitions. Water International, 10(3): 111-120.
2340 Wilhite, D.A., Svoboda, M.D. and Hayes, M.J., 2007. Understanding the complex impacts of
2341 drought: A key to enhancing drought mitigation and preparedness. Water Resources
2342 Management, 21(5): 763-774.
2343 Wilkinson, S.L., Verkaik, G.J., Moore, P.A. and Waddington, J.M., 2020. Threshold peat burn
2344 severity breaks evaporation-limiting feedback. Ecohydrology, 13(1): e2168.

2345 Willis, K.J., Jeffers, E.S. and Tovar, C., 2018. What makes a terrestrial ecosystem resilient?
2346 Science, 359(6379): 988-989.
2347 Woellert, K., Ehrenfreund, P., Ricco, A.J. and Hertzfeld, H., 2011. Cubesats: Cost-effective
2348 science and technology platforms for emerging and developing nations. Advances in
2349 Space Research, 47(4): 663-684.
2350 Wold, S., Esbensen, K. and Geladi, P., 1987. Principal component analysis. Chemometrics and
2351 Intelligent Laboratory Systems, 2(1-3): 37-52.
2352 Wu, J. et al., 2015. Drought monitoring and analysis in China based on the Integrated Surface
2353 Drought Index (ISDI). International Journal of Applied Earth Observation and
2354 Geoinformation, 41: 23-33.
2355 Wu, X. et al., 2018. Differentiating drought legacy effects on vegetation growth over the
2356 temperate Northern Hemisphere. Global Change Biology, 24(1): 504-516.
2357 Xie, P. and Arkin, P.A., 1997. Global precipitation: A 17-year monthly analysis based on gauge
2358 observations, satellite estimates, and numerical model outputs. Bulletin of the American
2359 Meteorological Society, 78(11): 2539-2558.
2360 Xie, P., Arkin, P.A. and Janowiak, J.E., 2007. CMAP: The CPC merged analysis of precipitation,
2361 Measuring Precipitation from Space. Springer, pp. 319-328.
2362 Xie, Q. et al., 2018. Vegetation indices combining the red and red-edge spectral information for
2363 leaf area index retrieval. IEEE Journal of Selected Topics in Applied Earth Observations
2364 and Remote Sensing, 11(5): 1482-1493.
2365 Xie, S. et al., 2010. Global warming pattern formation: Sea surface temperature and rainfall.
2366 Journal of Climate, 23(4): 966-986.

2367 Xu, C. et al., 2019. Increasing impacts of extreme droughts on vegetation productivity under
2368 climate change. Nature Climate Change, 9(12): 948-953.
2369 Xu, Z., Zhou, G. and Shimizu, H., 2010. Plant responses to drought and rewatering. Plant
2370 Signaling & Behavior, 5(6): 649-654.
2371 Xue, J. and Su, B., 2017. Significant Remote Sensing Vegetation Indices: A Review of
2372 Developments and Applications. Journal of Sensors, 2017: 1353691.
2373 Yager, R.R., 1996. Quantifier guided aggregation using OWA operators. International Journal of
2374 Intelligent Systems, 11(1): 49-73.
2375 Yan, G. et al., 2019. Review of indirect optical measurements of leaf area index: Recent
2376 advances, challenges, and perspectives. Agricultural and forest meteorology, 265: 390-
2377 411.
2378 Yang, X. et al., 2018a. FluoSpec 2—an automated field spectroscopy system to monitor canopy
2379 solar-induced fluorescence. Sensors, 18(7): 2063.
2380 Yang, Y. et al., 2015. Comparison of three dual-source remote sensing evapotranspiration
2381 models during the MUSOEXE-12 campaign: Revisit of model physics. Water Resources
2382 Research, 51(5): 3145-3165.
2383 Yang, Y., Roderick, M.L., Zhang, S., McVicar, T.R. and Donohue, R.J., 2019. Hydrologic
2384 implications of vegetation response to elevated CO_2 in climate projections. Nature
2385 Climate Change, 9(1): 44-48.
2386 Yang, Y. et al., 2018b. Post-drought decline of the Amazon carbon sink. Nature
2387 Communications, 9(1): 1-9.

2388 Yebra, M. et al., 2013. A global review of remote sensing of live fuel moisture content for fire
2389 danger assessment: Moving towards operational products. Remote Sensing of
2390 Environment, 136: 455-468.
2391 Yi, Y. et al., 2013. Recent climate and fire disturbance impacts on boreal and arctic ecosystem
2392 productivity estimated using a satellite-based terrestrial carbon flux model. Journal of
2393 Geophysical Research: Biogeosciences, 118(2): 606-622.
2394 Yoshida, Y. et al., 2015. The 2010 Russian drought impact on satellite measurements of solar-
2395 induced chlorophyll fluorescence: Insights from modeling and comparisons with
2396 parameters derived from satellite reflectances. Remote Sensing of Environment, 166:
2397 163-177.
2398 Yuan, M. et al., 2020. Impacts of preseason drought on vegetation spring phenology across the
2399 Northeast China Transect. Science of The Total Environment, 738: 140297.
2400 Yuan, W. et al., 2019a. Increased atmospheric vapor pressure deficit reduces global vegetation
2401 growth. Science Advances, 5(8): eaax1396.
2402 Yuan, X. et al., 2019b. Anthropogenic shift towards higher risk of flash drought over China.
2403 Nature Communications, 10(1): 1-8.
2404 Zaitchik, B.F., Santanello, J.A., Kumar, S.V. and Peters-Lidard, C.D., 2013. Representation of
2405 soil moisture feedbacks during drought in NASA Unified WRF (NU-WRF). Journal of
2406 Hydrometeorology, 14(1): 360-367.
2407 Zarco-Tejada, P.J., Rueda, C. and Ustin, S., 2003. Water content estimation in vegetation with
2408 MODIS reflectance data and model inversion methods. Remote Sensing of Environment,
2409 85(1): 109-124.

2410 Zargar, A., Sadiq, R., Naser, B. and Khan, F.I., 2011. A review of drought indices.
2411 Environmental Reviews, 19(NA): 333-349.
2412 Zeng, Q. et al., 2018. Inter-comparison and evaluation of remote sensing precipitation products
2413 over China from 2005 to 2013. Remote Sensing, 10(2): 168.
2414 Zhang, A. and Jia, G., 2013. Monitoring meteorological drought in semiarid regions using multi-
2415 sensor microwave remote sensing data. Remote Sensing of Environment, 134: 12-23.
2416 Zhang, B., AghaKouchak, A., Yang, Y., Wei, J. and Wang, G., 2019a. A water-energy balance
2417 approach for multi-category drought assessment across globally diverse hydrological
2418 basins. Agricultural and Forest Meteorology, 264: 247-265.
2419 Zhang, B. et al., 2019b. A Framework for Global Multicategory and Multiscalar Drought
2420 Characterization Accounting for Snow Processes. Water Resources Research, 55(11):
2421 9258-9278.
2422 Zhang, J., 2010. Multi-source remote sensing data fusion: status and trends. International Journal
2423 of Image and Data Fusion, 1(1): 5-24.
2424 Zhang, J. et al., 2016a. Multi-Radar Multi-Sensor (MRMS) quantitative precipitation estimation:
2425 Initial operating capabilities. Bulletin of the American Meteorological Society, 97(4):
2426 621-638.
2427 Zhang, K., Kimball, J.S. and Running, S.W., 2016b. A review of remote sensing based actual
2428 evapotranspiration estimation. Wiley Interdisciplinary Reviews: Water, 3(6): 834-853.
2429 Zhang, L., Jiao, W., Zhang, H., Huang, C. and Tong, Q., 2017a. Studying drought phenomena in
2430 the Continental United States in 2011 and 2012 using various drought indices. Remote
2431 Sensing of Environment, 190: 96-106.

2432 Zhang, X., Chen, N., Li, J., Chen, Z. and Niyogi, D., 2017b. Multi-sensor integrated framework
2433 and index for agricultural drought monitoring. Remote Sensing of Environment, 188:
2434 141-163.
2435 Zhang, Y. et al., 2013. Monitoring and estimating drought-induced impacts on forest structure,
2436 growth, function, and ecosystem services using remote-sensing data: recent progress and
2437 future challenges. Environmental Reviews, 21(2): 103-115.
2438 Zhang, Y., Song, C., Band, L.E., Sun, G. and Li, J., 2017c. Reanalysis of global terrestrial
2439 vegetation trends from MODIS products: Browning or greening? Remote Sensing of
2440 Environment, 191: 145-155.
2441 Zhao, F. et al., 2011. Measuring effective leaf area index, foliage profile, and stand height in
2442 New England forest stands using a full-waveform ground-based lidar. Remote Sensing of
2443 Environment, 115(11): 2954-2964.
2444 Zhao, M., Heinsch, F.A., Nemani, R.R. and Running, S.W., 2005. Improvements of the MODIS
2445 terrestrial gross and net primary production global data set. Remote Sensing of
2446 Environment, 95(2): 164-176.
2447 Zhao, M. and Running, S.W., 2010. Drought-induced reduction in global terrestrial net primary
2448 production from 2000 through 2009. Science, 329(5994): 940-943.
2449 Zheng, G. and Moskal, L.M., 2009. Retrieving leaf area index (LAI) using remote sensing:
2450 theories, methods and sensors. Sensors, 9(4): 2719-2745.
2451 Zhong, R. et al., 2019. Drought monitoring utility of satellite-based precipitation products across
2452 mainland China. Journal of Hydrology, 568: 343-359.
2453 Zhou, L., Chen, N., Chen, Z. and Xing, C., 2016. ROSCC: an efficient remote sensing
2454 observation-sharing method based on cloud computing for soil moisture mapping in

precision agriculture. IEEE Journal of Selected Topics in Applied Earth Observations and Remote Sensing, 9(12): 5588-5598.

Zhou, L. et al., 2014. Widespread decline of Congo rainforest greenness in the past decade. Nature, 509(7498): 86.

Zhou, S., Zhang, Y., Park Williams, A. and Gentine, P., 2019. Projected increases in intensity, frequency, and terrestrial carbon costs of compound drought and aridity events. Science Advances, 5(1): eaau5740.

Zhu, X., Chen, J., Gao, F., Chen, X. and Masek, J.G., 2010. An enhanced spatial and temporal adaptive reflectance fusion model for complex heterogeneous regions. Remote Sensing of Environment, 114(11): 2610-2623.

Zhu, X., Skidmore, A.K., Darvishzadeh, R. and Wang, T., 2019. Estimation of forest leaf water content through inversion of a radiative transfer model from LiDAR and hyperspectral data. International Journal of Applied Earth Observation and Geoinformation, 74: 120-129.

Zhu, X. et al., 2015. Comparison of monthly precipitation derived from high-resolution gridded datasets in arid Xinjiang, central Asia. Quaternary International, 358: 160-170.

Zscheischler, J. et al., 2020. A typology of compound weather and climate events. Nature Reviews Earth & Environment: 1-15.

Zuromski, L.M. et al., 2018. Solar-induced fluorescence detects interannual variation in gross primary production of coniferous forests in the Western United States. Geophysical Research Letters, 45(14): 7184-7193.

2477 **Table 1.** Summary of major drought related satellite products that can be incorporated into integrated drought characterization.

	Data	Temporal resolution	Spatial resolution	Coverage	Data period	References
Precipitation	CPC-Global	Daily	0.5°	Global	2006-present	(Xie et al., 2010)
	GPCP	Daily/Monthly	1°/2.5°	Global	1979-present	(Adler et al., 2003)
	GPM	30 min/3h/Daily	0.1°	60°S-60°N	2015-present	(Hou et al., 2014; Hou et al., 2008)
	GSMaP	1h/Daily/Monthly	0.1°	60°S-60°N	2002-2012	(Kubota et al., 2007)
	CMAP	Monthly	2.5°	Global	1979-present	(Xie and Arkin, 1997; Xie et al., 2007)
	TRMM	3h/Daily/Monthly	0.25°/0.5°	50°S-50°N	1998-2015	(Huffman et al., 2007)
	PERSIANN-CCS	30 min/3h/6h	0.04°	60°S-60°N	2003-present	(Sorooshian et al., 2000)
	PERSIANN-CDR	3h/6h/Daily	0.25°	60°S-60°N	1983-present	(Ashouri et al., 2015)
Land Surface Temperature	Landsat	16 days	60 m	Global	1999-present	(Sobrino et al., 2004)
	MODIS	Twice daily	0.01°	Global	2000-present	(Wan, 2008; Wan and Li, 1997)
	ASTER	Twice daily	90 m	Global	1999-present	(Jiménez-Muñoz and Sobrino, 2009)

	AVHRR	Twice daily	~1.1 km	Global	1978-present	(Kerr et al., 1992)
	AATSR	35 days	~1 km	Global	2004-present	(Prata, 2002)
Soil Moisture	AMSR-E	Daily	25 km	Global	2002-2011	(Paloscia et al., 2006)
	AMSR2	Daily	25 km	Global	2012-present	(Kim et al., 2015)
	SSM/I	Daily	25 km	Global	1987-present	(Paloscia et al., 2001)
	ASCAT	3 Days	12.5/25 km	Global	2007-present	(Brocca et al., 2011)
	SMAP	2-3 Days	3 /9 /36 km	Global	2015-present	(Das et al., 2010)
	SMOS	2-3 days	35 km	Global	2010-present	(Kerr et al., 2012)
Groundwater/Surface water storage	GRACE	Monthly	220 km	Global	2002-present	(Ruzmaikin et al., 2014)
	GRACE-FO	Monthly	180 km	Global	2017-present	(Flechtner et al., 2016)
Snow	MODIS	5 min/Daily/8 days/Monthly	1 km	Global	2000-present	(Hall et al., 2002)
	IMS	Daily	1 km /4 km/24 km	0-90^{o}N	1997-present	(Helfrich et al., 2007)
	CMC	Daily	24 km	0-90^{o}N	1998-present	(Brown et al., 2003)
	AMSR-E	Daily/5 days	25 km	Global	2002-2011	(Chang and Rango, 2000)
	SSM/I	Daily	25 km	Global	1978-present	(Pulliainen and Hallikainen, 2001)
	AMSR2	Daily	25 km	Global	2012-present	(Kim et al., 2015)
Evapotranspiration	MODIS	8 Days	500 m	Global	2000-present	(Mu et al., 2011)

	GLEAM	Daily	0.25°	Global	1980-2018	(Miralles et al., 2011)
	GLDAS	3 h/month	1°	Global	1979-2016	(Liu et al., 2016a)
	METRIC	16 days	30 m	Global	2011-present	(Allen et al., 2007)
Vegetation vigor	AVHRR NDVI/EVI	bi-week	0.083°	Global	1982-present	(Tucker et al., 2005)
	MODIS NDVI/EVI	8 Days/Monthly	500 m	Global	2000-present	(Beck et al., 2006)
	Landsat NDVI	16 days	30 m	Global	1972-present	(Beck et al., 2011)
	MODIS LAI	8 days	500 m	Global	2000-present	(Myneni et al., 2002)
	SMOS VOD	Daily	~40 km	Global	2009-present	(Vittucci et al., 2016)
	GOME-2 SIF	Daily	0.5°	Global	2007-present	(Joiner et al., 2011)
	TROPOMI SIF	Daily	7 km×3.5km	Global	2017-present	(Köhler et al., 2018)
	OCO-2 SIF	Daily	2.25 km × 1.29 km	Global	2014-present	(Frankenberg et al., 2014; Sun et al., 2017)
	SCIAMACHY SIF	Daily/Monthly	1.5°/1°	Global	2002-2012	(Köhler et al., 2014)
	MODIS GPP/NPP	8 days	500 m	Global	2000-present	(Zhao et al., 2005)

Table 2. Synthesis from the last decade summarizing various approaches for the development of multi-sensor integrated drought indices.

Model Type		Index	Data	References
Data driven models	Simple linear combination models	MIDI	Precipitation (TRMM), Soil moisture (AMSR-E), LST (AMSR-E)	(Zhang and Jia, 2013)
		SDCI	Precipitation (TRMM), Vegetation (MODIS NDVI), LST (MODIS)	(Rhee et al., 2010)
		ADI	Vegetation (AVHRR NDVI, GPP), Soil moisture (ASCAT, AMSR-E, SMMR, SSM/I)	(Wang et al., 2018)
		Optimal SDCI	Precipitation (TRMM, GSMaP), Vegetation (MODIS NDVI), LST (MODIS)	(Guo et al., 2019)
		OVDI	Precipitation (TRMM), Vegetation (MODIS NDVI), LST (MODIS), Soil moisture (AMSR-E)	(Hao et al., 2015)
		OMDI	Precipitation (TRMM), LST (MODIS), Soil moisture (AMSR-E)	(Hao et al., 2015)
	PCA models	SDI	Precipitation (TRMM), LST (MODIS), Vegetation (MODIS NDVI)	(Du et al., 2013)
		IDCI	Precipitation (TRMM), LST (MODIS), Vegetation (MODIS NDVI)	(Meng et al., 2016)

	Machine learning models	HSMDI	Precipitaiton (TRMM), LST (MODIS), Vegetation (MODIS NDVI, EVI, LAI), ET (MODIS), Soil moisture (AMSR-E)	(Park et al., 2017)
		CMDI	Precipitation (TRMM), LST (MODIS), Vegetation (MODIS NDVI), ET (MODIS)	(Han et al., 2019)
		ISDI	Vegetation (MODIS), LST (MODIS), Land cover (IGBP)	(Wu et al., 2015)
		VPID	Precipitation (GPM, IMERG), Vegetation (VIIRS), Soil moisture (METOP, ASCAT), LST (S-NPP), ET (MODIS)	(Son et al., 2021)
	Fuzzy weighting models	Nonparametric-SPI	Precipitation (CHOMPS, GPCP, CMAP, PERSIANN-CD, TRMM, GLDAS-2, MERRA-2)	(Alizadeh and Nikoo, 2018)
		GIIDI	Precipitation (TRMM), Vegetation (MODIS NDVI), LST (MODIS), Soil moisture (AMSR-E)	(Jiao et al., 2019b)
Process based models		PADI	Precipitation (GPCC), Vegetation (AVHRR NDVI), Soil moisture (GLDAS)	(Zhang et al., 2017b)
Water balance models		SZI	Precipitation (GLDAS-2), ET (GLDAS-2), PET (GLDAS-2), Runoff (GLDAS-2)	(Zhang et al., 2019a)

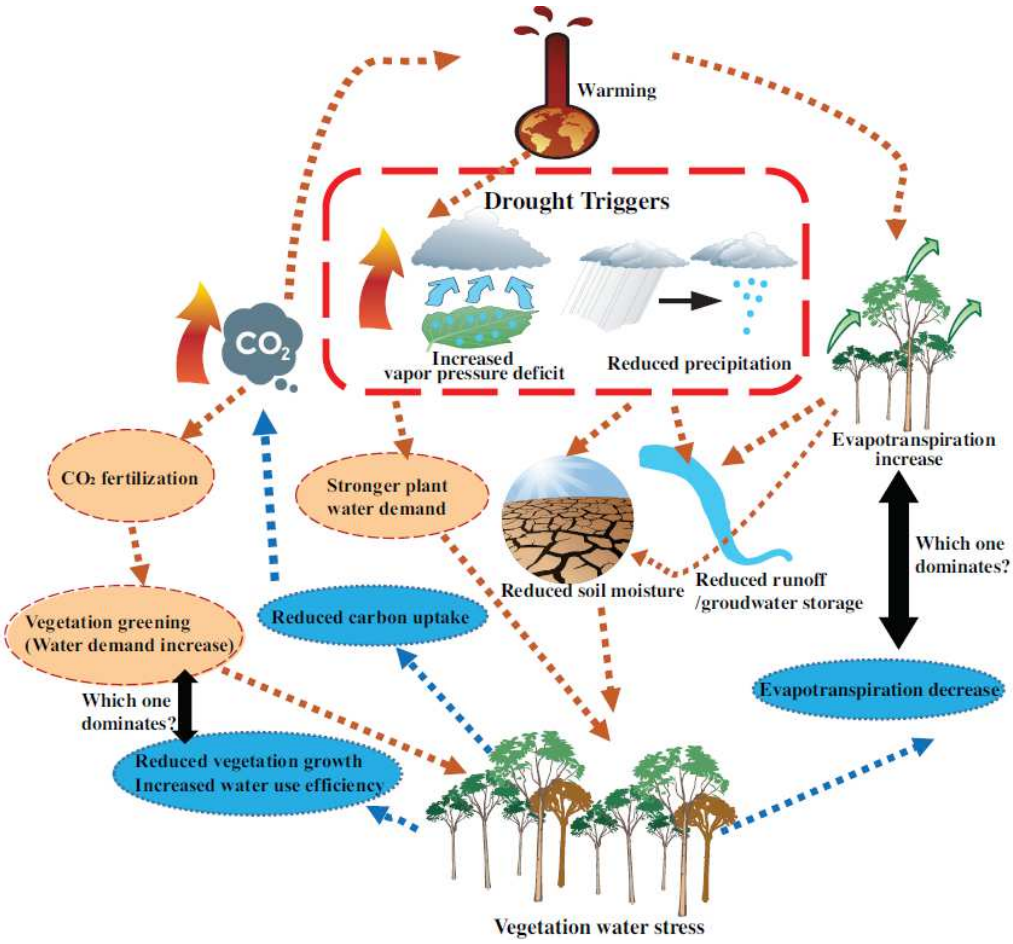

2483

2484 **Figure 1.** Conceptual diagram of drought impacts and the potential ecosystem feedbacks under

2485 global warming. Brown arrows in indicate the components of drought impacts and how global

2486 warming potentially exacerbate drought; blue arrows indicate potential drought feedbacks to

2487 climate.

2488

2489

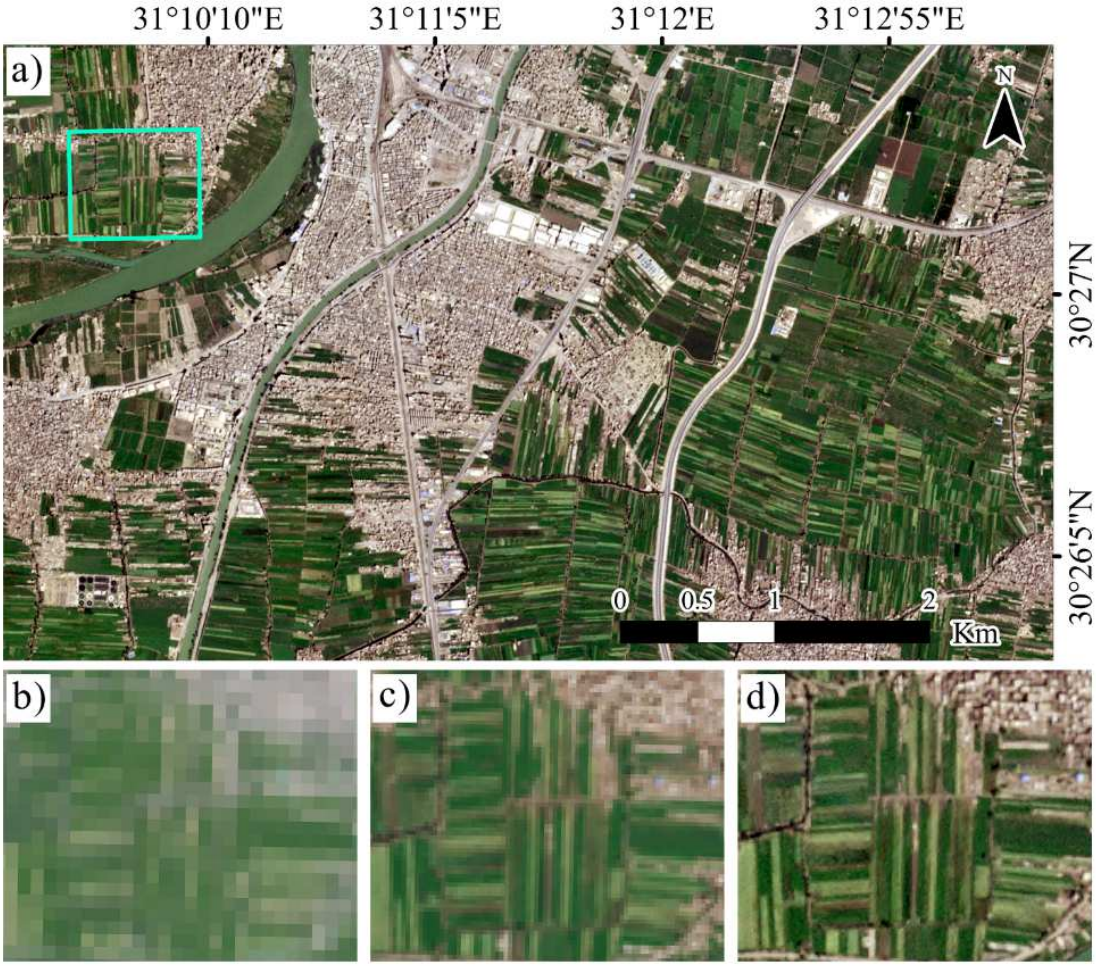

Figure 2. Natural color representation of an agricultural area along the Nile River near Banha, Egypt that demonstrates the spatial resolution advantage of CubeSats. Panel a) shows a 3 m spatial resolution CubeSat image from Planet, where small agricultural fields and urban structures can be discerned. Panels b) to d) show a zoomed-in view of the area contained by the cyan rectangle for b) Landsat 8, c) Sentinel-2A and d) Planet at 30, 10, and 3 m resolutions, respectively. The Landsat image was acquired on March 31,2020, and both Planet and Sentinel-2A images were acquired on March 29, 2020.

Acronym dictionary:

AGC:	Aboveground biomass carbon
AMS:	American Meteorological Society
AOD:	Aerosol optical depth
ASCAT:	Advanced Scatterometer
AVHRR:	Advanced Very High Resolution Radiometer
BRT:	Boosted regression trees
CART:	Classification and regression tree
CCI:	Climate Change Initiative
CDMI:	Combined drought monitoring index
COT:	Cloud optical thickness
ECOSTRESS:	ECOsystem Spaceborne Thermal Radiometer Experiment on Space Station
EDDI:	Evaporative demand drought index
ENSO:	El Nino-Southern Oscillation
EPMC:	Evolution Process-based Multi-sensor Collaboration
ERSATSR:	European Remote Sensing Satellite–Along Track Scanning Radiometer
ESA:	European Space Agency
ESI:	Evaporative Stress Index
FDA:	flexible discriminant analysis
FIDI:	Fuzzy Integrated Drought Index
FLEX:	FLuorescence EXplorer
fPAR:	fraction of absorbed photosynthetic active radiation
GEDI	Global Ecosystem Dynamics Investigation
GEO:	Geostationary Earth orbit
GFED:	Global Fire Emissions Database
GNSS:	Global Navigation Satellite System
GPCP:	Global Precipitation Climatology Project
GPP:	Gross primary productivity
GRACE:	Gravity Recovery and Climate Experiment
GWR:	Geographically weighted regression
HiFIS :	High-fidelity imaging spectroscopy
HLS:	Harmonized Landsat and Sentinel-2
HSMDI:	High resolution Soil Moisture Drought Index
ICESat-2:	Ice, cloud, and land elevation satellite-2
IDI:	Integrated Drought Index
IMS:	Ice Mapping System
INFORM:	Invertible forest reflectance model
InSAR:	Interferometry of Synthetic Aperture Radar
ISDI:	Integrated Surface Drought Index

JAXA:	Japan Aerospace Exploration Agency
KECA:	Kernel entropy component analysis
LAI:	Leaf area index
LEO:	Low Earth orbit
LFMC:	Live fuel moisture content
LiDAR:	Light detection and ranging
LST:	Land surface temperature
MAIAC:	Multi-Angle Implementation of Atmospheric Correction
MARS:	Multivariate adaptive regression splines
MIDI:	Microwave Integrated Drought Index
MODIS:	Moderate Resolution Imaging Spectroradiometer
MRMS:	Multi-Radar Multi-Sensor
NASA:	National Aeronautics and Space Administration
NDII:	Normalized Difference Infrared Index
NDVI:	Normalized Difference Vegetation Index
NDWI:	Normalized Difference Water Index
NIR:	Near infrared radiation
NIR_V:	Near-infrared reflectance of vegetation
NISAR:	NASA-ISRO Synthetic Aperture Radar
NLDAS-2:	North American Land Data Assimilation System-2
NOAA:	National Oceanic and Atmospheric Administration
OMDI:	Optimized Meteorological Drought Index
OVDI:	Optimized Vegetation Drought Index
PADI:	Process-based Accumulated Drought Index
PAR:	Photosynthetically active radiation
PCA:	Principal component analysis
PCI:	Precipitation Condition Index
PDSI:	Palmer drought severity index
PERSIANN:	Precipitation Estimation from Remotely Sensed Information using Artificial Neural Networks
PHDI:	Palmer Hydrologic Drought Index
PLSR:	Partial least squares regression
PRI:	Photochemical reflectance index
QuickDRI:	Quick Drought Response Index
RCI:	Rapid change index
RF:	Random forests
RTM:	Radiative transfer models
SDCI:	Scaled Drought Condition Index
SDI:	Synthesized drought index
SESR:	Standardized evaporative stress ratio
SIF:	Solar-induced chlorophyll fluorescence

SKPCA:	Sparse KPCA
SMCI:	Soil Moisture Condition Index
SMMR:	Scanning Multi-channel Microwave Radiometer
SMRI:	Standardized Snow Melt and Rain Index
SPEI:	Standardized Precipitation Evapotranspiration Index
SPI:	Standardized Precipitation Index
SSM/I:	Special Sensor Microwave Imager
SVI:	Standardized Vegetation Index
SVM:	Support vector machines
SWSI:	Surface Water Supply Index
SZI:	Standardized Moisture Anomaly Index
Tandem-X:	TerraSAR-X add-on for Digital Elevation Measurement
TCI:	Temperature Condition Index
TRMM:	Tropical Rainfall Measuring Mission
TWS:	Terrestrial water storage
USGS:	United States Geological Survey
VCI:	Vegetation condition index
VegDRI:	Vegetation Drought Response Index
VIS/IR:	Visible and infrared radiation
VOD:	Vegetation optical depth
VPD:	Vapor pressure deficit

2501

2502